

Fall 12-18-2020

Feasibility of Geothermal Energy Piles in New Orleans Alluvial Soils

Patrick A. Thurmond
University of New Orleans, pathurmo@uno.edu

Follow this and additional works at: <https://scholarworks.uno.edu/td>



Part of the [Civil Engineering Commons](#), and the [Geotechnical Engineering Commons](#)

Recommended Citation

Thurmond, Patrick A., "Feasibility of Geothermal Energy Piles in New Orleans Alluvial Soils" (2020).
University of New Orleans Theses and Dissertations. 2845.
<https://scholarworks.uno.edu/td/2845>

This Thesis is protected by copyright and/or related rights. It has been brought to you by ScholarWorks@UNO with permission from the rights-holder(s). You are free to use this Thesis in any way that is permitted by the copyright and related rights legislation that applies to your use. For other uses you need to obtain permission from the rights-holder(s) directly, unless additional rights are indicated by a Creative Commons license in the record and/or on the work itself.

This Thesis has been accepted for inclusion in University of New Orleans Theses and Dissertations by an authorized administrator of ScholarWorks@UNO. For more information, please contact scholarworks@uno.edu.

Feasibility of Geothermal Energy Pile Use in Alluvial Deposits in New Orleans Area

A Thesis

Submitted to the Graduate Faculty of the
University of New Orleans
in partial fulfillment of the
requirements for the degree of

Master of Science
in
Engineering
Civil and Environmental

by

Patrick Andrew Thurmond

B.S. University of Oklahoma, 2015
M.S. University of New Orleans, 2018

December, 2020

Table of Contents

List of Figures	v
List of Tables	vii
Abbreviations.....	viii
Abstract	xi
Chapter 1 - Introduction.....	1
1.1 Background.....	1
1.2 Problem Statement	4
1.2.1 Primary Objective.....	5
1.2.2 Experimental Approach.....	6
1.2.3 Report Organization	6
1.3 Geological Setting.....	7
1.3.1 Late Quaternary Mississippi River Evolution.....	7
1.3.2 Holocene Delta Formation	11
1.3.3 Pleistocene Deposits	13
1.3.4 Fluvial Deposits	14
1.3.5 Fluvial-Marine	17
1.3.6 Paludal Environments	19
1.3.7 Marine Environments.....	21
1.3.8 Geology Summary	24

Chapter 2: Theory and Literature Review	26
2.1 Overview	26
2.2 Vapor Compression Cycle	26
2.3 Underground Thermal Energy Storage	29
2.4 Ground Heat Exchangers	30
2.4.1 Open-Loop Systems.	30
2.4.2 Closed-Loop Systems.....	32
2.4.3 Geothermal Energy Piles	33
2.5 Governing Thermodynamics	35
2.6 Thermal Conductivity	39
2.7 Theoretical and Empirical Models for Thermal Conductivity	43
2.7.1 Early Methods Proposed by Kersten (1949).....	43
2.7.2 Complex Model by de Vries (1963)	44
2.7.3 Normalization of λ by Johansen (1975).....	44
2.7.4 Introduction of Soil Texture Factors by Côté and Konrad (2005).....	47
2.7.5 Alternative Normalized Conductivity by Lu and Horton (2007) and Lu et. al (2014)	48
2.7.6 Other Relevant Work	49
2.7.7 Summary of Theoretical and Empirical Models	49
2.8 Laboratory Testing of Thermal Conductivity	49
2.9 In Situ Testing of Thermal Conductivity	54
2.9.1 Field Testing Using a Needle Probe.....	54
2.9.2 Testing of Thermal Properties at Depth.....	54

2.9.3 Development of the Thermal Cone Test	56
2.10 Previous Study of Geothermal Properties in Louisiana	58
2.11 Available Studies of System Efficiency	62
2.11.1 General Summary of System Efficiencies	62
2.11.2 Efficiency in Cooling Dominated Climates by Khan and Wang (2014) and Akrouch (2014).....	65
2.11.3 Other Relevant Work	69
Chapter 3: Methodology.....	72
3.1 Define Scope of Work	73
3.2 Conduct Literature Review.....	73
3.3 Develop Case Study Soil Types	74
3.4 Estimate λ from Empirical Correlations	74
3.5 Validation by Lab Testing.....	75
3.6 Evaluation of In Situ Testing Methods	75
Chapter 4: Analysis.....	77
4.1 Case Study Soil Types	77
4.2 Empirical Estimates of λ.....	79
4.3 Results of Laboratory Testing.....	79
4.4 In Situ Thermal Cone Testing	85
4.4.1 Calibration Testing	85
4.4.2 Field Testing	90

Chapter 5: Results and Discussion 97

5.1 Geotechnical Feasibility of Energy Piles in New Orleans.....97

5.2 Design Responsibilities99

5.3 Determination of λ 101

5.4 Recommendations for In Situ Testing of λ 102

5.5 Limitations and Future Research103

References..... 105

Vita 113

List of Figures

Figure 1: Typical Pile Foundations	3
Figure 2: Seasonal Heat Storage Process.....	4
Figure 3: Mississippi River during Pleistocene (from Kolb & Van Lopik, 1958)	9
Figure 4: Historical Lobes of the Mississippi River.....	Error! Bookmark not defined.
Figure 5: Typical stages of deltaic deposition	13
Figure 6: Barrier Island Formation (Roberts & Blum, 2012)	23
Figure 7: Pine Island Barrier Trend (from New Orleans Geological Society)	24
Figure 8: Vapor Compression Cycle in GHP (from Tidewater Mechanical, LLC)	27
Figure 9: Open-Loop System (from Underground Energy, LLC).....	31
Figure 10: Closed Loop Systems (from SintonAir, LLC)	33
Figure 11: GHX loops fitted to pile reinforcement cages (from Narsilio, et al., 2014)	34
Figure 12: Relationship between thermal conductivity and saturation (from Brandl, 2006).....	37
Figure 13: Transfer of heat in an energy pile (from Akrouch, 2014).....	39
Figure 14: Thermal dryout curves (from IEEE 442-2017).....	42
Figure 15: Thermal probe as proposed by Lutenegger and Lally, 2001.....	55
Figure 16: Thermal profile in New Orleans (adapted from Bou-Mekhayel, 2019)	59
Figure 17: Correlation as proposed by Bou-Mekhayel (2019)	61
Figure 18: Measured HCF Temperature and Calculated Heat Exchange (from Akrouch, 2014).....	68
Figure 19: Research Methodology.....	72
Figure 20: Thermal probe with electronic cone penetrometer	76
Figure 21: Predicted vs measured values of effective thermal conductivity.....	84
Figure 22: Example thermal curve for calibration test of thermal probe.....	86
Figure 23: Example of simplified slope method during heating cycle	87
Figure 24: Locations of field testing.....	91

Figure 25: Temperature during CPT sounding	92
Figure 26: Typical thermal loading cycle during field testing	93

List of Tables

Table 1: Typical values for thermal conductivity (<i>Adapted from Côté & Konrad, 2005; IEEE Std 442-2017</i>)	39
Table 2: Values of texture parameters (<i>from Cote and Konrad, 2005</i>)	47
Table 3: Equivalency between thermal and hydraulic flows (from Briaud, 2014).....	57
Table 4: Summary of Measured Dry Thermal Conductivity (from Bou-Mekhayel, 2019)	60
Table 5: Summary of Case Studies of Installed Systems (adapted from Laloui and Donna, 2013)	62
Table 6: Comparison of heat transfer by pile and soil material types (from Laloui and Donna, 2013)	64
Table 7: Summary of expected payback period (from Tapia, 2017).....	70
Table 8: Summary of Selected Parameters for Generalized Soil Types	77
Table 9: Typical Values of Thermal Conductivity for Generalized Soil Types	79
Table 10: Accuracy and precision of predicted versus measured values of thermal conductivity	81
Table 11: Average thermal conductivity by depositional environment	85
Table 12: Result of calibration testing for thermal probe using stabilized water	90
Table 13: Summary of results for in situ testing of thermal conductivity	94
Table 14: Summary of previous economic studies (adapted from Khan and Wang, 2014; Akrouch, 2014)	98

Abbreviations

ACIP	Augered Cast-In-Place
AD	Abandoned Distributary
ASHP	Air-Source Heat Pump
ASHRAE	American Society of Heating, Refrigerating, and Air-Conditioning Engineers
ATES	Aquifer Thermal Energy Storage
BHX	Borehole Heat Exchanger
BS/NG	Baysound/Nearshore Gulf
CH	High Plasticity (Fat) Clay
CL	Low Plasticity (Lean) Clay
COP	Coefficient of Performance
CPT	Cone Penetration Test
CSP	Closed End Steel Pipe
CTES	Cavern Thermal Energy Storage
EER	Energy Efficiency Ratio
GCHP	Ground-Coupled Heat Pump
GHE	Ground Heat Exchanger
GHG	Greenhouse Gas
GSHP	Ground Source Heat Pump
GWHP	Ground-Water Heat Pump
HDPE	High Density Polyethylene
HCF	Heat Carrying Fluid
HVAC	Heating, Ventilation, and Air Conditioning
ID	Interdistributary
LGM	Last Glacial Maximum
NL	Natural Levee
ML	Silt
OH	Organic Clay

OSP	Open End Steel Pipe
PHX	Pile Heat Exchanger
PB	Point Bar
PD	Prodelta
PT	Peat
PWP	Pore Water Pressure
RB	Relict Beach
S/M	Swamp/Marsh
SM	Silty Sand
SP	Poorly-Graded Sand
SPC	Square Precast Concrete
TCT	Thermal Cone Test
TID	Thermally Independent Depth
USACE	U.S. Army Corps of Engineers
UTES	Underground Thermal Energy Storage
C	Volumetric heat capacity
D	Diameter
E	Voltage
f_a	Sand fraction
f_{cl}	Clay fraction
f_g	Gas fraction
f_q	Quartz fraction
I	Electrical current
K	Hydraulic conductivity
L	Length
n	Porosity
Q	Heat exchange rate
R	Electrical resistivity
r	Radius
S	Saturation
SG	Specific gravity

t	Time
T	Temperature
u	Pore pressure
u_{50}	At 50% dissipation
u_i	Initial
u_o	Hydrostatic
α	Thermal diffusivity
γ	Unit weight
γ_d	Dry
γ_w	Water
Δu	Excess
θ	Volumetric water content
λ	Thermal conductivity
λ_{dry}	Dry
λ_e	Effective
λ_m	Lab measured
λ_n	Normalized
λ_p	Probe measured
λ_s	Solids
λ_{sat}	Saturated
ρ	Density
ρ_b	Bulk
ρ_w	Water
ω	Gravimetric water content

Abstract

Geothermal energy piles offer the benefits of modifying existing construction practices to reduce costs associated with heating and cooling. A major obstacle today in effective utilization of these systems is a general lack of site-specific data on the thermal properties of subsoils. To maximize the potential efficiency of these systems, engineers require an understanding of the potential impact of this technology on existing foundation design methodology as well as a means for quantifying potential heat transfer through soil by determination of the soil's thermal conductivity. This study examines the feasibility of energy piles with a focus on alluvial soils found in the New Orleans and Lower Mississippi River valley areas by evaluating available empirical means for estimating thermal conductivity coupled with a field and laboratory investigation. These values for thermal conductivity were then compared with values in other studies performed on the efficiency of systems in other cooling dominated climates.

Keywords: Geothermal; Thermal Conductivity; Thermal Cone Test; Ground Coupled Heat Pump;

Thermal Properties of New Orleans Alluvium

Chapter 1 - Introduction

1.1 Background

The widespread availability of energy resulting from the Industrial Revolution precipitated one of the longest sustained periods of development in human history. Electricity produced using coal and other fossil fuels allowed the mechanization of manufacturing reducing the cost of common goods; the industrialization of agriculture alleviating much of the world's food shortages; and further specialization in the workforce leading to a breathtaking pace for advances in tech, medicine, and nearly every other aspect of modern day life. Unfortunately, the cost of these rapid advances becomes more apparent as the consequences of greenhouse gases (GHG) on the stability of the global climate are better understood. These consequences have resulted in a widespread push for the development of not just responsible and sustainable energy sources but also technology to maximize the efficiency of these sustainable energy sources.

The development of heating, ventilating, and air conditioning (HVAC) systems continued this trend of industrialization and altered the way and eventually the places that people live. Initially, the invention of modern air conditioning resulted in relatively local effects. The ability to cool theaters during the peak of summer heat saw the birth of the "summer blockbuster" as crowds sought an entertaining escape from the heat (Friedman, 1984). Factories and businesses, able to continue work throughout the summer months, saw jumps in productivity and sales; one study of Detroit Edison workers in 1938 saw an increase of 51% in productivity (Friedman, 1984). As the technology matured, more lasting effects were observed. The ability to provide

ventilation, in conjunction with the electric lightbulb, permitted architects to construct ever larger structures with interior spaces far from windows, giving rise to the modern skyscraper.

On a more macro scale, the ability to provide climate control started a demographic trend in the United States as more and more people moved to previously underdeveloped areas in the southern third of the country, commonly referred to as the Sun Belt. This trend saw the growth of cities like Atlanta, Houston, Las Vegas, and Phoenix from regional hubs to global cities. The Gulf Coast including Southern Louisiana and New Orleans grew by 150%, more than doubling the national growth average, between 1960 and 2008 (U.S. Census Bureau, 2010).

Today, HVAC systems account for approximately 42% of residential primary energy use and 32% of commercial building primary energy use (Buildings Energy Data Book, 2011). The significant energy usage for space heating and cooling has been identified by the United Nations as one of the key goals for sustainable development, particularly in the face of rising global temperatures (Keeping Cool in the Face of Climate Change). Geothermal heat pumps (GHPs), referred to as ground source heat pumps (GSHPs) by the American Society of Heating, Refrigerating, and Air-Condition Engineers (ASHRAE), utilize the moderated subsurface temperatures to boost the efficiency of heating and cooling systems. In fact, when compared to a traditional air-source heat pump (ASHP) system, a GHP may provide primary energy savings of 30% to 60% for spacing cooling and heating alone, while also providing domestic water heating (Tapia, 2017). The method with which the traditional HVAC system interacts with the subsurface is typically referred to as the ground heat exchanger (GHE).

Geothermal energy piles serve as one method of a GHE. Commonly installed as a deep foundation element to provide structural support in soft or compressible soils, such as those found in the New Orleans area, piles can be comprised of steel, concrete, grout, or timber and can extend to depths exceeding 60 meters (200 feet) below the ground surface. An example of pile foundations is shown in **Figure 1**.



Figure 1: Typical Pile Foundations

By virtue of their deep embedment, particularly below the hydrostatic water table, these piles offer an attractive opportunity in underground thermal energy storage (UTES), or the process of circulating heat through a heat retaining medium beneath the ground surface. These mediums, generally comprising naturally occurring ground water or occasionally crystalline bedrock, allow the storage of heat over time. Thus, a common application of this process is the

storage of heat during the summer for use in heating a building during the winter. In an ideal case, the inverse can also be true, and the building can also be cooled during the summer by transferring heat stored below the ground surface. This process is illustrated in **Figure 2**.

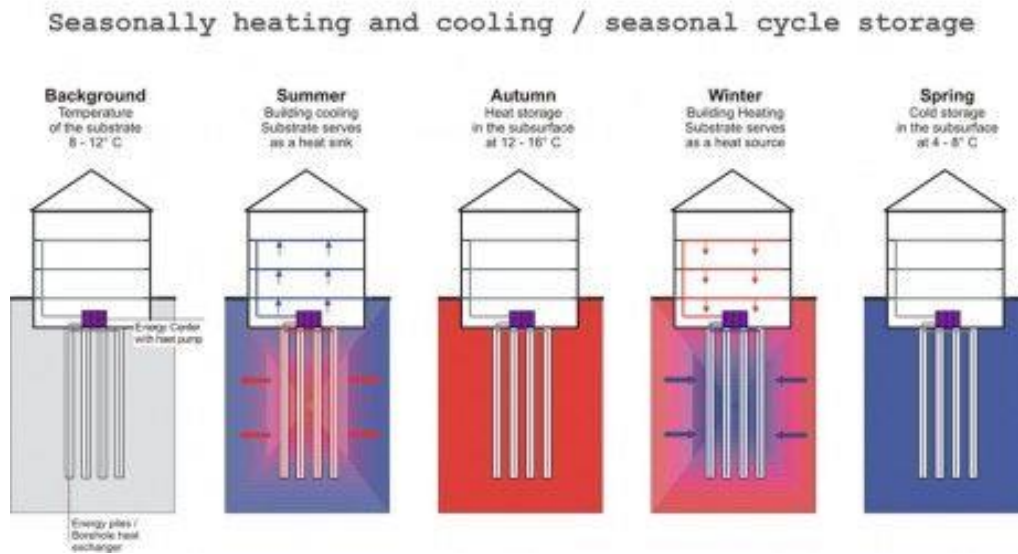


Figure 2: Seasonal Heat Storage Process

1.2 Problem Statement

GHPs and UTES provide the ability to modulate the seasonal energy requirements of a building by utilizing the stable thermal mass of the subsurface to store solar heat and provide a more efficient thermal gradient in HVAC systems. By its nature, the technology offers a reduction in operating costs over the lifespan of the building but requires an initial capital expenditure. Although energy piles are fairly common in Europe and to a lesser extent, Asia, research describing their design and case studies evaluating their efficacy, particularly in the New Orleans

and Lower Mississippi River Valley areas, are still relatively limited. Successful installation of energy pile systems within the United States has been limited primarily due to three factors:

- Hesitation from design teams based on the limited literature available;
- High initial installation costs with unclear payback periods; and
- Lack of public awareness.

The presence of very shallow groundwater and significant granular deposits in the New Orleans Area makes this technology attractive, particularly with respect to the near necessity of deep foundations. However, adaptations to the processes and methods commonly seen in Europe and Asia must be made to adjust for the much lower differential between average seasonal temperatures and the increased requirements for cooling rather than heating.

1.2.1 Primary Objective

While others have evaluated the economic feasibility of GHP systems within South Louisiana (Tapia 2017) or the efficiency of such systems (Desmedt 2010; Akrouch 2014), this work is meant to provide a general understanding of the suitability of soils and basic expectations for system efficiencies within the alluvial deposits encountered in the New Orleans area. To provide a means for qualitative comparison of the geotechnical conditions in New Orleans to previous case studies available in the literature, average or “typical” soil properties will be estimated for common geological subunits within New Orleans area alluvial soils, and the thermal properties of these soils will be evaluated through the thermal conductivity, λ , as estimated through a variety of theoretical and empirical methods, laboratory testing, and a new in situ testing method referred to as the thermal cone test (TCT).

1.2.2 Experimental Approach

This research focuses on the geological and geotechnical design aspects of energy piles to provide a quantitative evaluation of the feasibility of energy piles within New Orleans alluvial soils. To accomplish this, the geological setting as delineated in previous studies will be used to produce a set of typical soil types commonly encountered in geotechnical design. The efficiency of potential energy piles within these soils will be evaluated based on the thermal properties of the soils, namely, thermal conductivity, thermal resistivity, and thermal diffusion. These properties will be both evaluated using common empirical methods based on material index properties; measured using laboratory testing of undisturbed samples; and in situ through the performance of TCTs. Estimated ranges in the thermal properties of the soils will be used to compare to efficiency studies performed in different geological settings to provide a qualitative estimate of the viability of these systems. Please note this research is intended to answer questions regarding the subsoil's viability; additional factors including climate, hydrogeology, and economics may still govern and are not addressed herein.

1.2.3 Report Organization

- Chapter 1 provides the introduction to the problem while identifying the primary problem and presenting the objectives of this research. The remainder of Chapter 1 provides a review of the geological processes that created the current Mississippi River delta.
- Chapter 2 presents a substantial review of the most important works recently performed regarding energy piles, including basic theory of the refrigeration cycle; mechanisms for heat transfer; and methods for evaluating thermal conductivity of soils.

- Chapter 3 presents the methodology for the proposed scope of work.
- Chapter 4 was performed in two parts. First, a desktop study taking common index properties was used in conjunction with empirical methods to estimate the thermal properties of specific soil types of interest. Second, these estimates were compared to the results of tested values through laboratory testing of undisturbed samples and in situ tests. Further discussion on recommended procedures for future testing of thermal properties are also provided.
- Chapter 5 compares the estimated thermal properties as presented in Chapter 4 against selected case studies to provide an evaluation of the feasibility of energy piles in addition defining areas within the New Orleans metro where particular opportunities for energy pile installation may exist. Recommendations for future research important to enhance our understanding of how energy piles work are presented.

1.3 Geological Setting

1.3.1 Late Quaternary Mississippi River Evolution.

The surficial geology of the New Orleans area is relatively young and largely governed by the Mississippi River. During the course of the late Quaternary (approximately last half-million years), the river has served as both a sediment supply and filter, reacting to long term trends in sea level change resulting in a complex formation of depositional environments. As the river changes course, a process referred to as delta switching or avulsion, layers of these depositional environments create a complex and interbedded stratigraphy.

The creation of the modern Mississippi River system begins during the Miocene Epoch as the proto-Mississippi became the dominant source of sediment in the Gulf of Mexico basin along with a paleo-Tennessee River that would later be captured (Galloway et al., 2011). Sedimentation into the northern Gulf of Mexico became the foundation for shelf-edge progradation through the middle to late Miocene and would continue into the Pleistocene Epoch (Winker, 1982; Galloway et al., 2000).

The Pleistocene Epoch, beginning approximately 2.6 mya, was a period of high amplitude climate shifts resulting in highly variable global ice volume and sea level (Lisiecki and Raymo, 2005). Various interpretations of the fluvial axes for drainage during the Pleistocene exist (Saucier, 1994; Galloway et al., 2011); however, creation of the modern delta system is understood to have accelerated approximately 71-29 kya (Bentley et al., 2016). Over this time, increased glaciation that led to the last glacial maximum (LGM) approximately 18 kya resulted in a lowering of sea level to as much as 120 m (400 ft) below current (Fisk, 1944; Kolb & Van Lopik, 1958; Autin et al., 1991; Blum, 2007; Rittenour et al. 2007). The approximate location of the ancient shoreline is depicted in **Figure 3**. This lowering of sea level resulted in an increased gradient for gulfward-flowing streams and tributaries leading to a much higher energy river that carried coarser deposits and incised into the existing substrate. The Mississippi River created a wide valley approximately 20 to 50 km (10 to 25 miles) across with gently sloping sides that trended southeasterly across the coastal plain debouching into the Gulf of Mexico near the approximate location of modern Houma, Louisiana. Other smaller drainage basins to the east and west of this fluvial system drained directly into the Gulf.

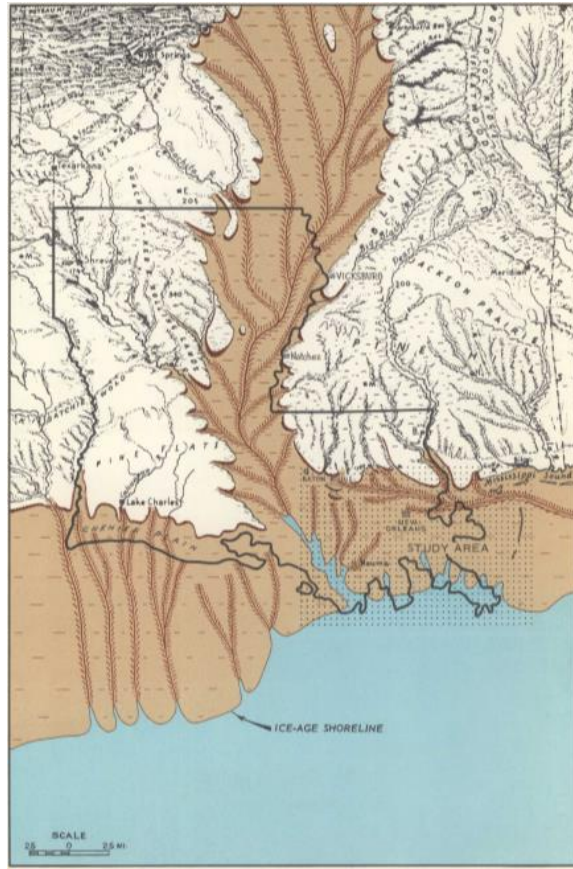


Figure 3: Mississippi River during Pleistocene (from Kolb & Van Lopik, 1958)

Following the LGM sea level began to rise occurring as conditions transitioned into the present interglacial phase. As sea level change shifted from falling to rapidly rising, a reduction in stream energy shifted stream behavior from erosional to depositional (Bentley et al., 2016). Braid belts of extremely coarse materials were transported by large flood pulses of glacial meltwater, the youngest of which formed approximately 11 to 13 kya (Bentley et al., 2016) and are commonly referred to as substratum deposits in local engineering practice. Global sea-level rise decelerated and stabilized ca. 9-6 kya (Bentley et al., 2016) at which time the modern delta system began to form. Although sediment loads of clay and silt continued to be transported into

the Gulf, relatively coarser sediments were now deposited near the mouth of the river, which allowed the construction of subaerial deltaic deposits.

By the start of the current interglacial period approximately 9-6 kya (Bentley et al., 2016), sea level rise stabilized. Relatively rapid deltaic progradation occurred as the rate of deposition exceeded the rate of sea level rise, turning the formerly erosional tributary system into a depositional distributary system typical of a lobate delta. These lobate deltas continued to prograde basinward, preceded by a stratum of brackish to marine-brackish prodelta clay, overlain by intradelta complexes consisting of distributary front sands, interdistributary clays, and natural levee clays and silts (Kolb & Van Lopik, 1958).

As a lobate delta of alluvial deposits advanced further into the gulf, it reached a point where the stream would abandon a low energy gradient course in favor of a shorter and more direct route to the sea. During the course of the last 5,000 to 7,000 years, this process of delta switching formed seven identified delta complexes as shown on **Figure 4**.

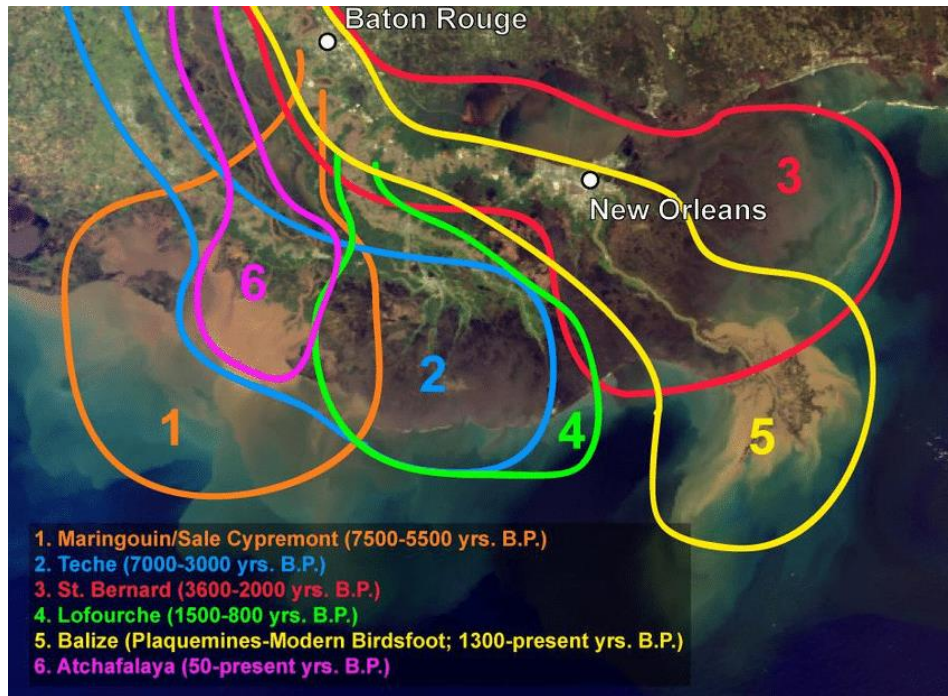


Figure 4: Historical lobes of the Mississippi River (after Bloom, 1998; from Day et al., 2007)

1.3.2 Holocene Delta Formation

Within the relatively low wave and tidal energy environment of the Gulf of Mexico, the formation of these deltas is largely a fluvial dominated process. Kolb & Van Lopik (1958) recognized four groups of stratigraphic units each of which possesses soils of different engineering properties as a result of the depositional environment in which they were deposited:

- Fluvial, comprise relatively narrow bands of sediment that are a direct result of riverine processes within active streams and former stream channels. Fluvial deposits can be further subdivided into natural levee, point bar, abandoned course, and abandoned distributary environments;
- Fluvial-marine, a combination of riverine and open water processes (e.g., waves and tides) typically encountered at the interface between river channels and the

Gulf. These deposits are estimated to constitute 75% of Holocene deposits within the deltaic plain (Deubert, 1982). Common subdivisions include prodelta, intradelta, and interdistributary;

- Paludal, typically wetlands characterized by a large amount of organic sediment within a low energy environment. This can include fresh, brackish, and saline marsh, inland and mangrove swamp, tidal channels, or lacustrine deposits; and
- Marine, deposited within shallow coastal waters subjected to erosion, reworking, and sorting by action of waves and tides. Typical deposits include bay-sound, reef, beach, and nearshore gulf deposits.

As the course of the river shifted during the past 7,000 years, different delta lobes migrated across one another creating the modern deltaic plain with very little to almost no vertical relief, but a complex stratigraphy as shown in **Figure 5**. In the words of Kolb & Van Lopik (1958), this region is “a land between earth and sea – belonging to neither and alternately claimed by both.”

An understanding of the depositional environments and the associated soil types is essential for understanding the engineering characteristics of those soils. Because the fluvial, marine, and paludal deposits within the deltaic plain are so complexly interwoven, stratigraphically substantial geotechnical variations can exist across short distances. The following provides a discussion of the most common soil types and their associated depositional environments, the distribution of these deposits, and a brief discussion of the physical properties.

Typical engineering properties are taken from Kolb and Van Lopik (1958); Montgomery (1974); and Saucier (1963).

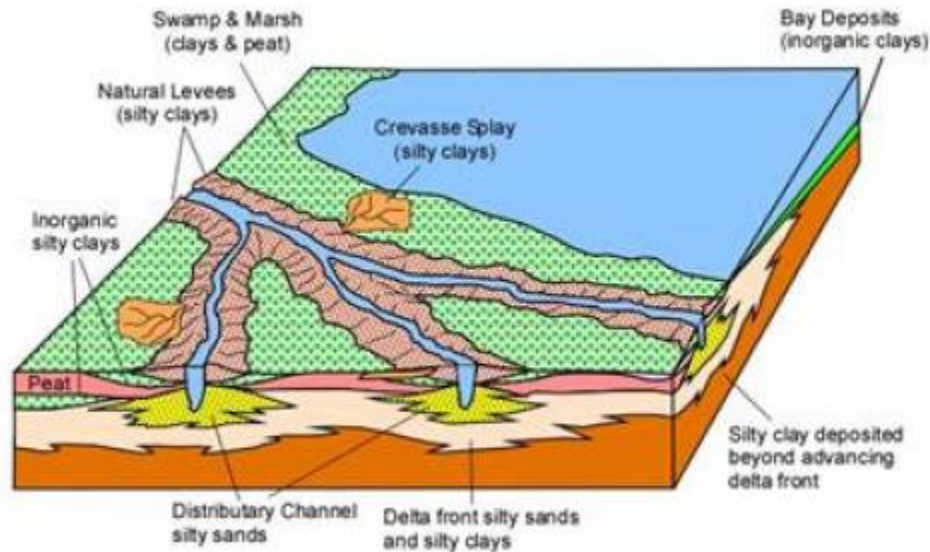


Figure 5: Typical stages of deltaic deposition

1.3.3 Pleistocene Deposits.

Pleistocene deposits are typically treated as a separate unit for geotechnical engineering deposits. Surficially encountered along the present day North Shore of Lake Pontchartrain from Slidell to Baton Rouge, these deposits dip to the south under Holocene alluvium from an average depth of approximately 25 meters in the New Orleans area to in excess of 200 meters at the current mouth of the river (Fisk, 1944). Incision into the Pleistocene surface that occurred prior to the previous LGM are common; the most notable being the ancient Mississippi River entrenchment near Houma. Pleistocene deposits were subjected to thousands of years of consolidation, dessication, and oxidation. As a result, typical deposits consist of primarily stiffer, overconsolidated soils. The uppermost Pleistocene is characterized by oxidized mottled tan, light

gray, or yellow colors, which can sometimes be mistaken for natural levee deposits, which are also subject to oxidation. At greater depths, tan and greenish-gray become more common.

Other defining characteristics of the Pleistocene interface include (Kolb and Van Lopik, 1958):

- Noticeable decrease in the natural moisture content
- Noticeable increase in the total unit weight
- Marked increase in soil strength

Predominant soil types of Pleistocene deposits include clay or silty clay, although sands, silts, and even organic deposits may also be encountered. Average moisture contents are commonly below 30%. Typical shear strengths range from approximately 40 to 120 kPa with unit weights often in excess of 18 kN/m³ (Saucier, 1963). A “crust” of highly overconsolidated soils is commonly encountered at the upper Pleistocene interface, returning to normally consolidated with greater depth.

1.3.4 Fluvial Deposits

Natural Levee. Natural levees (NL) are formed by the deposition of the coarsest sediments in the suspended load of seasonal floodwaters at the top of the riverbanks along distributary channels. The height of natural levees is typically governed by the subsidence and consolidation rates of underlying soils as well as available sediment load within the channel. The width of natural levees along common distributary channels and bayous can be measured in the tens of meters, whereas the main channel of the Mississippi River may have a natural levee as wide as 8 kilometers (Kolb & Van Lopik, 1958). Natural levees are typically the thickest immediately along the channel with a backslope largely governed by stream size that slopes

down towards flanking marsh or intertributary areas. Along the Mississippi River, the natural levee is typically 3 to 10 meters thick and is characterized by medium stiff to stiff gray and tan clays or silty clays with some sandy silty or silty sand seams found along the channel. Grain size typically decreases with distance from the channel. Moisture content of natural levee deposits tends to range from 20% to 50%. Typical shear strength of cohesive materials ranges from approximately 20 to 60 kPa with unit weights commonly between 15.5 and 18.5 kN/m³. As these deposits are usually only partially submerged during seasonal floods, oxidation may occur, leading to the tanner color. Natural levees can also sometimes be identified through aerial or satellite imagery by the presence of vegetation like oak or pine trees, which are surrounded by marsh or swamp vegetation.

Point Bar. Point bar (PB) deposits result from the lateral migration of the river channel. As the channel meanders, deposition of relatively coarse sediments like silt and silty sand occurs on the inside bend. Mostly associated with the primary channel of the Mississippi River, point bar deposits tend to be relatively insignificant along tributary channels. Meandering of the Mississippi River channel tends to be more common within the upper alluvial valley due to more prevalent deposits of relatively easily erodible medium to coarse sands. South of Baton Rouge, the river crosses the deltaic plain that was constructed primarily from finer deposits of less erodible clay and silt, resulting in less meandering. Within the Lower Mississippi River valley, point bar deposits tend to be relatively elongate along the inside bend of channels with distinct vertical transitions (in some cases as steep as 1H:1V). As the particle size tends to be influenced by seasonal water levels within the river, these deposits are highly interbedded with a fine-

grained topstratum approximately 10 to 20 meters thick overlaying coarser deposits of sandy silts and silty sands with frequent lenses and layers. The fine-grained topstratum generally comprises well interbedded gray clay or silty clay with natural moistures generally between 30% and 50%; typical shear strengths ranging from 20 to 50 kPA; and unit weights ranging from 17.3 to 19.0 kN/m³. Sands found in point bar deposits tend to be medium dense to dense in relative density with typical natural moisture contents of approximately 20% to 35% and unit weights ranging from 18.0 to 19.0 kN/m³. Point bar sands can typically be differentiated from marine sands by the relative lack of shell fragments.

Abandoned Course/Abandoned Distributary. Abandoned course deposits are the sediments that infill the primary channel after a lobe avulsion when the flow of the river switches to a new channel. After the avulsion, the channel is a fairly deep, elongate water body that gradually fills with a wedge of coarser sediments upstream at the head of the abandoned course becoming progressively thinner and finer downstream. Abandoned distributaries (AD), essentially an abandoned course on a much smaller scale, form an integral part of delta advance. These distributaries can range in width from just a few meters to in excess of 300 meters to as much as 15 meters deep. As with abandoned courses, abandoned distributaries are typically filled with coarser gray sand deposits near the head of the channel forming a wedge that thins in a downstream direction. Sand deposits are generally loose to medium dense in relative density. An upper zone of finer cohesive materials, deposited in the final stages of filling, is commonly encountered with high natural moisture contents, high organic content, and relatively low shear strengths.

As studied by Welder (1954), the formation of a distributary channel network is a function of the water depth of the receiving water body. Coarse sand deposits carried in the bed load of the distributary channel are deposited at the mouth of the channel, forming a shoal. This shoal can eventually cause the channel to bifurcate. Shallow water at the mouth of the distributary channel causes more frequent bifurcations resulting in a complex network of minor channels. In deeper water, shoals are typically longer developing resulting in fewer, larger distributary channels as seen at the Head of Passes in the modern Balize delta lobe. More complex distributary systems can be seen today from the formation of a crevasse, a location where the natural levee of a channel is overwhelmed by floodwaters. Ancient crevasse splays, leaving a complex formation of abandoned distributaries, today form the foundation of developed areas like Laplace and Thibodaux, Louisiana.

1.3.5 Fluvial-Marine

General. Estimated to comprise approximately 75% of all deltaic deposits including as much as 400 to 500 million tons of annual sediment (Kolb & Van Lopik, 1958), fluvial-marine deposits consist of the sediment carried as both bedload and suspended load in the Mississippi River that is deposited into depositional environments influenced by marine processes.

Prodelta. Prodelta (PD) deposits include terrigenous clays and silty clays carried in suspension from the river mouth that become widely distributed by marine and fluvial currents within the marine environment. Prodelta clays are typically the first deposits of a delta as they advance in a wide arc ahead of the distributary channels. The deposits are typically graded by particle size with the finest particles traveling the farthest from the river mouth (thus typically

the first deposits) followed by silty clays and occasionally sandy clays very close to the mouth of an active distributary. Prodelta clays are typically relatively homogenous due to their depositional nature and commonly overlie Pleistocene materials, substratum sands and gravels of the ancient Mississippi River channel, or nearshore gulf deposits. The thickness of these deposits is commonly in the order of a few meters; however, this thickness increases in an offshore direction with large homogenous strata more than 120 m (400 ft) encountered off the Balize delta. The majority of prodelta deposits consist of fat gray clays (CH) with natural moisture contents between 30% and 90%; unit weights of 14.0 to 18.5 kN/m³; and cohesive shear strengths between 10 and 30 kPA with a straight-line increase in shear strength versus depth due to consolidation of overburden pressures.

Intradelta. Intradelta deposits are essentially coarse materials deposited at the mouths of distributary channels. In engineering practice, there is some overlap between intradelta deposits (placed at the mouth of an active distributary channel) and abandoned distributaries (as much of the abandoned distributary was placed as intradelta deposits). Distributary channels can form from bifurcation of an existing channel due to intradelta deposits at the channel mouth or by crevassing of the natural levee along the channel. In either case, coarser sediments will fall out of suspension at the mouths of these channels as the transport energy drops. Intradelta deposits commonly form triangular or diamond shaped wedges at the base of an abandoned distributary. The deposits are typically coarser with primarily gray silts and fine sands but relatively high clay contents as well.

Interdistributary. As the name implies, interdistributary (ID) sediments are typically fine-grained materials carried in suspension and trapped between the subaqueous or low, subaerial natural levees of distributary channels. Fines may also be transported inland from the river mouth by wave action and settle in these triangular basins between distributaries. Given the significant amount of fine sediments carried by the Mississippi River, interdistributary deposits comprise a substantial proportion of delta deposits with considerable thicknesses and aerial extents. These clays are often placed over a basement of prodelta clays. As sedimentation continues and the water depth decreases, these environments typically trend more towards paludal rich with organics. These deposits are typically fairly homogenous gray clays (CH), although very thin silt or fine sand lenses may be present as a result of large seasonal floods pushing coarser deposits further. Natural moisture contents in these deposits are typically fairly high, ranging from 50% to 110% and correspondingly low unit weights between 14.0 and 16.5 kN/m³. Cohesive shear strengths of interdistributary deposits are related to the age of the materials. These deposits tend to be deposited in relatively quick succession; therefore, underconsolidated materials are frequently observed in younger deposits located near the current Balize delta. Older deposits tend to trend towards normally consolidated with a linear increase in strength proportional to the overburden as consolidation is allowed to occur. Typical cohesive shear strengths range from 15 to 30 kPa.

1.3.6 Paludal Environments

General. As the water depth within interdistributary zones decreases with continued sedimentation organic content increased due to vegetative growth. The decaying biomass of

sedges and other marsh grasses serves as an additional sediment trap, promoting land growth and ultimately a transition from fresh to brackish and saline wetlands. This decrease in salinity promotes the growth of vegetation like mangroves and cypress trees found in freshwater swamps, resulting in even greater sediment capture and retention. Subsidence or a decrease in sediment supply results in an imbalance in elevation change and associated increase in salinity. Vegetative die-off as a result of salinity increases accelerates erosion creating a complex, tortuous, ever-changing coastline of open water marshes and isolated, shallow lakes.

Marsh. Marshes describe the nearly featureless grasslands found on the Louisiana coastline where land and water meet. Typically less than half a meter above sea level, these expanses may be subjected to tidal flooding depending on distance from open water. Although this flooding frequently captures additional fine sediments, organic biomass comprises a significant portion of sedimentation. As grasses and sedges die, the organic material is pushed below the water surface where oxidation processes are limited. Additional seasons of plant growth augments and densifies this subaerial biomass, providing for a “firmer” land surface. These deposits of peat are typically brown to black fibrous masses with partly decomposed plant remains. Interspersed within the organic matter can be sediments of any range in particle size dependent on their distance to a distributary channel. Gray, dark gray, or black clay high in organic content is most commonly observed, but coarser sediments may be encountered as well. Kolb & Van Lopik (1958) subdivided marsh environments into freshwater marsh, floating marsh, brackish-freshwater marsh, and saline-brackish water marsh as a way to evaluate the potential composition between organic clays, peats, and humus. In any case, natural moisture contents of

these materials tends to be extremely high exceeding 100% with very low unit weights between 9 and 14 kN/m³. Shear strengths of these materials also tends to be extremely low, although fibrous materials can lead to misleadingly high shear test results.

Swamps. Swamps are freshwater wetlands primarily identified by the presence of dense growths of trees like cypress or mangrove. Cypress swamps, also referred to as inland swamps, are seasonally flooded low-lying areas with low tolerance for salinity intrusions. These deposits are characterized by gray and dark gray clay or organic clay with higher moisture contents and significant amounts of decayed wood. Some peat or humus may be present; however, it is less common than in marsh deposits. Cohesive strengths and unit weights of these deposits are typically very low.

Lacustrine. Development of lakes within the paludal environment normally occurs during the deterioration of marshes. Lakes can vary widely in size from a few meters to tens of kilometers. The depths within these lakes rarely exceed 2 to 3 m. Because sediment supply to these environments is typically low, these deposits are often mistaken and/or classified as either marsh or interdistributary deposits depending on organic content and color. Some varved clays may be observed with extremely thin silt lenses in larger lakes.

1.3.7 Marine Environments

As a relatively shallow basin with a microtidal regime, the Gulf of Mexico experiences much smaller wave and tidal energies than other coastlines. While this has resulted in the fluvial-dominated birdsfoot delta seen today, the delta coastline is not immune to the effects of coastal processes. These processes can result in a winnowing, sorting, and/or reworking of soil particles.

Deposits formed within marine environments comprise a relatively limited proportion of the areal extent of the delta; yet are important components in the overall structure of the delta. Some deposits commonly associated with marine environments include bay-sound, nearshore gulf, and beaches/barrier islands.

Bay-sound/Nearshore Gulf. Bay-sound and nearshore gulf (BS/NG) deposits can comprise any deltaic or marsh deposit that is reworked by wave action to sort the materials by particle size. These materials result from open bodies of water with sufficient fetch and depth to allow the formation of waves large enough to scour the bottom, transporting and reworking fines inland while allowing coarser silts and sands to settle. Bay-sound deposits display many of the same sedimentary characteristics as nearshore gulf deposits, but are typically finer grained and more finely interbedded, intermediate in that regard between nearshore gulf and lacustrine deposits (Saucier, 1963). Strata of bay-sound/nearshore gulf deposits typically dip gently and increase in thickness gulfward. These deposits range in thickness from 1 to 5 meters and can be generally characterized as gray silty sand to sandy silt with some fine sand and frequent to many shell fragments. Nearshore gulf deposits typically comprise poorly graded, fine-grained sands with significant shell fragments.

Barrier Islands/Beaches. Longshore transport is a significant process along the Gulf Coast to the east in Mississippi, Alabama, and Florida as well as to the west in Texas. Coarse deposits of sand are deposited at the mouth of an active, progradational delta distributary channel. Upon abandonment of the distributary channel, subsidence, erosion, and a general lack of sediment supply result in a retrogradational delta. The coarser sand deposits at the mouths of these

channels, although typically less susceptible to subsidence, become stranded from the marsh by open bays eventually to be reworked by wave action and longshore transport into long, barrier arcs (Fig. 6). These barrier islands typically have fairly steep foreshores with backslopes grading into protected marshes ringing the backbays. Wave action commonly transports these barrier island sediments toward the shore while tidal channels form as a function of volume of the backbay.

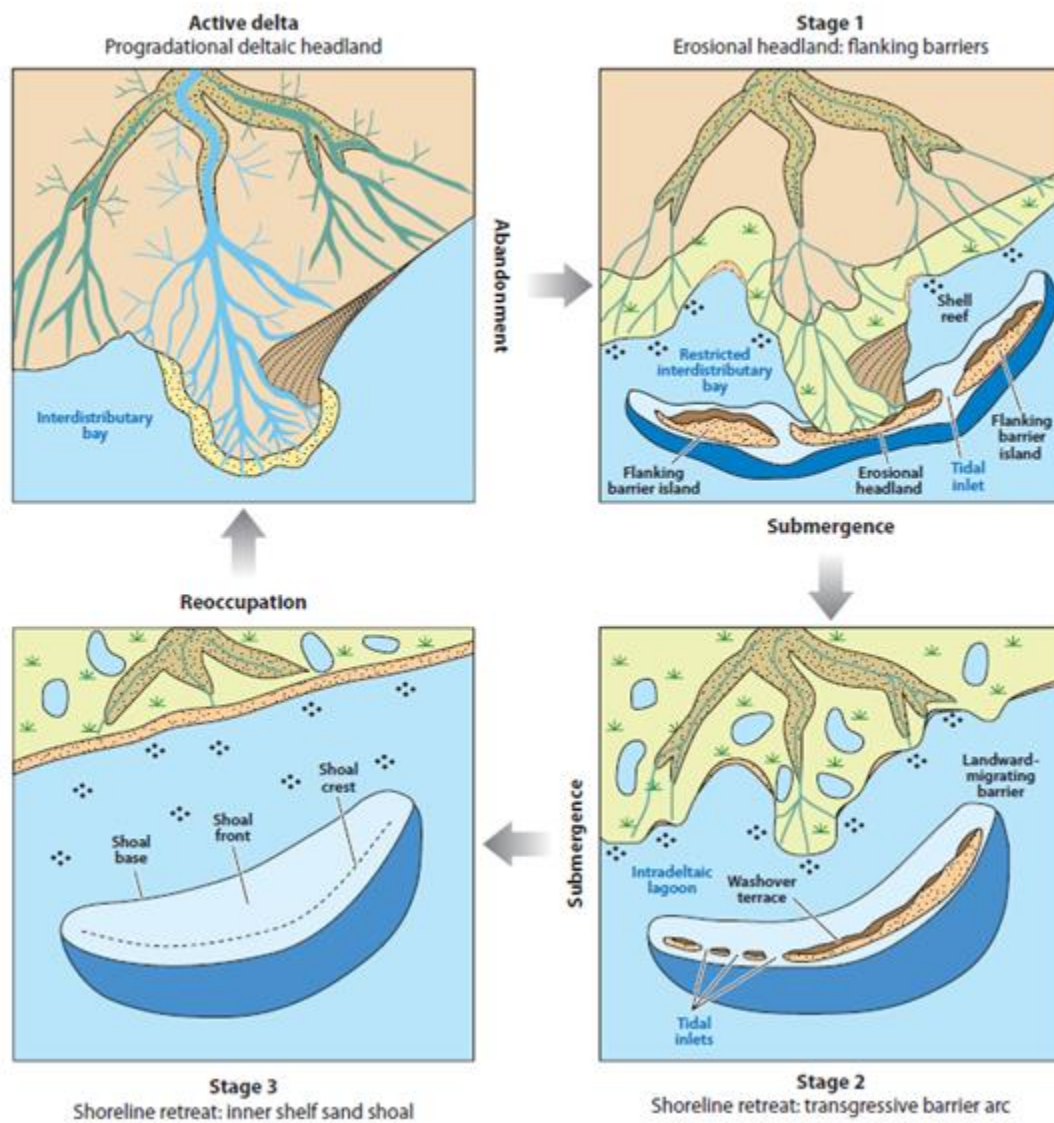


Figure 6: Barrier Island Formation (Penland et al., 1988)

Although critical as protection for a healthy delta environment, barrier islands typically comprise a relatively minor areal extent of Holocene deposits

The Pine Island Beach trend stretches from near the modern Pearl River outlet through Metairie, Louisiana. Consisting of sand deposits carried by longshore transport from the Pearl River westward approximately 5-6 kya at the beginning of the modern delta formation, these relict beaches (RB) form a relatively sturdy foundation across much of New Orleans and can occasionally be found only a few meters from the surface. The approximately extent of relict beaches in the New Orleans area as delineated by Saucier (1963) is shown in **Figure 7**.

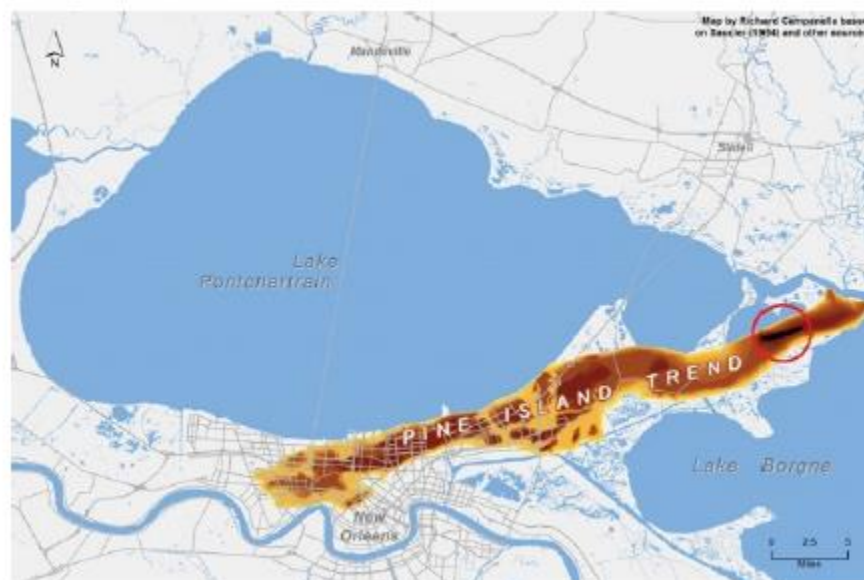


Figure 7: Pine Island Barrier Trend (from New Orleans Geological Society)

1.3.8 Geology Summary

The landforms and geology of New Orleans alluvial soils are the result of a complex interplay between sediment supply, depositional patterns, and relative sea level rise. Horizons of different deltaic lobes with a wide range of depositional environments create a complicated

subsurface stratigraphy challenging for geotechnical design. Within the New Orleans metro area, relatively coarse deposits of point bar and natural levee sands and silts along the Mississippi River provided areas of higher elevation that were most suitable for development. To the north, abandoned distributaries formed the Gentilly and Metairie Ridges that can be observed today in street layouts. Between these high points, the presence of backswamp organics and large amounts of interdistributary clays has led to subsidence within the city as a result of the compaction of these sediments.

Chapter 2: Theory and Literature Review

2.1 Overview

From ancient times, the insulating effects of soil have been used to moderate the temperature of a variety of structures. The Pueblo people of the American Southwest utilized thick clay walls, often carved directly from canyon walls, to moderate the diurnal temperature variations seen in the desert. In ancient Iran, a clever combination of airflow introduced by windcatchers and underground water channels, referred to as qanats, provided up to 15°C in passive cooling (Bahadori, 1978); baori, commonly referred to as stepwells, have served as both water source and cooled gathering spot for centuries in India. All three of these architectural features take advantage of the large difference in the way that soil and air absorb heat. By introducing a mechanism for heat exchange between the air and the subsurface, diurnal, and annual temperature variations can be modulated passively.

2.2 Vapor Compression Cycle

Traditional HVAC systems consist of a heating and cooling unit and the duct system to distribute/remove heat from the building. The refrigeration cycle is the basic premise for modern HVAC systems and takes advantage of the fact that energy in the form of heat in a fluid or gas can be manipulated through two mechanisms: temperature or pressure. As governed by the second law of thermodynamics, heat cannot flow from colder to hotter environments without work. This work can be seen when an air conditioner moves heat from the room temperature

interior to the warmer exterior or in the reverse when heat is taken from the relatively cooler outside to warm the interior. In either case, this work (along with other aspects) is performed by HVAC systems during the refrigeration cycle. At their core, these systems essentially consist of four primary components as shown in **Figure 8**.

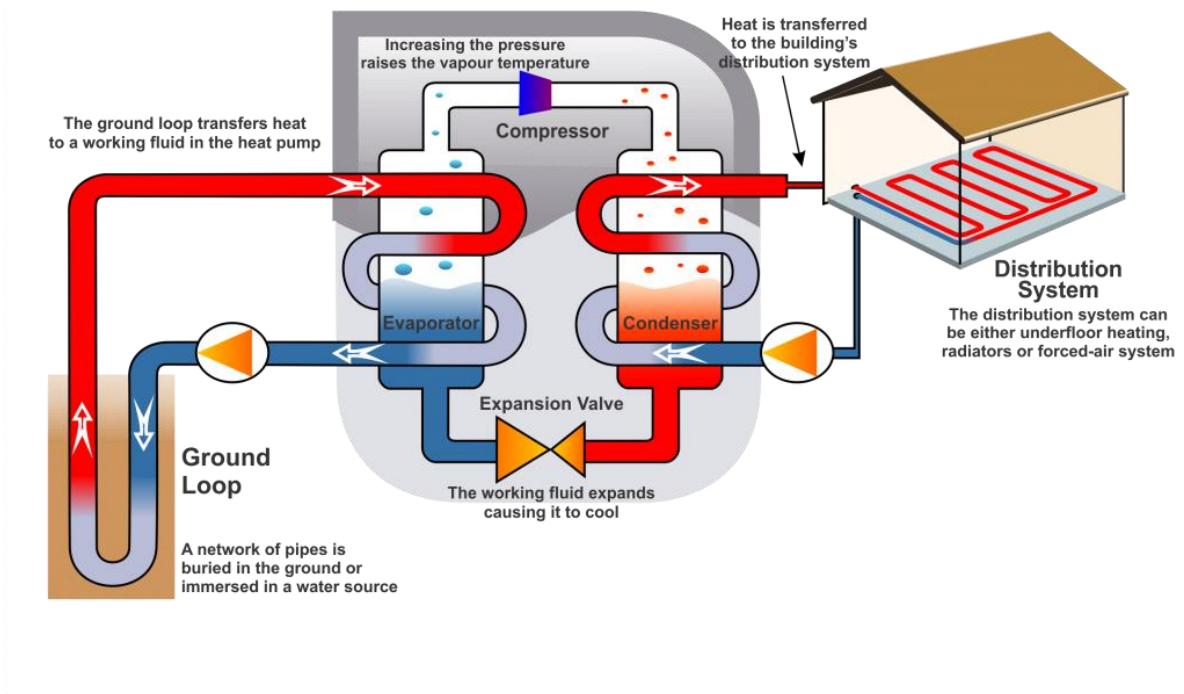


Figure 8: Vapor Compression Cycle in GHP (from Tidewater Mechanical, LLC)

Working fluid, referred to as the refrigerant, is circulated through the four phases of the cycle:

- 1) The work in the system is input through the use of an electrical compressor. The refrigerant enters the compressor as a low pressure and low temperature vapor. As the name would indicate, the compressor increases the pressure of

this vapor and resulting in an associated increase in temperature at constant volume;

- 2) The superheated high-pressure vapor enters the condenser, a heat exchanger in which air is passed over a long series of coils by a fan. As the superheated vapor passes through these coils, heat is rejected into the relatively cooler ambient air, allowing the refrigerant to return to liquid form;
- 3) The refrigerant, now a heated, high pressure liquid, enters the expansion device. This device rapidly reduces the pressure of the liquid causing some evaporation of the refrigerant;
- 4) Finally, the cooled vapor mix of refrigerant passes through the second heat exchanger, the evaporator. As with the condenser, the refrigerant is circulated through a series of coils over which air is circulated by a fan. As the air passes over the coils, heat is rejected into the relatively cooler refrigerant causing it to fully evaporate into a gas. This gas is then returned to the compressor, completing the cycle.

In the cooling mode, the evaporator is located within the interior space being cooled and rejects heat into the ambient air. This system is commonly referred to as an “air source heat pump” or ASHP. In a heating mode, the flow is reversed, and a heat exchanger located outside serves as the evaporator serving to heat the interior.

The efficiency of these systems is measured by the coefficient of performance (COP). This is calculated as the ratio of the heat exchanged and the work input to cause the heat exchange.

The energy efficiency ratio (EER) is an equivalent term used in the United States for cooling systems specifically. The EER is the ratio of output cooling energy to electrical input energy. This efficiency is limited by the laws of thermodynamics to be proportional to the thermal gradient between interior and exterior temperatures.

2.3 Underground Thermal Energy Storage

Underground thermal energy storage (UTES) is the process of circulating heat through a heat retaining medium beneath the ground surface using a GHP. Subsurface materials, generally naturally occurring ground water, sediments, or crystalline bedrock, have specific heat capacities generally 2 to 5 times greater than that of air (Hamdhan, 2010), which allows the storage of heat over time. By storing seasonal heat underground, designers are able to further improve the efficiency of HVAC systems by increasing the positive thermal gradient between the climate-controlled building and the heat source/sink.

A GHP in the modern sense was first developed by Robert C. Webber in 1940 (David B. L., 2008). A modern GHP system comprises three general components: the primary circuit, secondary circuit, and a heat pump (Narsilio, et al., 2014). The primary, or ground, circuit comprises a ground heat exchanger (GHE) system that circulates HCF through the subsurface to reject/extract heat. The secondary, or building, circuit includes the traditional ductwork or piping system required to circulate heat through a climate-controlled space. The heat pump is the connection between the two circuits and provides the energy required to move heat between them.

The utilization of a GHP provides a more beneficial thermal gradient between the climate-controlled space and the heat source/sink by taking advantage of the fact that below a certain depth, ground temperatures remain constant near the average annual air temperature. This depth is commonly referred to as the thermally independent depth (TID).

Depending on the climate and resulting ratio of heating and cooling loads, the building temperature can potentially be maintained purely through heat exchange with the subsurface. This period is referred to as “free cooling” and may vary between 1,000 hours per year along the Gulf Coast to over 8,000 hours per year in the upper Great Plains (DOE, 2008).

2.4 Ground Heat Exchangers

There are a variety of methods of exchanging heat between the above heating/cooling system and the subgrade. Broadly speaking, these can be divided into open-loop systems, closed-loop systems, and energy foundations (energy piles). As can be surmised, these categories are differentiated by the way the heat carrying fluid (HCF) interacts with the substrate.

2.4.1 Open-Loop Systems.

Open-loop systems are the simplest and most efficient UTES method developed. Most commonly achieved by aquifer thermal energy storage (ATES), open-loop systems extract and inject water with the ambient environment for use as the HCF. Alternative open-loop systems include cavern thermal energy storage (CTES), which is obviously limited to specific geologic setting, and open water systems where the water source would be a lake or river. In an open-loop system, water is extracted directly from the environment, circulated through the GHP for

heat exchange, and then injected back into the ground through a different well. Direction of the system flow is governed by seasonal temperatures. ASHRAE commonly refers to all open-loop systems as ground-water heat pumps (GWHPs). An example of an ATEs system is shown in **Figure 9**.

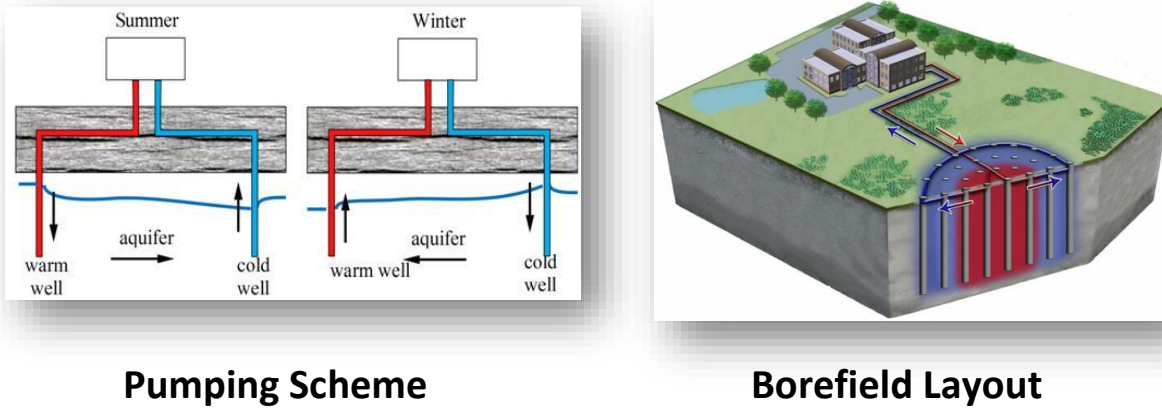


Figure 9: Open-Loop System (from Underground Energy, LLC)

The main advantage of open-loop systems are the high heat capacity and ready availability of groundwater. While this results in high system efficiency, the design is limited by site specific conditions. There must be an aquifer with sufficient permeability to permit groundwater flow. Additionally, care must be taken in separating the extraction and injection wells to prevent thermal short circuiting. Finally, soil and groundwater chemistry often present issues with HVAC systems. Minerals such as iron and calcium carbonate accumulate within the system, causing maintenance issues and reducing efficiency. Heat storage can also be an issue as regional groundwater flow can be difficult to model and result in a loss of stored heat.

2.4.2 Closed-Loop Systems

A closed-loop system consists of high-density polyethylene (HDPE) loops installed in the subsurface that circulate the HCF between the subsurface and the heating/cooling system. These loops may be placed either horizontally in shallow trenches (slinky configuration) or vertically in using borehole heat exchangers (BHX). Borehole systems may also be referred to as borehole thermal energy storage (BTES) systems. Horizontally placed loops are generally above the TID and as such the efficiency of these systems is relatively lower with respect to other GHE. However, installation costs for these systems are much less than for a vertical loop system. Vertical boreholes are generally 5 to 15 cm (2 to 6 in) in diameter with lengths ranging from 20 to 300 m (60 to 1000 ft) deep (Lee, 2013). The HDPE loops can be arranged in a variety of ways within the borehole; however, the most common is a double pipe loop forming a U shape.

The HCF, typically a water/antifreeze mixture, is passed through the loops and exchanges heat with the surrounding soil. These systems are governed by the thermal conductivity of the soils and are therefore less efficient than an open-loop system. However, because the soil is the primary heat medium, closed-loops systems are possible in a wide variety of site conditions and face less maintenance issues arising from soil/groundwater chemistry. Closed-loop systems are commonly referred to as ground-coupled heat pumps (GCHPs) by ASHRAE. An example of a slinky and borehole GHE is shown below in **Figure 10**.

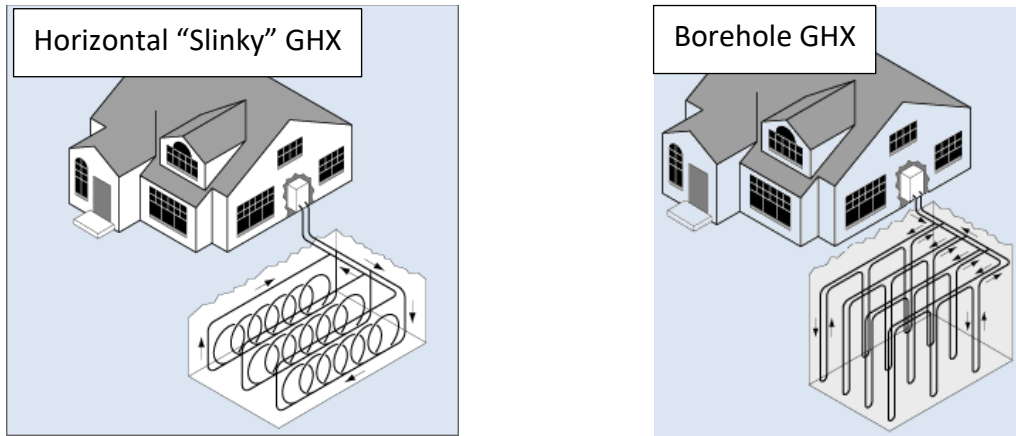


Figure 10: Closed Loop Systems (from SintonAir, LLC)

2.4.3 Geothermal Energy Piles

Both closed- and open-loop systems are characterized by very deep lengths (often 150 to 300 m; 500 to 1000 ft) and high installation costs. These wells and boreholes are drilled expressly for heat exchange; thus, the high installation costs often dissuade their use in construction. One method of heat exchange for GHPs that is gaining popularity is the inclusion of heat exchange loops within foundation elements. These have been included in basement/tunnel walls or footings; however, the focus of this study is the use of heat exchange loops within deep foundation elements, often referred to as energy piles or pile heat exchangers (PHX).

This practice began gaining acceptance in the 1980s and has been the focus of much research (Laloui et al., 2003; 2006; 2011). The primary advantage is the dual use of energy piles as both heat exchangers and structural support. Within the New Orleans area, the most commonly used pile types include timber; square, precast concrete (SPC); open-end steel pipe (OSP); and augered, cast-in-place (ACIP) piles. The inclusion of loops for circulation of a HCF

through timber piles would be difficult; therefore, they offer limited opportunity for use as GHX elements. Although a circulation system could be included with OSP piles, protection of the system during driving would likely be cost prohibitive. Additionally, these piles are most commonly used in industrial and marine applications, which commonly lack large space heating/cooling loads. Although additional research for industrial applications of this technology could be beneficial, these piles are not the focus of this study.

SPC piles are precast offsite, transported to the site, and driven into the ground using a pile-driving hammer. ACIP piles consist of a continuous flight auger that drills to a predetermined depth, then pumps grout into the ground during retraction of the auger. Structural steel is then placed within the uncured grout. In either case, HDPE loops can easily be incorporated into either of these pile types during construction, often tied to the structural steel for support. An example of structural steel cage with HDPE loops fitted is shown in **Figure 11**.



Figure 11: GHX loops fitted to pile reinforcement cages (from Narsilio, et al., 2014)

As with other closed-loops systems, HCF is circulated through the loops to extract/inject heat into the subsurface, depending on the climate and season. The constant temperature of the soils provides an excellent moderating influence on the fluid, while design of the system can

allow heat to build during the cooling season in the summer that can later be extracted during the winter. Heat will generally be injected into the center of the building footprint and extracted from the edges to prevent heat loss into the surrounding soils (Brandl, 2006). However, in a cooling dominated climate, such as the Gulf Coast, the imbalance between heating and cooling demands often results in a long-term temperature rise within the subsoils (Akrouch, 2014). The efficiency of the system is largely governed by length of the GHE loops and the thermal properties of the subsoils (Brandl, 2006).

2.5 Governing Thermodynamics

According to the second law of thermodynamics, heat will flow from high to low entropy systems, i.e., from hot to cold environments. This heat transfer, defined as the heat flux q , occurs through three processes: conduction (heat transfer between particles), convection (heat transfer through a moving fluid, i.e. groundwater flow), and radiation (Akrouch, 2014). Latent heat transfer may occur as the result of a phase change in free ground water such as evaporation/condensation or freeze/thaw cycles (Brandl, 2006). Research has indicated that radiation heat transfer is negligible in soils and can be less than 1% of the overall heat transfer within sands (Rees et. Al, 2000). Convection can be significant when groundwater flow is occurring; however, most research to date focuses primarily on heat transfer through conduction (Akrouch, 2014).

Conduction is a process of heat transfer whereby molecules at a high temperature collide and excite neighboring particles, thus raising their temperature, and is governed by the well-

known Fourier's Law (Fourier, 1822). According to Fourier's Law, the heat flux to occur over a given thermal gradient due to conduction may be written as seen in Eq. 2.1.

$$q_{cond} = -\lambda \frac{dT}{dx}$$

As a porous material, soil has three constituent parts that influence the thermal properties of the system. These include solids (soil grains), liquid (water), and gas (air). The porosity of the soil (n) describes the ratio of solid particles to void spaces. The ability of the soil particles to transmit and absorb heat depends on a variety of factors, namely saturation, porosity, and mineral composition. Properties that describe a soil's thermal characteristics include thermal conductivity (λ), thermal diffusivity (α), and volumetric heat capacity (C).

Thermal conductivity is a measure of the soil's ability to transmit heat across a length for a given thermal gradient. The volumetric heat capacity is the amount of heat required to raise a unit volume of a material by 1°C. The volumetric heat capacity can be thought of as the thermal equivalent to the elasticity modulus of a material. Thermal diffusivity is the ratio of thermal conductivity to the specific heat capacity. Thermal conductivity can be thought of as the rate that thermal energy is transmitted across a material, the volumetric heat capacity is the material's ability to absorb that thermal energy, and thermal diffusivity, as a ratio of the two, is the rate a material absorbs thermal energy. While the thermal properties of a material are temperature dependent, the typical range of temperatures in applications for GHP are typically such that these effects may be neglected (Brandl, 2006) except in the case of potential phase changes, i.e., freezing.

In unsaturated soils above the hydrostatic groundwater table, these pores are filled with a combination of water and air, depending on the saturation (S) of the soil. In a fully saturated soil, the pores are filled with water. In unsaturated soils, heat transfer occurs primarily through conduction between soil particle interactions as the thermal conductivity of air is negligible, and it essentially acts as a thermal insulator (Akrouch 2014). As the saturation of the soil increases, the thermal conductivity of the system increases given the high thermal conductivity of water. This relationship is shown below in **Figure 12**.

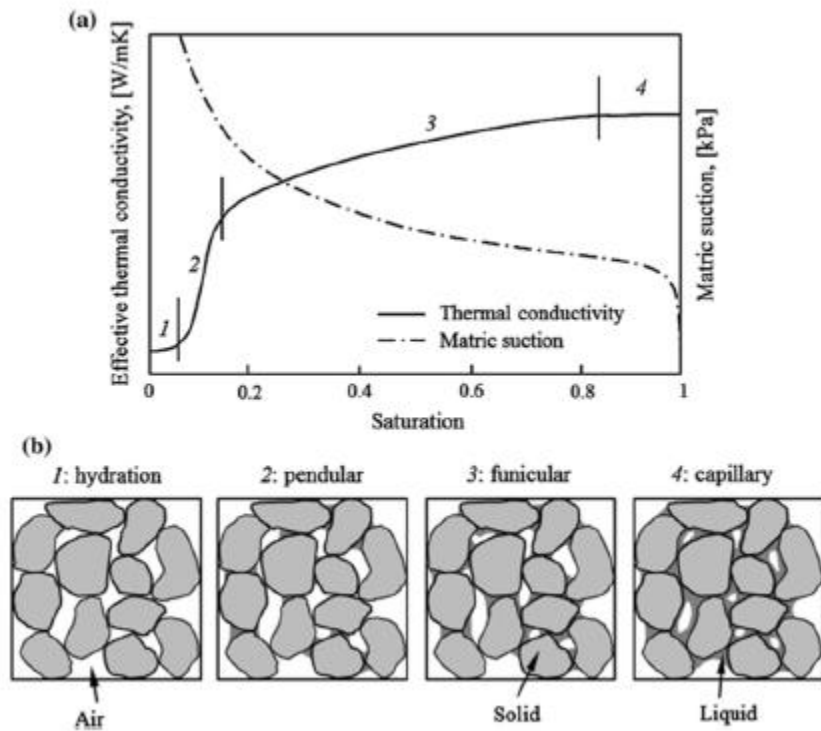


Figure 12: Relationship between thermal conductivity and saturation (from Brandl, 206)

This is taken to an extreme in an aquifer or open water system, where the water becomes the primary heat sink, and the soil particle interaction becomes negligible. When an aquifer is

unavailable or unsuitable for use as a heat sink, the soil particles' ability to absorb and transmit heat becomes more important. Heat transfer that occurs by fluid convection can be written as:

$$q_{conv} = c_w \rho_w v_w (T - T')$$

Where c_w is the specific heat capacity of the groundwater, ρ_w is the density of the groundwater, and v_w is the relative velocity of groundwater flow. T' in this case is a reference temperature (Brandl, 2006). Neglecting the negligible contribution of radiation heat transfer and the unlikely presence of latent heat transfer, the total heat flux for the subject problem can be given as:

$$q_{tot} = q_{conv} + q_{cond}$$

The process for heat transfer from the HCF to the soil through an energy pile is shown below in **Figure 13**. Convection occurs as the fluid passes along the HDPE pipe, exchanging heat with the pipe material. This heat then transfers through the HDPE pipe (Point A to point B in the figure) through conduction with some amount of heat being absorbed by the pipe. This heat continues through the pile section (point B to point C) again by conduction. As the heat enters the soil, some combination of conduction through the soil and groundwater particles as well as convection from groundwater flow (if present) propagates and absorbs the heat radially.

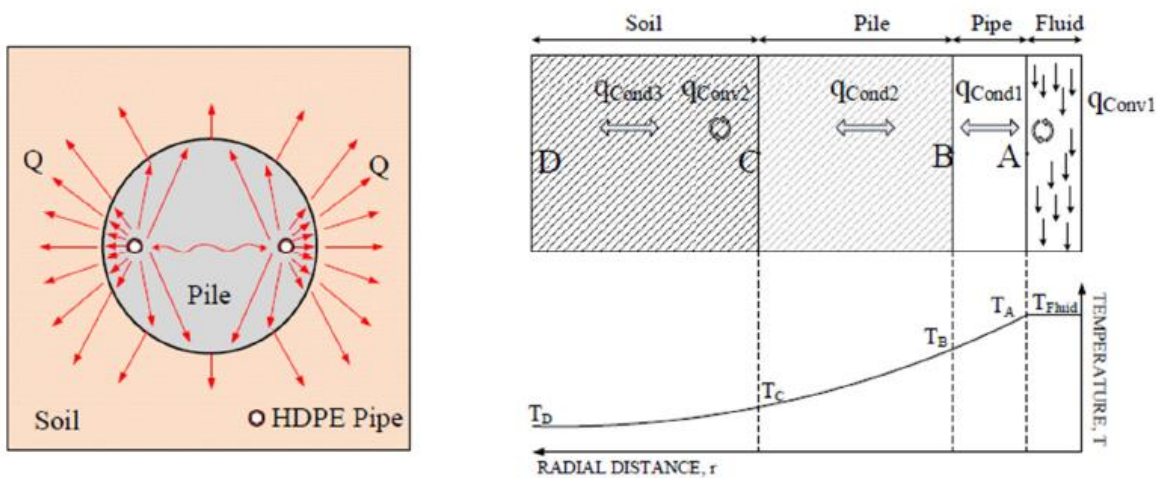


Figure 13: Transfer of heat in an energy pile (from Akrouch, 2014)

2.6 Thermal Conductivity

As can be seen, the rate of heat transfer for energy piles in the absence of groundwater flow is largely governed by the thermal conductivity, λ (often previously given as k). For a given type of soil, the magnitude of λ depends on the porosity of the soil, n ; volumetric water content, θ ; bulk density of the soil ρ_b ; and mineral composition (de Vries, 1963; Campbell, 1985). Some typical values of λ for common materials are provided in **Table 1** below.

Table 1: Typical values for thermal conductivity (Adapted from Côté & Conrad, 2005; IEEE Std 442-2017)

Material	λ (W/m.k)
Quartz grains	5.0 to 9.0
Granite grains	2.5 to 3.9
Limestone grains	2.2 to 2.5
Sandstone grains	1.7 to 3.0
Silt and clay	1.0 to 2.9
Organics	0.15 to 0.65
Liquid Water	0.58 to 0.61
Ice	2.2 to 2.4
Air	0.025

Please note, the estimated values presented in Table 1 are general estimates of observed values for thermal conductivity. Soil is a heterogenous material, thus the thermal conductivity is a function of the constituent parts of the soil. These constituent parts impact the observed or “effective” thermal conductivity, λ_e through:

- **Mineral Content:** Sediments at their core are comprised of weathered particles of various forms or types of minerals. As can be seen in the table above, the range in typical values of λ for different minerals can range widely. The source material for a given sediment will strongly influence the way heat is transferred.
- **Porosity:** The thermal conductivity of minerals is greater than that of water or air, the other two primary constituents of soil. Therefore, an increase in porosity decreases the effective thermal conductivity of a soil by causing an increase in the volumetric fraction of air and water.
- **Density:** Porosity is largely a function of the density of the soil. Thus, soils compacted to a higher density (naturally or through compactive effort) will have greater particle to particle contact and exhibit a higher effective thermal conductivity.
- **Water Content:** Similarly, the thermal conductivity of water is much higher than that of air. As such, an increase in the moisture content of a soil up to the point of saturation, i.e. all voids are filled with water, will increase the effective thermal conductivity of a soil by providing a fluid contact between particles and potentially allowing for convection to occur.

- **Temperature:** Thermal conductivity of ice is approximately four times greater than that of water; therefore, significant changes to effective thermal conductivity of a soil occur below the freezing point. Substantial data regarding the effects of freezing on the effective thermal conductivity are available in the literature (Kersten, 1949; Penner et al., 1975; Farouki, 1982; Hansson et al., 2004; Côté and Konrad, 2005); however, the Gulf Coast region is not in a climatic zone where soils are susceptible to freezing. As the frost depth be highly likely to exceed more than 0.5m, freezing of soils has been neglected for this study and all values of thermal conductivity discussed refer to the unfrozen state.

Thus, to speak of “the” thermal conductivity of a soil, without specifying water content, density, temperature, and composition, is meaningless. In most applications, the density and composition of the in-situ soils will be relatively fixed, and the temperature range can be considered small enough to be neglected (assuming no freezing occurs). Therefore, the primary driver for variability in thermal conductivity for a given material is the moisture content (Campbell, 1985).

The relationship between water content and soil thermal conductivity for a given soil at a specified density is sometimes referred to as the thermal dryout curve. The boundary conditions for a thermal dryout curve are the lower limit condition of thermal conductivity for a completely dry sample ($\theta = 0$; $S = 0$), termed as λ_{dry} . The upper limit for a given soil at a specified density would be the thermal conductivity for a fully saturated sample ($\theta = \theta_{sat}$; $S = 1$), termed as λ_{sat} . An example of this relationship is shown in **Figure 14** below.

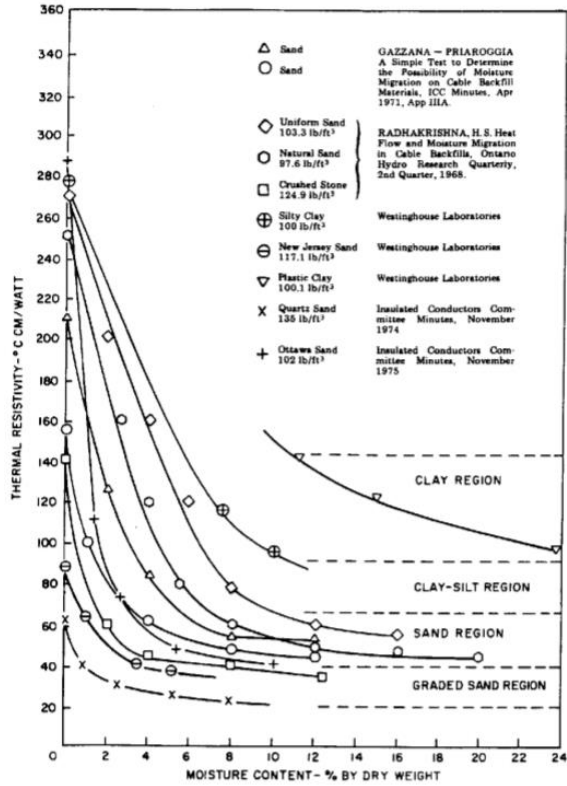


Figure 14: Thermal dryout curves (from IEEE 442-2017)

In practical application, it may be desirable to reference the effective thermal conductivity, that is, the thermal conductivity for a given soil composition at a specified density and moisture content, as "the" thermal conductivity. While it is important to remember that this value is variable as a function of the moisture content, density, and temperature of the soils as described previously, λ_e is essentially the in situ value for thermal conductivity as would be observed through laboratory testing of undisturbed samples or in situ testing. Therefore, λ_e will be treated as roughly analogous to λ within this work.

2.7 Theoretical and Empirical Models for Thermal Conductivity

Many empirical models (Kersten, 1949; Gemant, 1952; Van Rooyen and Winterkon, 1957; De Vries, 1963; Johansen, 1975; Hillel, 1982; Ingersoll, 1988; Campbell, 1985; Côté and Konrad, 2005; Lu and Horton, 2007; Lu et. al 2014; Nikoosokhan et. al 2015) have been introduced to the literature to predict the effective thermal conductivity for soils as logarithmic functions of water content and dry density. Farouki (1982) provided a fairly exhaustive review of the models available at the time, suggesting that Johansen (1975) gave the best overall prediction for sands and fine-grained soils. Further modifications to the Johansen (1975) model were provided by Côté and Konrad (2005); Lu and Horton (2007; 2014); and Nikoosokhan et. al (2015) to better reflect the influence of particle diameter and texture on effective thermal conductivity.

2.7.1 Early Methods Proposed by Kersten (1949)

Kersten (1949) provided the basis for much of the early research on the thermal properties of soils during extensive testing on soil samples provided by the U.S. Army Corps of Engineers (USACE) – St. Paul Division. From the results of this testing, Kersten (1949) proposed a basic correlation for thermal conductivity of clays and sands using gravimetric moisture content (ω) and unit weight as inputs. These correlations for λ are provided below. Please note these correlations have been modified to provide λ in SI units; however, the dry unit weight of the soil γ_d should be in units of pounds per cubic foot.

$$\lambda_{clay} = 0.1442 * [0.9 \log(\omega) - 0.2] * 10^{0.01\gamma_d (pcf)}$$

$$\lambda_{sand} = 0.1442 * [0.7 \log(\omega) + 0.4] * 10^{0.01\gamma_d (pcf)}$$

2.7.2 Complex Model by de Vries (1963)

De Vries (1963) proposed a more complex model to estimate the soil thermal conductivity as a weighted average of the three phases of soil: gas, liquid, and solid.

$$\lambda = \frac{k_g f_g \lambda_g + k_w f_w \lambda_w + \sum_{i=1}^n k_i f_i \lambda_i}{k_g f_g + k_w f_w + \sum_{i=1}^n k_i f_i}$$

where k is a weight factor and f is the volumetric fraction of each constituent. The subscripts g , w , and i indicate the gas, liquid, and solid phases, respectively. As the solids are more than likely a composite containing sand, silty, clay, and organic matter, the individual volumetric fractions and thermal conductivities for “ n ” number of constituents is summed. De Vries (1963) reported typical thermal conductivities for sand, silt, clay, and air as 8.53, 2.93, 2.93, and 0.025 W/m.K, respectively. Campbell (1994) provides a review of the methods to calculate each of the weight factors as well as proposed modifications to account for latent heat components within the “fluid” gas and liquid phases.

2.7.3 Normalization of λ by Johansen (1975)

As a means of better defining the effective thermal conductivity within the framework of a thermal dryout curve, Johansen (1975) proposed the normalization of the thermal conductivity for a soil with respect to the saturation level of the tested sample in relation to the λ_{dry} and λ_{sat} values for that material. The normalized thermal conductivity, λ_n , can be defined as:

$$\lambda_n = f(S) = \frac{\lambda - \lambda_{dry}}{\lambda_{sat} - \lambda_{dry}}; \text{ where } 0 < \lambda_n < 1$$

Rearranging this equation to solve for λ provides:

$$\lambda = \lambda_n * (\lambda_{sat} - \lambda_{dry}) + \lambda_{dry}$$

Johansen (1975) proposed the following as empirical predictions for λ_n as a function of the saturation, S for various soil textures:

Unfrozen medium and fine sands: $\lambda_n = 0.7 \log(S) + 1$

Unfrozen fine-grained soils: $\lambda_n = \log(S) + 1$

Unfrozen peat: $\lambda_n = 0.029(36^S - 1)$

Obviously, values for λ_{sat} and λ_{dry} must be obtained to allow for the normalization of thermal conductivity; however, most data available in the literature focuses on λ_e as additional sample preparation is necessary for λ_{sat} and λ_{dry} . Many theoretical models exist to estimate λ_{sat} ; however, in cases where the thermal conductivities of constituent materials of a sample do not vary by more than an order of magnitude, a simple geometric mean may be used (Sass et al. 1971). Thus, the unfrozen, saturated thermal conductivity of a soil may be estimated as proposed by Johansen (1975):

$$\lambda_{sat} = \lambda_s^{1-n} \lambda_w^n$$

Where λ_s and λ_w are the thermal conductivities of the constituent solid particles and ground water, respectively, and n is the porosity of the soil. Thermal conductivity of water is typically taken to be approximately 0.6 W/m.k. To distinguish from λ_{dry} , λ_s is defined as the thermal conductivity of the soil solid material only and is theoretically independent of porosity. As described by Chen (2020), λ_s is theoretically an intrinsic material property related to the mineral content only. While the thermal conductivity of a pure material such as water, paraffin, or even pure minerals may readily be determined through laboratory testing, the compositions and geometry of soil solid particles are complex and variable to the point that there is no effective

method for measuring λ_s without some influence of gaps between particles (Chen, 2020). The most effective measurements of λ_s are suggested by Chen (2020) to be made by an inversion of the Johansen (1975) model for estimating λ presented herein, suggesting that further research to calibrate appropriate local values for λ_s is necessary. As a practical solution, Côté and Konrad (2005) presented typical values of λ_s for silt/clay and peat (the most common soil constituents in the New Orleans area) to be 2.90 and 0.25 W/m.K, respectively. Additional values for selected rock-forming minerals are given in Horai, 1971.

Sass et. al (1971) used a simple geometric mean for calculating λ_s when the complete mineral composition was known. Johansen (1975) proposed a simplified solution by assuming the soil solid phase is divided into two components: quartz, with an average thermal conductivity of 7.7 W/m.K, and other minerals, with an assigned average value of 2 W/m.K. Based on these assumptions, λ_s can be estimated using f_q , the volume fraction of quartz in the solid particles, by:

$$\lambda_s = \begin{cases} (2.0^{1-f_q})(7.7^{f_q}); & f_q > 0.2 \\ (3.0^{1-f_q})(7.7^{f_q}); & f_q \leq 0.2 \end{cases}$$

In contrast to λ_s , estimates of λ_{dry} are relatively simple to obtain from laboratory testing with some additional sample preparation. Lacking fluid providing particle to particle connections, λ_{dry} is largely a function of the porosity and correspondingly the bulk density of the soil. Johansen (1975) proposed a semi-empirical equation utilizing only bulk density to estimate λ_{dry} .

$$\lambda_{dry} = \frac{0.135\rho_b + 64.7}{2700 - 0.947\rho_b}$$

2.7.4 Introduction of Soil Texture Factors by Côté and Konrad (2005)

Utilizing the large data set obtained by Kersten (1949), Côté and Konrad (2005) proposed a refined model for estimating λ utilizing a normalized function. Based on Johansen's (1975) work, Côté and Konrad (2005) introduced a dimensionless soil texture factor, κ , to account for the range in mathematical expressions used to estimate the normalized thermal conductivity for different soil types. Additionally, Côté and Konrad (2005) proposed new relationships for λ_{dry} as a function of porosity instead of bulk density as suggested by Johansen (1975). These expressions are written as:

$$\lambda_n = \frac{\kappa S}{1 + (\kappa - 1)S}$$

$$\lambda_{dry} = \chi 10^{-\eta n}$$

where χ and η are dimensionless texture parameters. Values for κ , χ , and η as recommended by Côté and Konrad (2005) are provided in **Table 2**.

Table 2: Values of texture parameters (from Cote and Konrad, 2005)

Soil Type	κ	
	Unfrozen	Frozen
Gravels and coarse sands	4.60	1.70
Medium and fine sands	3.55	0.95
Silty and clayey soils	1.90	0.85
Organic fibrous soils (peat)	0.60	0.25

Soil Type	χ	η
Crushed rocks and gravel	1.70	1.80
Natural mineral soils	0.75	1.20
Organic fibrous soils (peat)	0.30	0.87

Building on the work of Côté and Konrad (2005), Nikoosokhan et. al (2015) utilized the normalized thermal conductivity with a soil texture factor to estimate λ_e . Nikoosokhan et. al (2015) utilized the volume fraction of sand, f_a , to estimate κ by:

$$\kappa = 4.4f_a + 0.4$$

Nikoosokhan et. al (2015) also proposed λ_{dry} be estimated as a function of both particle texture and dry unit weight of the soil, as shown below.

$$\lambda_{dry} = 0.087f_a + 0.019\gamma_d$$

2.7.5 Alternative Normalized Conductivity by Lu and Horton (2007) and Lu et. al (2014)

Based on a different database of tested values, Lu and Horton (2007) developed an alternative expression for λ claimed to be more accurate for soil thermal conductivity predictions than either Johansen (1975) or Côté and Konrad (2005). This method was further refined by Lu et. al (2014) to produce:

$$\lambda = \lambda_{dry} + e^{\beta - \theta^{-\alpha}}$$

where α and β are dimensionless shape factors utilizing the volumetric fractions of clay and sand, f_{cl} and f_a , respectively, with the bulk density as given by Lu et. al (2014):

$$\alpha = 0.67f_{cl} + 0.24$$

$$\beta = 1.97f_a + 1.87\rho_b - 1.36f_a\rho_b - 0.95$$

Lu and Horton (2007) recommended typical values for α of 0.86 and 0.27 for coarse and fine-grained soils, respectively, based on curve fitting of their prediction model to the tested data.

Lu and Horton (2007) also proposed λ_{dry} be estimated as a function of porosity by:

$$\lambda_{dry} = -0.56n + 0.51$$

2.7.6 Other Relevant Work

Campbell et al. (1994) published a predictive model for thermal conductivity as a function of bulk density, temperature, and water content based on the de Vries (1963) equation. Campbell et al. (1994) surmised that thermal conductivity increased dramatically with temperature, reaching values 3 to 5 times the ambient value at 90°C. Although these tested values may have been strongly influenced by free convection occurring in the heated samples, it is important to remember that the other models presented herein assume a relatively stable ambient temperature. The effects of GHP on long-term subsurface temperatures is not well defined; thus, the conductivities (and by extension efficiency) of the systems may be variable over time. Additional research is needed to better quantify these potential effects.

2.7.7 Summary of Theoretical and Empirical Models

As can be seen, some assumptions are necessary, particularly regarding λ_s ; however, reasonable estimates of λ may be made given good understanding of the bulk density, porosity, and water content of the soils. These estimates are likely sufficient for desktop studies and preliminary design but should be confirmed through in situ testing to properly understand the governing thermal properties of the subsoils.

2.8 Laboratory Testing of Thermal Conductivity

Procedures for laboratory testing of the thermal conductivity of various materials are fairly well developed as described by Lutenegger & Lally (2001) with the first use of a cylindrical probe method proposed by Schleiermacher (1888) and further developed by Stalhane and Pyk

(1931). These methods were utilized to measure thermal conductivity of liquids by Weishaupt (1940); van der Held (1949); and van Drunen (1949). Kersten (1949) performed substantial laboratory testing on a variety of soil samples and in conjunction with additional testing by Hooper and Lepper (1950) and Skieb (1950) provided the data set for many early empirical predictive models. Since then, many studies including laboratory testing of thermal conductivity of soils have been performed including Penner (1963), Weschler (1966), Falvey (1968), Winterkorn (1970), Mitchell and Kao (1978), Brandon and Mitchell (1989) Ewen and Thomas (1992), Lutenegger and Lally (2001), Lu and Horton (2007), Akrouch (2014), Tong et al. (2016), and many others.

The majority of these studies utilized the thermal needle under a transient heat method as now standardized under ASTM D5334-08 “Standard Test Method for Determination of Thermal Conductivity of Soil and Soft Rock by Thermal Needle Probe Procedure.” A similar standard utilized by electrical engineers for design of high voltage underground utilities is provided in IEEE Std 442-2017 “IEEE Guide for Thermal Resistivity Measurements of Soils and Backfill Materials.” In either case, the equipment comprises a small stainless steel needle containing a heating element and thermocouple as described by Mitchell et al. (1978); a constant current source able to monitor voltage; and datalogger able to measure temperature to the nearest 0.1°C.

As derived by Carslaw and Jaeger (1946) and adapted to soils by Van Royen and Winterkorn (1957); Von Herzen and Maxwell (1959) and Winterkorn (1970), a constant heat flux applied to a zero mass heater over a period of time will result in a temperature response by:

$$\Delta T = \begin{cases} -\frac{Q}{4\pi\lambda} Ei\left(\frac{-r^2}{4Dt}\right); & 0 < t < t_1 \\ -\frac{Q}{4\pi\lambda} \left[-Ei\left(\frac{-r^2}{4Dt}\right) + Ei\left(\frac{-r^2}{4D(t-t_1)}\right) \right]; & t > t_1 \end{cases}$$

where:

t = time from the beginning of heating in seconds

ΔT = temperature rise from time zero

Q = heat input per unit length of heater (W/m)

r = distance from the heated needle (m)

D = thermal diffusivity (m²/s)

Ei = exponential integral, and

t₁ = heating time

Although this provides the most precise method for determining the thermal conductivity, no explicit solution for λ and D exists; therefore, a non-linear least-squares inversion technique must be used. Weschler (1966) proposed a simplified solution assuming a line heat source of infinite length dissipating heat in an infinite medium as governed by:

$$\Delta T = \frac{Q}{4\pi\lambda} \ln \frac{t_2}{t_1}$$

where t₂ and t₁ are discrete times during the heating (or cooling) phase. Rearranging to solve for λ gives:

$$\lambda = \frac{Q}{4\pi(T_2 - T_1)} \ln \frac{t_2}{t_1}$$

Because this theory assumes zero mass for the heating element, a calibration factor, C , must be introduced to account for heat absorbed by the mass of the needle. This becomes more important with increased probe diameter as departures from the assumption of an infinitely thin probe cause statistically significant differences in estimation of the thermal conductivity due to non-negligible heat storage and transmission in the needle probe itself (ASTM D5334-08). The calibration factor is determined by performing tests on pure materials having known thermal conductivities. These materials are most commonly dry Ottawa sand or glycerine with a known thermal conductivity of 0.282 W/m.K at 25°C or water stabilized with 5 g agar per liter to prevent free convection with a known thermal conductivity of 0.607 W/m.K at 25°C. The calibration factor is then calculated as:

$$C = \frac{\lambda_{material}}{\lambda_{measured}}$$

Hanson et al. (2004) showed the calibration factor to be a function of thermal conductivity for large diameter needles and proposed the calibration factor be determined at a range of thermal conductivities to construct a calibration curve as a function of λ . Including the calibration factor, the tested value for thermal conductivity is given by:

$$\lambda = \frac{CQ}{4\pi(T_2 - T_1)} \ln \frac{t_2}{t_1}$$

This equation can be further simplified by selecting t_2 and t_1 to be one logarithmic cycle apart (e.g., 10 and 100 seconds) such that the equation is reduced to:

$$\lambda = \frac{2.3Q}{4\pi} \Delta T$$

The heat input, Q , is a function of the power supply and length and material properties of the heating wire located in the probe. Most modern testing units provide this value as an output of the test; however, it can also be calculated by:

$$Q = I^2 \frac{R}{L} = \frac{EI}{L}$$

where:

- I = current flowing through heater (A)
- R = total resistance of the heater (Ω)
- L = length of heated needle (m)
- E = measured voltage during heating (V)

The data points used to estimate thermal conductivity should be located on the linear section of the curve (ASTM D5335-14). Nonlinearity at the beginning of the test typically indicates transient heat influences from the probe are still present possibly as the probe temperature was not at equilibrium with the soil. Nonlinearity at the later portion of the test can indicate either boundary influences as a result of the sample diameter being too small or the duration of heating being too long. Care must be taken to prevent free convection that may occur as a result of redistribution of water due to sufficiently high thermal gradients. Typically, a 1-2°C increase in temperature is sufficient to observe linearity in the test curve while preventing free convection. Higher heat inputs should be avoided if possible.

Other laboratory testing methods besides the thermal probe method include: the Guarded Hot Plate test (ASTM C177), the Cylindrical Configuration test (Kersten, 1949), the Heat

Meter test (Scott, R.F., 1969), the Periodic Temperature Wave (Forbes, 1849), and the Thermal Shock Method (Shannon and Wells, 1947).

2.9 In Situ Testing of Thermal Conductivity

While laboratory testing of thermal conductivity is fairly common and well developed, there is a growing interest in the ability to perform similar testing in situ. Often, issues with sample collection, transport, and storage can cause sample disturbance and alter the material properties. Additionally, laboratory testing is constrained in its ability to properly model the in situ hydrogeological conditions, leaving the effects of convection on heat transfer through heat piles largely unstudied.

2.9.1 Field Testing Using a Needle Probe

Rao and Singh (1999) proposed a thermal probe based on the work of Hooper and Lepper (1950) and Mitchell and Kao (1978) for use in the design of high voltage buried power cables. Essentially a modified laboratory thermal needle, the probe was inserted by hand from the ground surface and a subsequent heat pulse measured. This method has gained popularity in the design of power cables and has been standardized under the IEEE 442-2017. While these probes may be as long as 2 meters, this method is limited to testing surficial or near-surficial materials.

2.9.2 Testing of Thermal Properties at Depth

An in-situ test based on the thermal probe method was proposed by Lutenegger and Lally (2001). The testing was performed using a probe 2.86 cm in diameter and 91.4 cm long with a

60° apex cone tip hydraulically pushed into the ground. The probe comprised three sections: a solid cone tip; a central heating and measuring body; and an upper drill rod adapter, as shown in **Figure 15**. The central portion of the probe was instrumented with three Type T thermocouples with a dual pass 26-gauge nichrome heating wire. The solid tip was designed such that the lowest thermocouple was positioned 30 cm from the probe tip as suggested by Winterkorn (1970). The thermocouples were placed on 30 cm centers flush with the outer surface of the probe body.

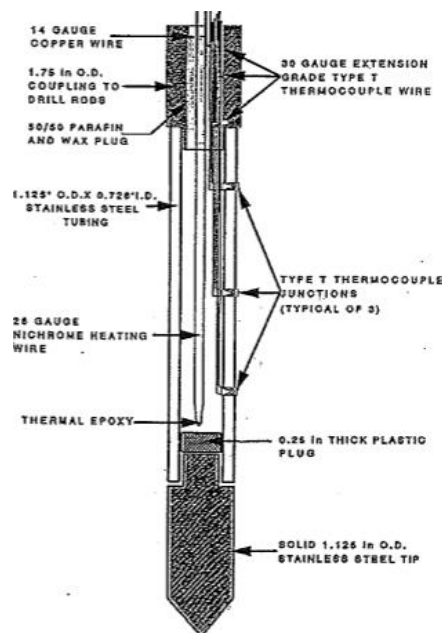


Figure 15: Thermal probe as proposed by Lutenegeger and Lally, 2001

During the thermal probe test, the probe was pushed to the desired test depth and subsequently brought to thermal and hydraulic equilibrium with the surrounding earth over a 24-hour period. Next, a thermal resistivity test based on the methods proposed by Winterkorn (1970) was performed by applying a constant heat load, and the resulting thermal response recorded. The thermal conductivity was calculated using a simple line heat source of infinite length (Weschler, 1966) as described previously.

2.9.3 Development of the Thermal Cone Test

Following the work of Lutenegeger and Lally (2001), Akrouch (2014) proposed an in-situ test for the thermal properties of soils based on the Cone Penetration Test (CPT). A CPT is an in-situ test performed in accordance with ASTM D-5778 to evaluate geotechnical engineering properties such as soil stratigraphy, strength, and compressibility. During this test, an instrumented cone penetrometer is hydraulically pushed into the ground at a constant rate and data are recorded at regular intervals. Modern cone penetrometers typically include two strain gauges measuring penetration resistance at the tip and friction on a sleeve along the shaft of the cone; a sensor measuring the pore water pressure near the cone tip; and a sensor measuring the inclination from vertical.

The soils at the tip of the cone penetrometer are in a quasi-steady state during the push; however, significant excess pore water pressure (u) may develop in low permeability saturated clays and silts. The soil hydraulic properties may be determined during the performance of a pore water pressure dissipation test (PWP) as described by Janbu and Senneset (1974); Wissa, et al. (1975); and Torstensson (1975). Once penetration of the cone is halted, excess pore pressure dissipates as a function of k . By observing the rate of decay, values for soil hydraulic conductivity, k , may be obtained by the empirical relation as proposed by Mayne (2007).

$$k \text{ (cm/s)} = \frac{1}{(251 * t_{50})^{1.25}}$$

where t_{50} is the time required after the cone is halted to achieve 50% dissipation of the excess pore water pressure, Δu . An example of a PWP test with initial pore water pressure, u_i , hydrostatic pore water pressure, u_0 , pore water pressure at 50% dissipation, u_{50} , and the excess

pore water pressure shown is provided on **Figure xx**. Briaud (2013) proposed an equivalency between hydraulic and thermal dissipations in soil. This equivalency is summarized in **Table xx** below.

Table 3: Equivalency between thermal and hydraulic flows (from Briaud, 2014)

PARAMETER	FLOW OF WATER	FLOW OF HEAT
Quantity	Volume, V (m ³)	Heat, Q (J)
Potential	Head, h (m)	Temperature, T (K)
Gradient	Hydraulic gradient, i _h (unitless)	Thermal gradient, i _t (unitless)
Flux	Flow rate, Q (m ⁴ /s)	Heat transfer rate, H (W)
Flux density	Velocity v (m/s)	Heat flow q (W/m ²)
Conductivity	Hydraulic conductivity, k (m/s)	Thermal conductivity, λ (W/m.K)
Law	Darcy	Fourier
Storage	Compressibility	Specific heat, c _p (J/kg.K)

Assuming pore pressure and heat decay occur similarly in soils, Akrouch (2014) proposed a thermal dissipation test, referred to as a thermal cone test (TCT) be performed in a similar manner. A similar relationship to the empirical method of estimating k from a pore pressure decay curve was proposed as:

$$\lambda = \frac{1}{(A * t_{50})^B}$$

where t₅₀ in this case is the time to achieve 50% dissipation of excess heat and A and B are dimensionless calibration factors. To determine the values of the calibration factors, Akrouch (2014) performed 11 thermal dissipation tests and compared the results to values obtained through laboratory testing using the thermal shock method (Shannon and Wells, 1947). Although Akrouch (2014) originally proposed to utilize a heating element to induce a thermal pulse, excess

heat produced as a result of friction during pushing the cone resulted in sufficient increases in temperature to observe the thermal decay. The tested soils comprised overconsolidated clays and medium dense clayey to fine sand from three sites in Southeast Texas. Based on the 11 samples, Akrouch (2014) proposed thermal conductivity could be measured from a thermal dissipation test performed during a CPT by:

$$\lambda = \frac{110}{(t_{50})^{0.968}}$$

It should be noted that the excess heat generated during pushing of the cone penetrometer resulted in a fairly uniform increase of 7-8°C within sand deposits but varied widely from 1.5-20°C in the tested clay deposits. These large temperature increases may have resulted in free convection of available ground water which would affect the observed thermal conductivity. Information regarding the location of the water table during these tests was not readily apparent.

2.10 Previous Study of Geothermal Properties in Louisiana

Bou-Mekhayel (2019) previously performed laboratory testing on a variety of alluvial soils within the vicinity of New Orleans using the thermal probe needle method in accordance with ASTM D5334-08 as part of a larger study of typical soil characteristics. Additionally, the TID was evaluated through the use of a thermistor string with temperature sensors at approximate 0.3m (1 foot) spacing to near the 15m depth (49 feet). The ambient air temperature was also monitored at the ground surface. Based on a series of measurements between August 2013 and January 2014, Bou-Mekhayel (2019) found that after a depth of approximately 4.5 to 6m (15 to

20 feet), the temperature remains relatively constant between approximately 21 and 25°C (70 to 75°F). The results of long-term measurements of the thermal profile are shown below in **Figure 16**.

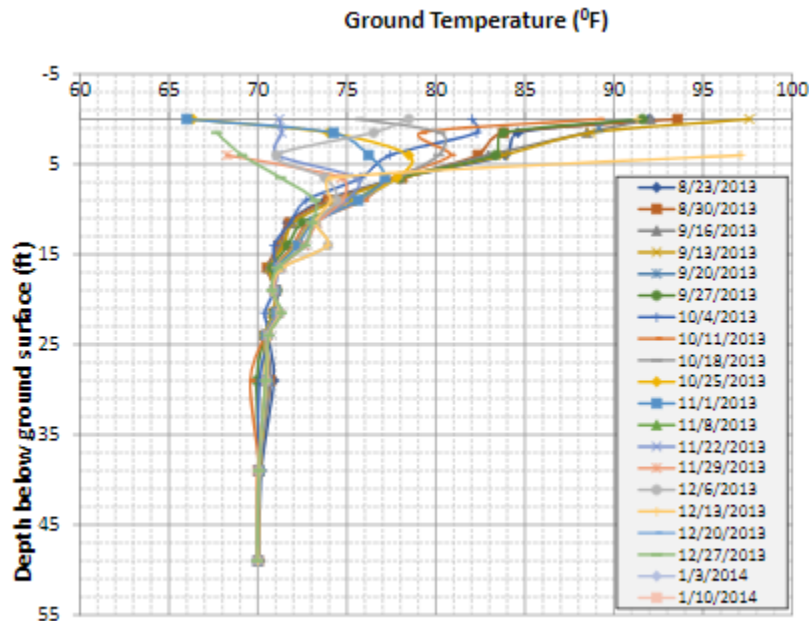


Figure 16: Thermal profile in New Orleans (adapted from Bou-Mekhayel, 2019)

Bou-Mekhayel (2019) performed testing of thermal conductivity on a variety of dry sand samples prepared in an apparatus as described by Lutenegger and Lally (2001). A sample of Ottawa sand ($\lambda_{\text{material}} = 0.292 \text{ W/m.K}$) was used for calibration of the thermal probe. Two tests were performed on each sample. A summary of the measured thermal conductivities of various dry sand samples as presented by Bou-Mekhayel (2019) are provided in **Table 4**. An average of the two tests for each material as presented by Bou-Mekhayel (2019) is also provided below.

Table 4: Summary of Measured Dry Thermal Conductivity (from Bou-Mekhayel, 2019)

Type of Soil	ρ_{dry} (kn/m ³)	γ_{dry} (pcf)	Measured Dry Thermal Conductivity, λ_{dry} (W/m.K)		
			Test 1	Test 2	Average
Ottawa Sand	14.6	93.1	0.17251	0.15907	0.166
Red Clay Sand	13.0	82.9	0.16157	0.16977	0.166
Pumped River Sand	13.6	86.2	0.18078	0.18049	0.181
Hass Pitt Sand	11.3	71.6	0.08784	0.16422	0.126
Grand Isle Sand	13.5	86.1	0.12442	0.13917	0.132
Lowes Sand	15.9	101.2	0.17568	0.22906	0.202

Bou-Mekhayel (2019) also performed thermal conductivity testing on a sample of pumped river sand at moisture contents of 0, 25% and 50% (extending across the range of typical values of moisture content seen for sand deposits along the Mississippi River). The results of thermal conductivity for pumped river sand at various moistures contents are shown in **Figure 17** below.

River Sand Thermal Conductivity Vs. Water Content

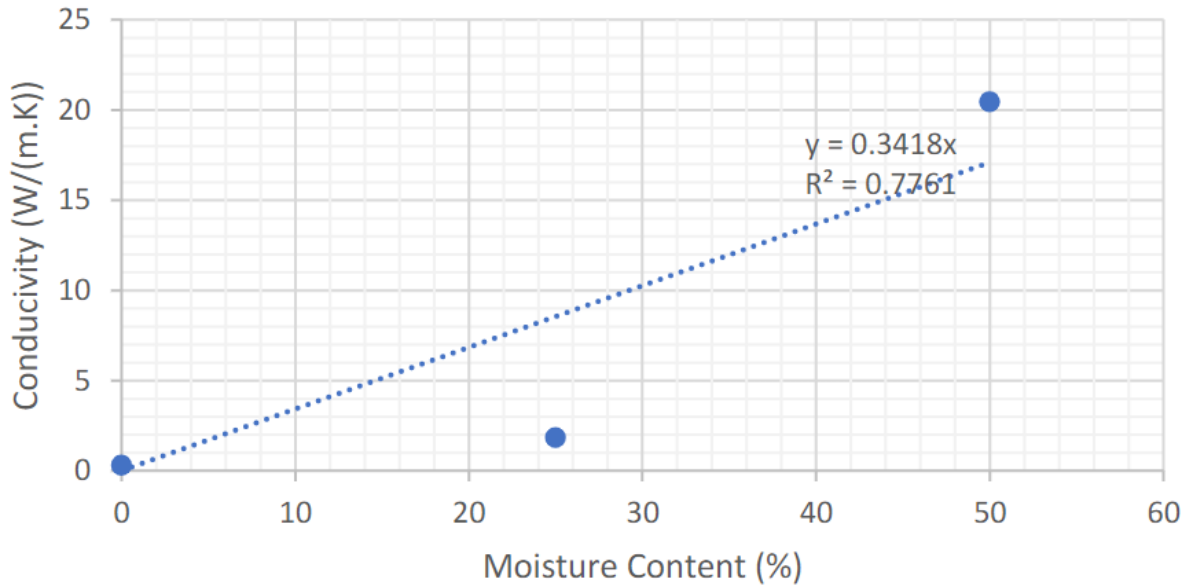


Figure 17: Correlation as proposed by Bou-Mekhayel (2019)

Linear regression was used to propose a relationship between moisture content and the thermal conductivity of the pumped river sand as described by:

$$\lambda_e = 0.3418\omega$$

where the moisture content is expressed as a percentage. It should be noted this expression provides an estimate for thermal conductivity beyond typical values for sedimentary materials. It is possible the tested value at 50% moisture content was influenced by free convection, providing a high estimate for thermal conductivity, and skewing the proposed relation.

2.11 Available Studies of System Efficiency

2.11.1 General Summary of System Efficiencies

Many studies of the thermal response of energy geostructures (including energy piles) have been performed with a fairly comprehensive review provided by Laloui and Donna (2013). The review by Laloui and Donna provided reports of operational and field test data from various pile types including bored cast in situ; augercast in situ; closed end, driven or screwed steel pipes that were either grout/sand or water filled; and precast concrete piles. A summary of works referenced by Laloui and Donna (2013) by pile type is provided in **Table 5** below.

Table 5: Summary of Case Studies of Installed Systems (adapted from Laloui and Donna, 2013)

Pile Type		Referenced Works
Bored Cast In Situ (Drilled Shafts)		Sekine et al. (2005) Brandl (2006) Laloui (2006) Pahud & Hubbuch (2006) Schnürer et al. (2006) Gao et al. (2008) Bourne-Webb et al. (2009) Kipry et al. (2009)
Augercast In Situ (ACIP)		Wood et al. (2009) Brettman et al. (2010)
Driven or Screwed Steel Tubes (CSP)	Sand/Grout Filled	Henderson et al. (1998) Jalaluddin et al. (2011)
	Water Filled	Morino & Oka (1994) Nagano et al. (2005) Katsura et al. (2009) Jalaluddin et al. (2011)
Precast Concrete (SPC)		Brandl (2006) Hamada et al. (2007) Katsura et al. (2009)

A summary of the results from the case studies referenced above can be found in Laloui and Donna (2013). It should be noted that the majority of these case studies were performed in Europe and Asia. Additionally, the heat transfer (Q) extracted and/or injected was traditionally reported in terms of Watts per meter (W/m), stemming from the industries origins and comfortability with BHX where the length to diameter (L/D) ratio is traditionally large enough that length is the governing dimension. Given the large lengths seen in BHX systems, the soils were also typically treated as homogenous and uniform. This makes direct comparisons somewhat difficult as variations in subsurface stratigraphy and groundwater conditions; pile type, size, and spacing; test methodology; and thermal loading conditions will have greater impact on the operational conditions yield of different energy piles systems (Laloui and Donna, 2013). However, while consideration to the potential impacts of these variables when reviewing the data summarized in Laloui and Donna (2013), some broad trends may be observed:

- The highest heat transfer appears to occur in fully saturated coarse-grained soils.
- Heat transfer into the ground (injection) may be slightly higher than heat extraction.
- Heat transfer may be slightly higher for steel piles than concrete.
- Heat pulses (or intermittent heat transfer) results in a higher heat transfer value than sustained, steady-state thermal loading.
- Larger diameters of piles (>0.6 m) may be difficult to model as their L/D ratio increases beyond the limits of the assumed infinite line source theory.

- As suggested by Brandl (2006), high-permeability soil with groundwater flow would be desirable for unbalanced climatic conditions where either heating or cooling dominates.
- The opposite is true in cases of balanced heating/cooling loads, where seasonal storage would be ideal. In this case, low-permeability soil with little groundwater flow to impact stored heat would be preferable.

Based on these broad trends and the reviewed case studies, Laloui and Donna (2013) provided the comparison of some typical heat transfers by pile and soil type shown in **Table 6** below. For comparison, Laloui and Donna (2013) also provide typical values for BHX recommended BS EN 15450 (2007), a design code commonly referenced for GHP systems using BHX. Note, values from BS 15450 are intended for pre-design of BHX and likely present somewhat un-conservative estimates for energy piles having much smaller L/D ratios.

Table 6: Comparison of heat transfer by pile and soil material types (from Laloui and Donna, 2013)

PILE MATERIAL	SOIL TYPE	HEAT TRANSFER, Q (W/m) ⁽¹⁾		BS 15450 VALUES BY SOIL TYPE
		INJECTION	EXTRACTION	
Concrete	Fine	15-60, max. 110	25-45	30-50
	Coarse	35, max 220	30-50	55-80
Steel tube with fluid infill	Fine	25-55, max. 140	15-20, max. 85	30-50
	Coarse	55-90	-	55-80

⁽¹⁾Includes both steady-state and transient thermal loadings. Laloui and Donna (2013) suggest heat transfer for transient loading conditions may be 2 to 4 times larger than steady-state conditions.

Olgun (2013) suggested typical values of heat transfer for energy piles equal to approximately 25, 50, and 75 W/m for poor, average, and excellent ground qualities, respectively.

As can be seen, while many studies of the efficiency of GHX systems are available in the literature and generally indicate excellent potential for the design approach, difficulty in direct comparisons exists because of the lack in uniformity of design approaches and control of variables. Measures to normalize and control the different variables that directly affect heat transfer in PHX systems are required.

2.11.2 Efficiency in Cooling Dominated Climates by Khan and Wang (2014) and Akrouh (2014)

While much research has been performed on the performance of energy pile systems in Europe and Asia, the issue is relatively new to the United States and particularly the Gulf Coast. Specific to South Louisiana, Khan and Wang (2014) performed a theoretical evaluation of a potential energy foundation design in New Orleans. Based on the work of Brandl (2006); Dupray et al. (2014); and Zarrella et al. (2013), Khan and Wang (2014) used an office building under construction in New Orleans as a case study for energy piles. The office building was a four-story structure with parking provided on the ground floor and approximately 696.77m² (7,500ft²) of office space on each of the upper floors. Khan and Wang (2014) estimated the cooling and heating loads for the building using LEED Plus software to be approximately 147.27kW/hr and 39.54kW/hr, respectively. The foundation plan for the structure comprised 145 piles arranged in 16 groups of 9 piles each at a spacing of approximately 1.22m (4 feet) on center. The pile lengths were designed based on structural loadings to have tip embedments approximately 24.4 m (80 ft) below the existing ground surface.

To avoid error resulting from potential interaction of energy piles, Khan and Wang (2014) assumed only the pile at the center of each pile group would be installed with GHX loops, giving

an effective spacing between energy piles of approximately 8.55m (28.06 feet). Each energy pile was modeled as a 0.25m (10 inch) diameter concrete pile installed with a single HDPE U-tube carrying pure water as the HCF with a 1492 W (2HP) variable speed circulation pump.

Typical values for the thermal properties of the soils were taken from the literature in modeling the efficiency of the system using the Ground Loop Design (GLD) 2012 software by Thermal Dynamics, Inc. Soil temperature was assumed to be 19.44°C (67°F). To be conservative, the soils were not assumed to be fully saturated. A uniform thermal conductivity value of 1.47 W/m.K was selected.

Based on these design assumptions, Khan and Wang (2014) estimated that approximately 20% of the cooling demand (29.3 kW) and 68% (26.9 kW) of the heating demand could be met through the installation of the 16 energy piles. The energy piles were estimated to provide approximately 1.8 kW in extraction (heating) and 1.7 kW in injection (cooling). Based on estimated costs for different energy sources, Khan and Wang (2014) concluded that the installation of the GHP system could reduce the annual HVAC operational costs by up to 92-93%.

While the overall cost reduction estimated by Khan and Wang (2014) is very encouraging, the heat transfer observed in their model (75 W/m and 68 W/m for heating and cooling, respectively) would be within the upper range of typical values as reported by Laloui and Donna (2013) and Olgun (2013) and thus may be indicative of an un-conservative estimate. One potential source of error may be the assumed ground temperature. As can be seen when comparing to the temperature profile as measured by Bou-Mekhayel (2019), a uniform ground temperature of 19.44°C (67°F) is somewhat un-conservative, particularly in the upper 4.5 to 6m

(15 to 20 feet). However, while the soils were assumed to not be fully saturated, in actuality saturations below the ground water table (approximately 1.5m per the geotechnical report prepared for the building) would likely be near or above 95%. This limiting assumption would strongly affect the thermal conductivity. Therefore, the values used for thermal conductivity in this theoretical study should be validated to compare the potential values of heat transfer.

Concurrent to Khan and Wang (2014), Akrouch (2014) performed an extensive study of GHP systems in cooling dominated climates using a building constructed on the Texas A&M University in College Station as the basis of research. This study included laboratory testing of the λ of foundation materials, construction of a GHP system for calibration of a full scale model, and an economic study of a full scale system using the Hybrid Ground Coupled Heat Pump (HyGCHP) software developed by the University of Wisconsin.

The evaluated building comprised five floors with a total area of 11,575m² (124,592ft²) supported on a deep foundation system comprising 263 ACIP piles each having a length of 18m (60 feet). Prior to construction, samples taken during the geotechnical exploration were used to perform laboratory testing of thermal conductivity by the thermal shock method (Shannon and Wells, 1947). The soils comprised primarily overconsolidated clays with an average water content of 28% and average thermal conductivity estimated as 0.61 W/m.K. During construction, three piles near the edge of the building were each installed with a single loop of HDPE pipe spaced 0.2 m (7.5 in) apart in the 0.45 m (18 in) diameter piles.

The HDPE pipes were connected to a GSHP located within the crawl space of the building separate from the main HVAC system but in a climate-controlled space kept at a constant

temperature. Temperatures were monitored throughout the length of the three piles; in three boreholes drilled at various distances from the instrumented piles; and at each inlet and outlet to monitor temperature of the HCF.

Using the three instrumented piles, Akrouch (2014) performed a field test of the GHP by operating the heat pump in a series of arbitrary heating and cooling cycles over an approximately 2-week period. Based on the measured, average change in HCF temperature between the inlet and outlet, the total heat exchange was estimated by Remund and Carda (2009). The measured HCF temperature at inlet and outlet for each pile and calculated heat exchange as published by Akrouch (2014) are provided in **Figure 18**.

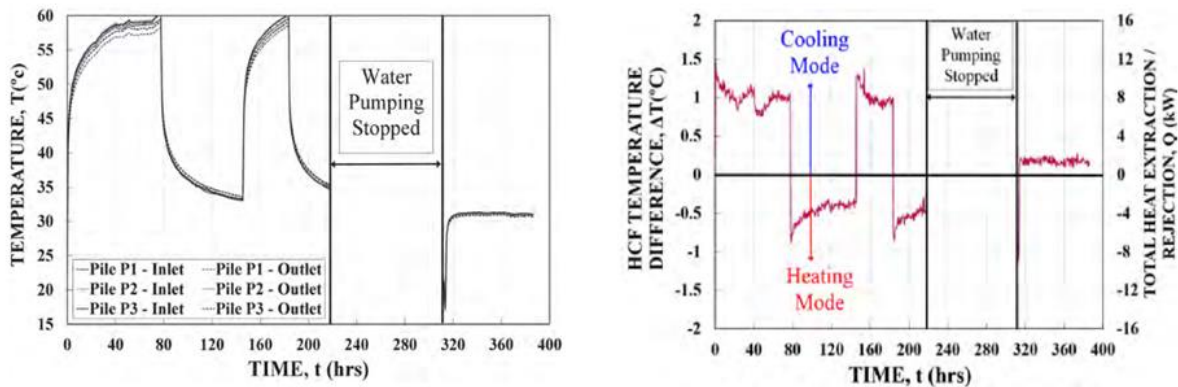


Figure 18: Measured HCF Temperature and Calculated Heat Exchange (from Akrouch, 2014)

Non-steady state conditions can be observed for the majority of the thermal loading periods, resulting in a reduction in heat exchange from the maximum seen at each switch. Temperature increases in the piles take the shape as seen in the HCF. Negligible changes in temperature were observed within the boreholes located as close as 0.72 m (2.3 ft) during the

testing period, although Akrouch (2014) suggests thermistors located in the boreholes may have been impacted during installation.

Akrouch (2014) estimated a total heat transfer of approximately 8 and 4 kW for heat injection (cooling) and extraction (heating), respectively. For the three piles, this gives a heat exchange rate of approximately 148.2 W/m and 74.1 W/m, respectively. Akrouch (2014) suggests these higher heat exchange rates may be the result of transient loading and under sizing of the system. The tested values were used to calibrate the system modeled by Akrouch (2014) in HyGCHP using a refined thermal conductivity equal to 1.87 W/m.K.

Using the calibrated $\lambda=1.87$ W/m.K, a ground temperature equal to 23°C, and actual HVAC loads for the Liberal Arts building monitored over the course of a year, Akrouch (2014) estimated a GHP system could supply 13.34% of the total cooling load, 63.51% of the total heating load, and 10.55 kW of domestic hot water heating for the building. Over a 30-year design life, this was estimated to reduce the electric power consumption by a total of 5,573 MWh. However, because of the cooling dominated climate, unbalanced heating and cooling loads resulted in an estimated 0.28°C increase in ground temperature per year. This increase in ground temperature results in an increase in the heating efficiency and decrease in cooling efficiency. Costs were estimated for the design, construction, and operation of the GHP to calculate a simple payback period of 13 years.

2.11.3 Other Relevant Work

Tapia (2017) performed a series of case studies on GHP systems located in South Louisiana to compare the energy usage and costs in hot and humid climates compared to traditional HVAC

systems. While comprising BHX and slinky systems used in residential applications, this study provides additional insight into potential payback periods. Tapia (2017) utilized four residences within New Orleans equipped with various GHP systems as case studies. Details of these four cases studies are summarized in **Table 7** below.

Table 7: Summary of expected payback period (from Tapia, 2017)

CASE STUDY	GROUND HEAT EXCHANGER SYSTEM		PAYBACK PERIOD (YEARS) ⁽¹⁾
	TYPE	LENGTH (m)	
GH1	Slinky	290.8	32 to 73
GH2	BHX	5 @ 76.2 each	2 to 7
GH3	BHX	3 @ 76.2 each	3.5 to 12
GH4	BHX	-	-

⁽¹⁾Lower bound of expected payback period includes all possible tax credits, while upper bound neglects any potential tax credits.

Tapia (2017) suggested the extremely high payback period seen in the first case study was the result of an overdesign based on limited experience by the GHP contractor that drastically increased the installation cost to a point that the payback on the investment is irrelevant. Moreover, the relatively high temperatures seen in the surficial 4 m (13 ft) in the New Orleans area likely strongly limits the efficiency benefits of a GHP. On the other hand, the deep systems installed by experienced contractors at Case Studies GH2 and GH3 provided excellent performance, low operating costs, and relatively quick payback periods, particularly with potential tax credits included. Although a deep system was installed at GH4, the system was installed by a contractor with no experience in GHP systems who kept no records to document the design. Without itemized costs or usage estimates, a payback period was impossible to calculate. Rather, this case study stands as a warning that since Louisiana lacks a system for

certification of GHP designers/installers, care must be taken to identify qualified and experienced contractors. Tapia (2017) concluded that while the initial cost of GHP systems in residential applications can be twice that of conventional ASHP systems, energy usage cost savings of 60% on average when combined with potential tax credits provide an opportunity for significant savings for landowners. Overall, homeowners with properly installed systems felt more satisfied with the performance of GHP systems than with the performance of conventional ASHP systems in hot and humid climates.

Chapter 3: Methodology

The contents of this chapter describe the methodology and research approach used to conduct this study on the thermal conductivity of alluvial soils in the New Orleans area. The objective for this research is to provide a basis for evaluation of the thermal properties of these soils to allow for more direct comparison to existing case studies in the literature. To achieve this objective, the research will answer the following questions:

RQ1: What typical values of thermal conductivity could be expected for various geological subunits of soils in the New Orleans area?

RQ2: How do the various empirical correlations used to estimate thermal conductivity of soils compare to tested values?

RQ3: Are proposed in situ methods of testing thermal conductivity practical and if so, do they provide additional context?

RQ4: How do these estimates of thermal conductivity compare to values assumed for previous economic studies of GHP systems?

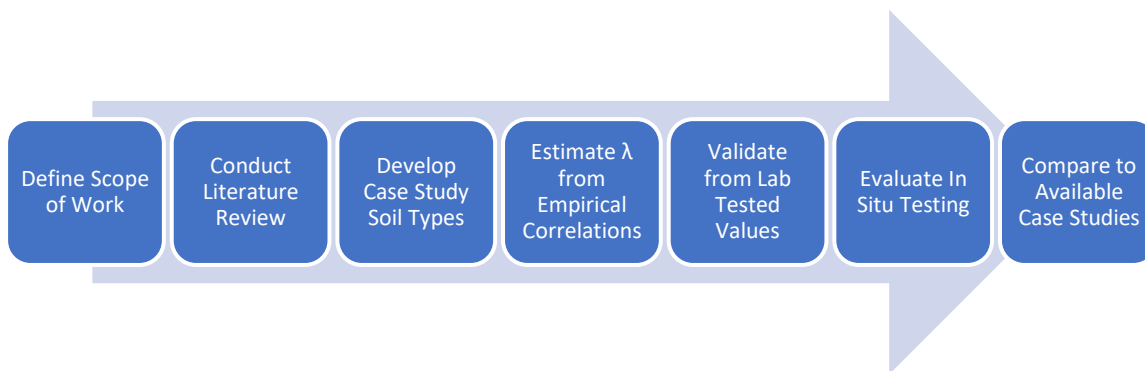


Figure 19: Research Methodology

3.1 Define Scope of Work

The focus of this research is to provide the foundation for application of energy piles in the New Orleans area by examining the geotechnical constraints and feasibility, as well as providing a basis for comparison of the geothermal properties encountered locally. As discussed previously, the metrics used to evaluate previous studies of GHP systems efficiency vary widely; therefore, this work proposes to use thermal conductivity of soil as a means of comparing the practicality of GHP systems, specifically energy piles, from a geotechnical perspective. This study is intended to support local engineering practice in providing a review of the factors influencing thermal conductivity and an evaluation of the various methods available to estimate thermal conductivity.

3.2 Conduct Literature Review

As a starting point for this study, the author reviewed in Chapter 1 the geological processes that led to the creation of the current Mississippi River alluvial delta to provide contextual background for the geotechnical environment in question. Basic conceptual aspects of GHP systems, particularly PHX, were examined with a focus on how these systems interact with the subsurface soils. Thermal conductivity was identified as the primary geothermal parameter in these systems, and various methods of estimating λ were considered. Although a significant number of studies evaluating the efficiency of GHP systems is available in the literature, the author suggests a disconnect exists in the various metrics used in these studies.

Thus, this research is intended to validate these studies with respect to the soils found in South Louisiana.

3.3 Develop Case Study Soil Types

As an initial step, foundation soils were subdivided by geological depositional environments with typical or average geotechnical properties assumed based on the work of Kolb and Lopik (1958); Saucier (1963); Montgomery (1974); and local engineering experience. The subdivided soils are not meant to be exhaustively comprehensive, but rather representative of the most common soils typically found in design of deep foundation systems. These case study soil types, when used in conjunction with available geological mapping performed by the USACE, can provide both a desktop study level understanding of thermal conductivity in the New Orleans area as well as spatial context for the tested values presented herein.

3.4 Estimate λ from Empirical Correlations

As shown in Chapter 2, various relationships for thermal conductivity based on material properties exist. Using the assumed geotechnical parameters for various case study soil types as described in the section above, these empirical correlations were used to estimate λ . Consideration was given to both the ease of use and accuracy of each of the methods to propose a recommended method for use in preliminary design or in cases where conservative values for thermal conductivity could be used in lieu of tested values.

3.5 Validation by Lab Testing

The results of laboratory measurements of thermal conductivity performed by the thermal needle probe method in accordance with ASTM D5334-14 were used to validate the accuracy of estimated values. The testing was performed with a KD2 PRO SML1-TPA-1 Thermal Conductivity Probe calibrated by the manufacturer. The testing was generally performed on undisturbed samples taken from borings.

3.6 Evaluation of In Situ Testing Methods

Lutenegger and Lally (2001) and Akrouch (2014) proposed methods for in situ testing of the thermal conductivity of soils. A thermal probe of similar construction as proposed by Lutenegger and Lally (2001) based on the work of Winterkorn (197) was constructed to perform in situ testing of thermal conductivity. The probe, shown in **Figure 20** below, consisted of a stainless-steel casing with a 6.99 cm (2.75-in.) outer diameter and total length of 91.4 cm (36-in.). The probe was designed to be pushed concurrently with a 3.72 cm (1.44-in.) diameter electronic cone penetrometer having a total length of approximately 30 cm (12-in.) below the bottom of the probe. Three Type-T thermocouple junctions were placed within the central body of the thermal probe at a center-to-center spacing of 30 cm (12-in.) positioned flush with the outer body of the probe. Heating was provided by a dual pass 26-gauge nichrome heating wire located in line with the thermocouples.



Figure 20: Thermal probe with electronic cone penetrometer

Chapter 4: Analysis

4.1 Case Study Soil Types

As described previously, geology in the New Orleans area is largely influenced by the Mississippi River. The various depositional environments that comprise the delta formation process strongly influence the geotechnical parameters of the soils. Commonly, identification of the depositional environments that could be anticipated in a profile through available geological mapping performed by USACE can provide an indication of the geotechnical parameters. Some deposits most pertinent to foundation design in the New Orleans area include natural levee silty clays, point bar silty sands, relic beach sands, interdistributary clays, swamp/marsh organics, prodelta clays, and Pleistocene clays. Although not comprehensive, this list encompasses the majority of generalized profiles in local engineering practice. Selected parameters for these soil types to be used in this study are provided in **Table 8** below. Average ranges are also provided in parentheses for reference.

Table 8: Summary of Selected Parameters for Generalized Soil Types

GENERALIZED SOIL TYPE	USCS	FINES FRACTION ⁽¹⁾ , f_{cl} (%)	NATURAL MOISTURE CONTENT, θ (%)	TOTAL UNIT WEIGHT, γ		POROSITY ⁽²⁾ , n (%)
				(kN/m ³)	(pcf)	
Natural Levee Silty Clay	CL/ML	90 (85 to 100)	35 (20 to 50)	17.3 (15.5 to 18.5)	110 (99 to 118)	0.48
Point Bar Silty Sands	SM	25 (0 to 50)	30 (30 to 50)	18.4 (17.3 to 19.0)	118 (110 to 121)	0.43

Relic Beach Sand	SP	5 (0 to 10)	25 (20 to 30)	18.8 (18.1 to 19.6)	120 (115 to 125)	0.43
Interdistributary Clays	CH	100 (90 to 100)	75 (50 to 110)	15.7 (14.0 to 16.5)	100 (89 to 105)	0.66
Swamp/Marsh Organic Clay	OH	100	180 (100 to 300)	11.8 (9 to 14)	75 (57 to 89)	0.83
Prodelta Clay	CH	95 (90 to 100)	60 (30 to 90)	16.0 (14.0 to 18.5)	102 (89 to 118)	0.62
Pleistocene Clay	CH/CL	90 (80 to 100)	30 (20 to 50)	19.2 (17.3 to 19.6)	122 (110 to 125)	0.44

Values for average ranges were taken from Kolb and Van Lopik (1958), Saucier (1963), Montgomery (1974), and local engineering experience. The fraction of fines is defined as the percent passing the U.S. Standard No. 200 sieve (0.074m particle diameter). Porosity of each soil type was calculated using the dry unit weight and an assumed specific gravity of 2.46 for the swamp/marsh organic clays and 2.70 for the remaining soil types. A range in fines is not provided for swamp/marsh deposits due to large organic materials being commonly observed in these deposits. For the purposes of this study of thermal conductivity, the organic clay was assumed to be 100% fines (i.e., no sand).

Within New Orleans, groundwater is commonly encountered within 1 to 3 meters (3 to 10 feet). For the purposes of this study, the generalized soil types were assumed to be fully saturated (below the ground water table). Based on mineral analyses of Mississippi River alluvial clays (USDA, 1970), fine grained materials are primarily montmorillonite, mica-illite, and vermiculite. The quartz fraction of point bar silty sands and relic beaches were assumed to be 25 and 50%, respectively. The solids thermal conductivity (λ_s) for clay minerals and quartz were assumed to be 2.90 and 7.70 W/m.K, respectively (Côté and Konrad, 2005).

4.2 Empirical Estimates of λ

Five empirical models for estimating thermal conductivity were considered for this study: Kersten (1949), Johansen (1970), Côté and Konrad (2005), Lu and Horton (2014), and Nikoosokhan (2015). A summary of these methods is provided in Chapter 2. The parameters for each of the generalized soil types as described in Section 4.1 were used to estimate thermal conductivity. The results of the analyses are provided in **Table 9** below. An average of the five methods for each generalized soil type is also provided.

Table 9: Typical Values of Thermal Conductivity for Generalized Soil Types

GENERALIZED SOIL TYPE	ESTIMATED SATURATED THERMAL CONDUCTIVITY (W/m.K)					
	Kersten (1949)	Johansen (1970)	Côté and Konrad (2005)	Lu and Horton (2014)	Nikoosokhan (2015)	Average
Swamp/Marsh Organic Clay	0.5	0.8	0.8	0.3	0.4	0.6
Interdistributary Clay	0.8	1.0	1.0	0.7	0.9	0.9
Prodelta Clay	0.9	1.1	1.1	0.8	1.0	1.0
Natural Levee Silty Clay	1.1	1.3	1.3	0.9	1.3	1.2
Pleistocene Clay	1.4	1.5	1.5	1.1	1.5	1.4
Point Bar Silty Sands	1.7	1.4	1.6	1.8	1.9	1.7
Relic Beach Sands	1.8	1.8	1.7	2.0	2.0	1.9

4.3 Results of Laboratory Testing

Laboratory testing performed in accordance with ASTM D5334-14 was used to evaluate the validity of the various methods for estimating thermal conductivity. Additional historical data were furnished by a local engineering firm and used to supplement the testing program. A total

of twenty-two tests were performed with seventy-nine historical tests made available. For each tested value, the moisture content, total unit weight, and dry unit weight were determined for the sample. These were used to estimate the porosity of the sample, n , by:

$$n = 1 - \frac{\gamma_{dry}}{\rho_w SG}$$

where SG is the specific gravity of the soil, assumed to be 2.46 for organic clays or peats and 2.70 for all other soils. Density of the sample, ρ_w , was taken to be equal to 62.4 pcf. Saturation of the sample was calculated by:

$$S = \frac{\theta}{\frac{\rho_w}{\gamma_{dry}} - \frac{1}{SG}}$$

Clay fraction was assumed to be 100% for samples classifying as CL or CH unless sand was noted in the description modifiers, in which case 85% was assumed. Unit weights for a number of the historical tested samples ($n=25$) were not provided; therefore, values were estimated using boring logs. Based on these input parameters, thermal conductivity was estimated using each of the models presented in Section 4.2. The results of these analyses for each method were plotted against the measured value as shown on **Figure 21 (A-E)**.

To provide quantitative measures of the accuracy and precision of the estimated values, the root mean square error (RMSE) and bias for each of the models was calculated by:

$$RMSE = \sqrt{\frac{\sum(\lambda_m - \lambda_p)^2}{m}}$$

$$Bias = \frac{\sum(\lambda_m - \lambda_p)}{m}$$

where λ_m and λ_p are the measured and predicted values, and m is the number of measurements. The results of these analyses are summarized in **Table 10** below and shown graphically on **Figure 21 (A-E)**.

Table 10: Accuracy and precision of predicted versus measured values of thermal conductivity

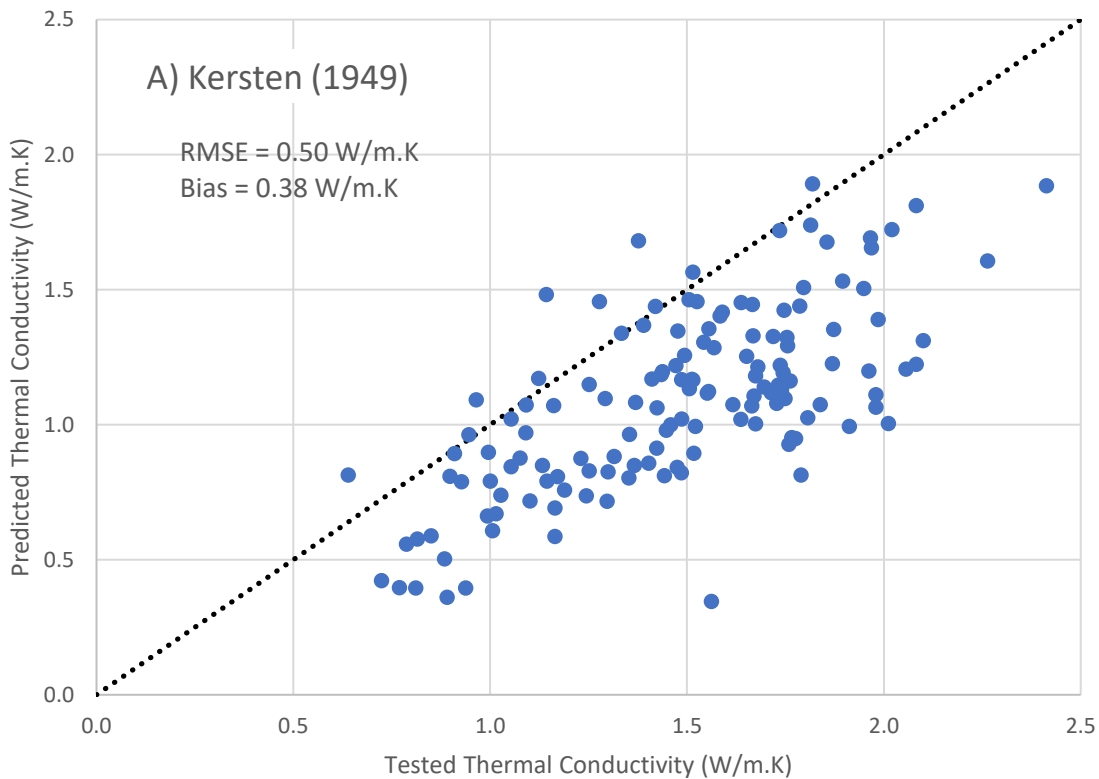
METHOD	RMSE (W/m.K)	BIAS (W/m.K)
Kersten (1949)	0.50	0.38
Johansen (1975)	0.38	0.23
Côté and Konrad (2005)	0.43	0.28
Lu and Horton (2014)	0.75	0.64
Nikoosokhan (2015)	0.57	0.41

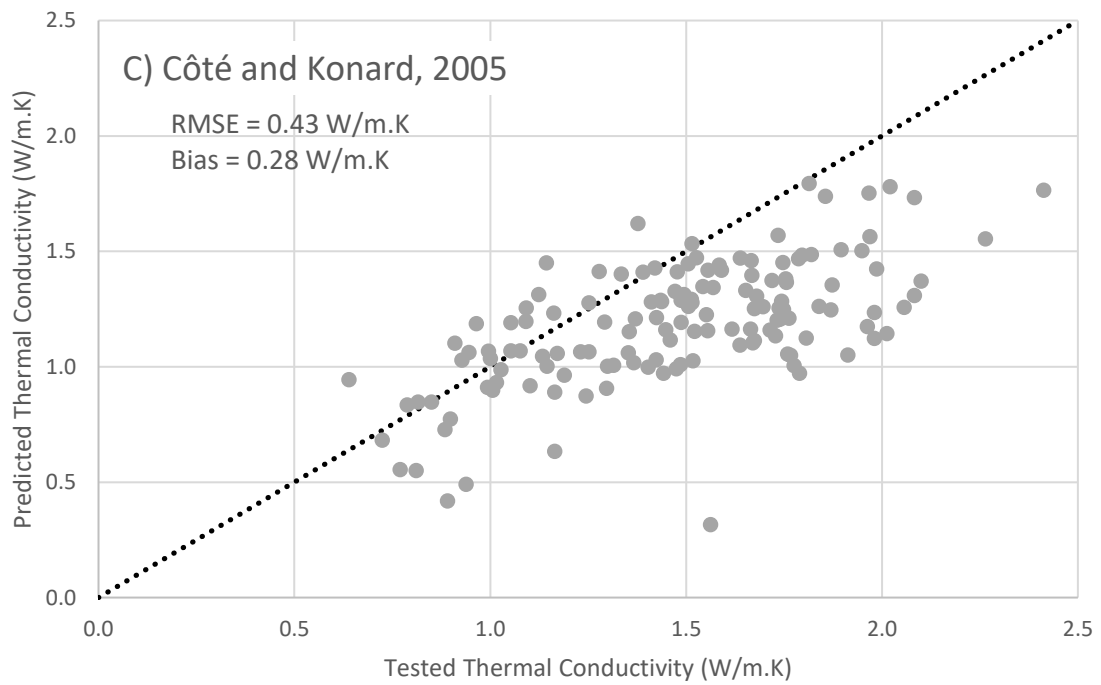
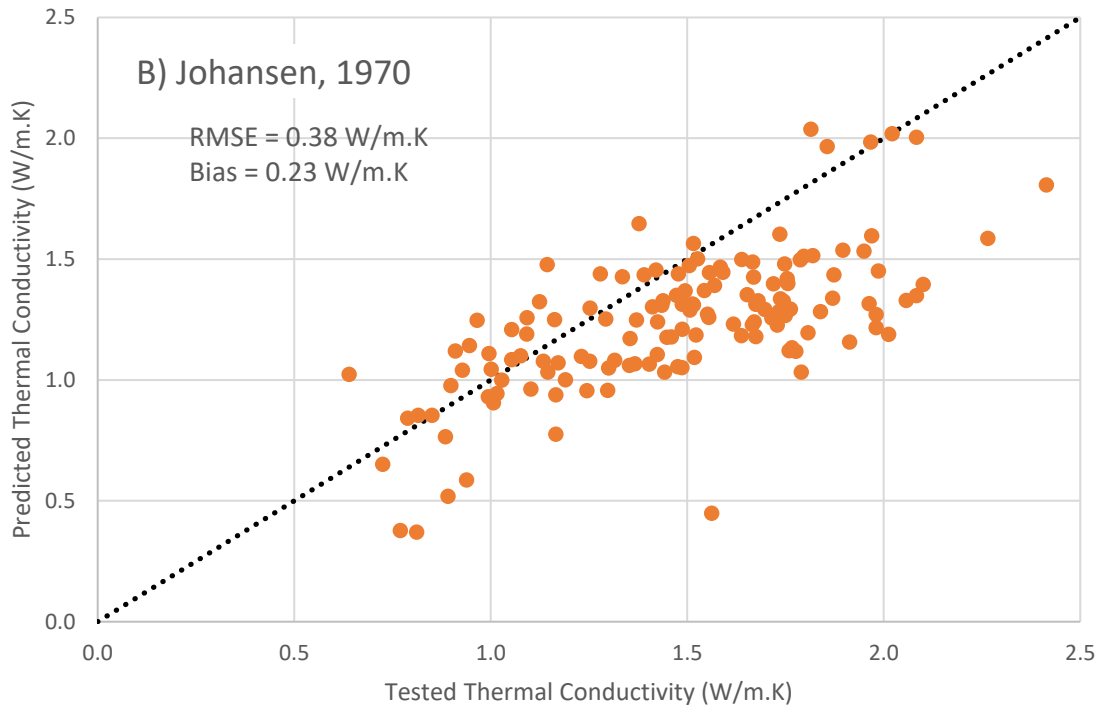
As can be seen in **Table 9** and **Figure 21 (A-E)**, all of the empirical models tend to underpredict the tested thermal conductivity, particularly at higher values. It should be noted the RMSE observed in the test data are 2 to 10 times larger than reported by Lu et al. (2007), but the Johansen and Côté and Konrad models were similarly reported to underpredict λ at higher moisture contents in that work. Interestingly, the test data provided by Kersten (1949) were utilized by both Johansen (1975) and Côté and Konrad (2005) in their analyses. Soils tested by Kersten (1949) comprised primarily alluvial sands and clays in the Upper Mississippi River, and it may be that similar mineral compositions of the soils result in the more accurate results of these empirical models.

Sensitivity analyses were performed by varying the assumed values for the solids thermal conductivity, λ_s and the clay fraction. Practically speaking, the assumption of 100% clay for many of the samples may be overly conservative. In actuality, many samples visually classified as clay may contain 5% to 10% sand by weight. At the same time, organic content tests performed on

similar soils indicate 5% to 10% organic content may also be possible. Decreasing the clay fraction to 51%, a classification of sandy clay, results in a relatively modest reduction in the RSME and bias for the Lu and Horton (2014) and Nikoosokhan (2015) models.

On the other hand, variations in λ_s used in the Johansen (1975) and Côté and Konrad (2005) provide a scalar effect on the predicted values. By varying the quartz content, q , the value for λ_s was increased from the lower bound assumed for clay minerals (montmorillonite, mica-illite, and vermiculite equal to 2.90 W/m.K) and an upper bound for pure quartz equal to 7.7 W/m.K. Although not supported in the literature as typical for the encountered materials, it is noted that values of λ_s of 4.94 W/m.K and 7.7 W/m.K reduce the bias to near zero for the Johansen (1975) and Côté and Konrad (2005) models, respectively.





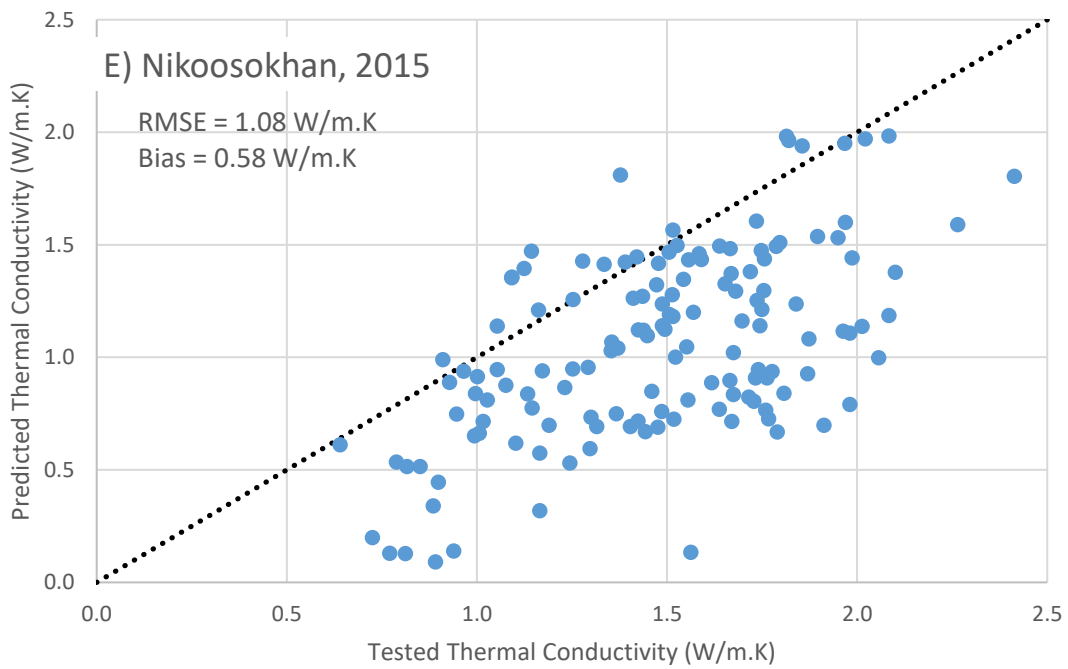
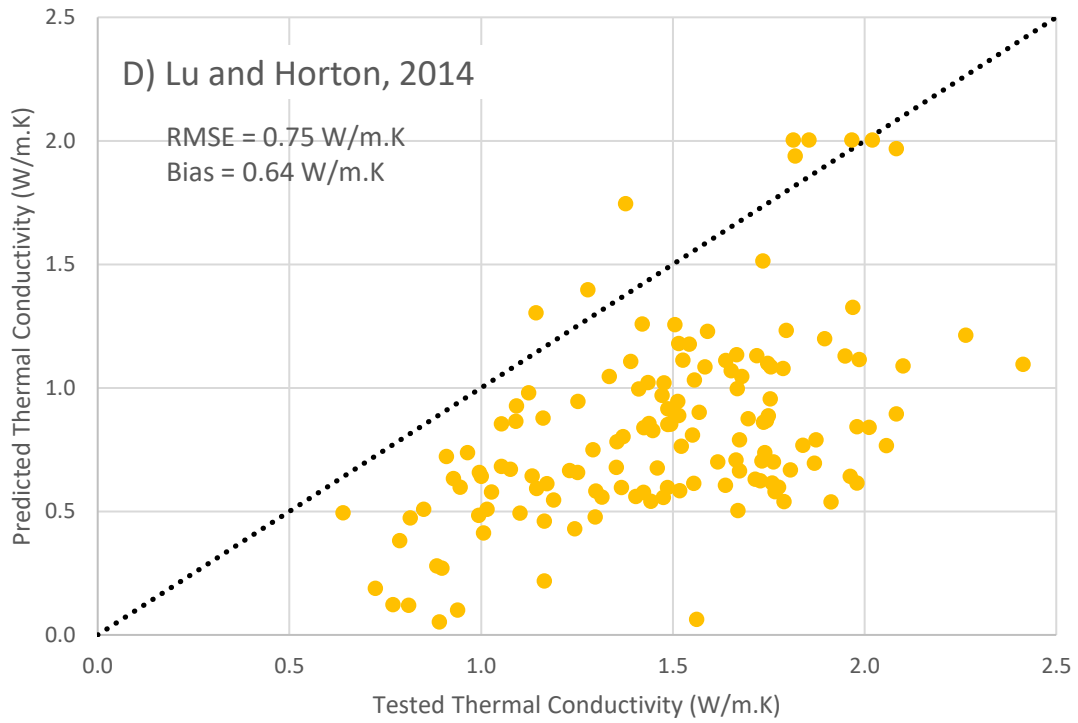


Figure 21: Predicted vs measured values of effective thermal conductivity

The tested samples were classified by likely depositional environment based on comparison of the sample location and depth with available geological mapping as well as the sample color and characteristics. The majority of the historical test data, performed for design of electrical conduits at large industrial facilities along the river, are classified as natural levee deposits. The results of laboratory testing by depositional environment are summarized in **Table 11** below.

Table 11: Average thermal conductivity by depositional environment

DEPOSITIONAL ENVIRONMENT	AVERAGE OF TESTED VALUES, λ_{avg} (W/m.K)	STANDARD DEVIATION, σ	POPULATION, n
Natural Levee	1.522	0.315	113
Interdistributary	1.214	0.225	6
Point Bar	1.940	0.146	4
Swamp/Marsh	0.891	0.120	12
Relic Beach	2.210	0.675	7

4.4 In Situ Thermal Cone Testing

4.4.1 Calibration Testing

Methods for in situ testing of thermal conductivity at depth following the work of Lutenegeger and Lally (2001) and Akrouch (2014) were evaluated. Calibration tests of the probe were conducted in a 0.5 m x 0.5 m x 1 m (approximately 20 in x 20 in x 40 in) HDPE container filled with water stabilized by approximately 5 g/L of agar having a known thermal conductivity of 0.607 W/m.K in accordance with ASTM D5334-14. During testing, a constant DC voltage was

applied using an Eventek KPS305D with a maximum rating of 30V/5A. Temperature at each of the thermocouples was recorded by an Omega RDXL450 four channel datalogger having a precision of 0.1°C. Power was maintained to induce a +1 to +3°C change in temperature, typically 15 to 20 minutes. The data were manually plotted during the test to ensure thermal dissipation had reached a linear slope in log space, usually 45 to 60 minutes. A typical thermal curve from the calibration tests is shown in **Figure 22**.

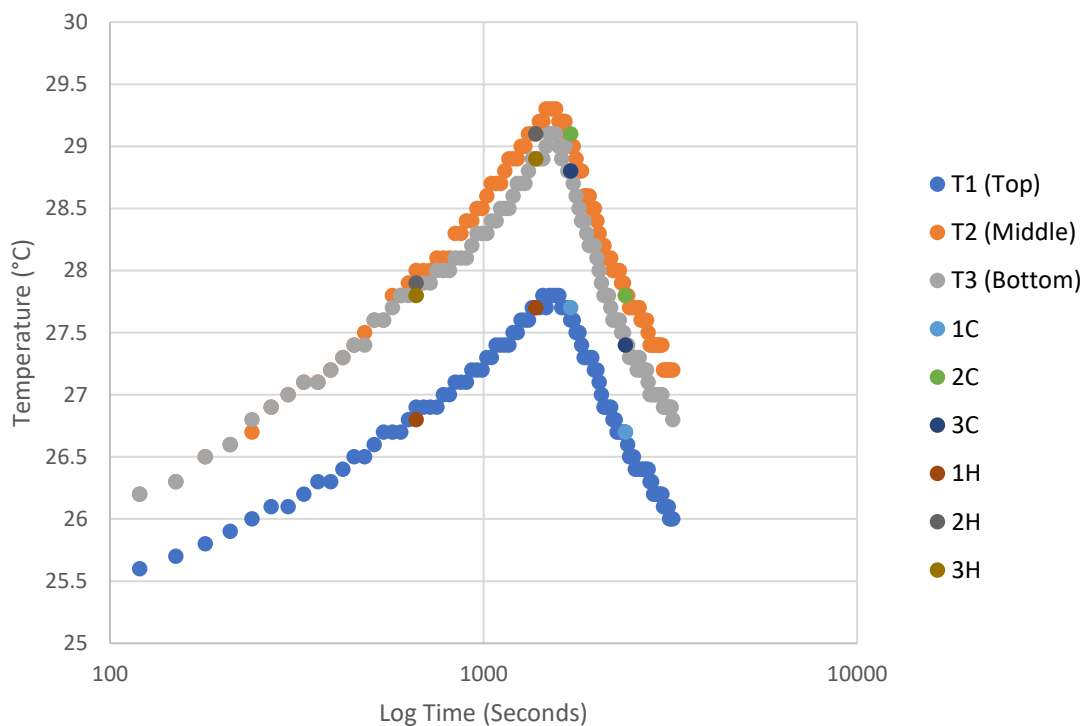


Figure 22: Example thermal curve for calibration test of thermal probe

Temperature was plotted versus time in log space, and the thermal conductivity was first evaluated by a simple line heat source analyses (Weschler, 1966) based on visual inspection of the linear portion of the curves during both the heating and cooling cycles. Linear regressions

along the curve used to estimate λ are indicated for the calibration test shown on **Figure 22** above. Thermal conductivity was then calculated from these linear regressions by:

$$\lambda = \frac{CQ}{4\pi(T_2 - T_1)} \ln \frac{t_2}{t_1}$$

where T_2 and T_1 are the temperatures at times t_2 and t_1 , respectively, and C is the calibration factor for the probe. As can be seen, nonlinearity of the thermal curve for the probe occurs due to the relatively high L/D ratio resulting in a departure from the infinite line theory. As a check for the fit of the linear regressions, the data were also evaluated by the “Simplified Slope Method” as described by ASTM D5334-14. In this method, temperature during the heating and cooling phases was plotted versus the $\ln t$ as shown in **Figure 23** below.

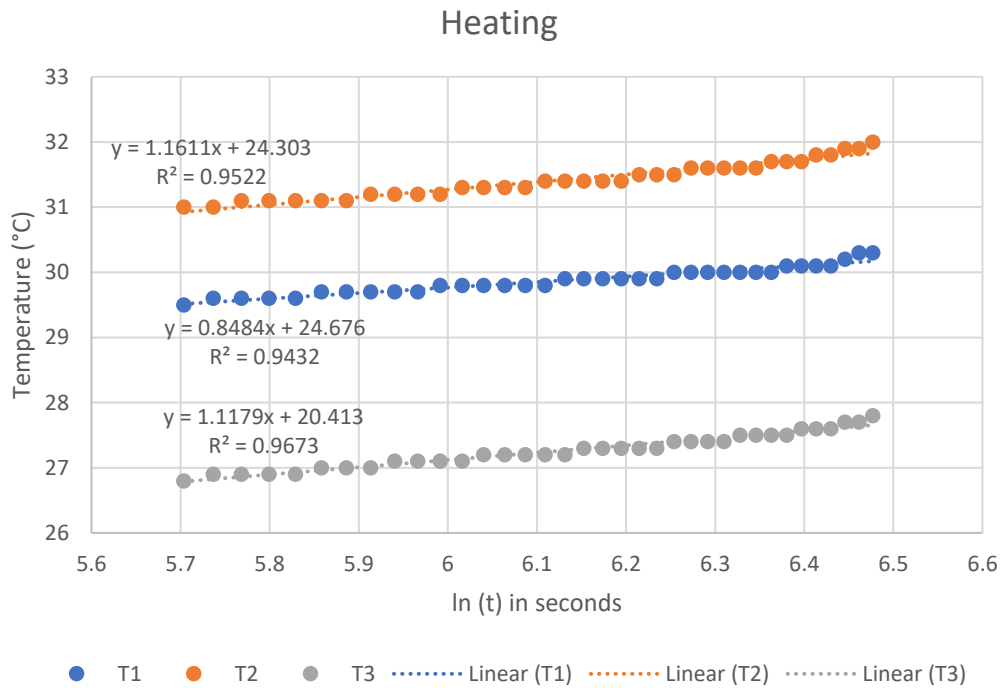
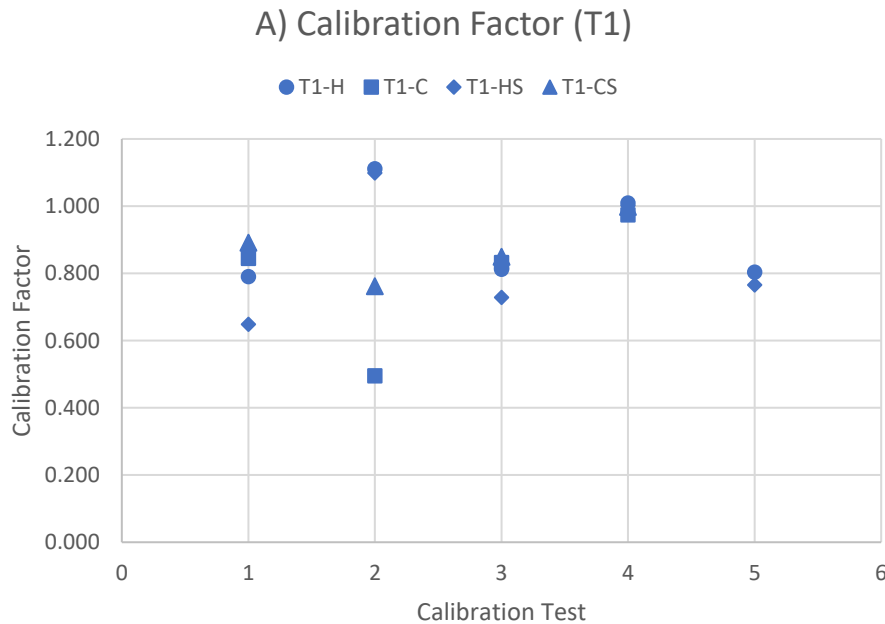


Figure 23: Example of simplified slope method during heating cycle

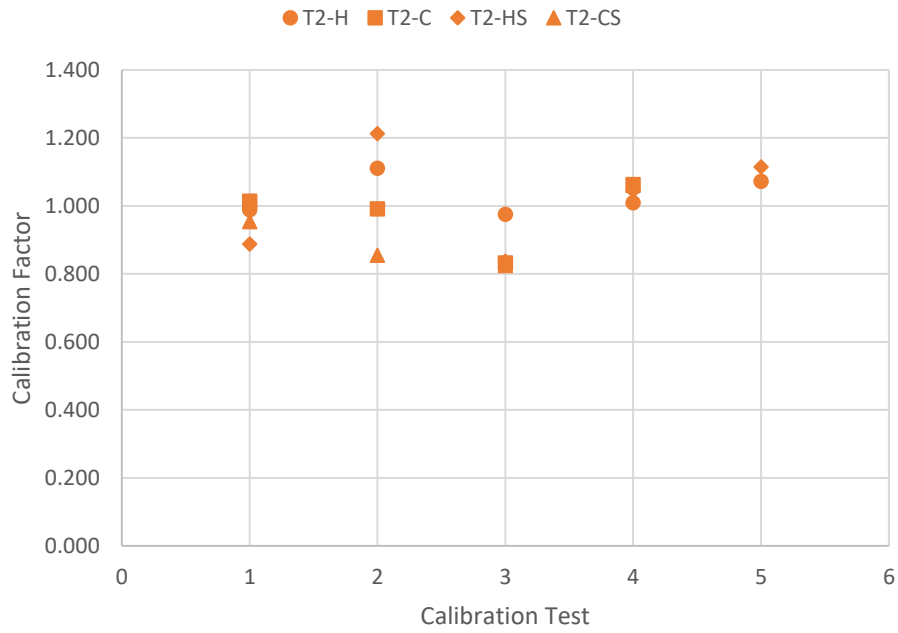
The slopes of linear regressions for the heating and cooling phases, S_H and S_C , respectively, were determined and used to calculate λ by:

$$\lambda = \frac{CQ}{4\pi S}$$

Early and late portions of the tests resulting from transient conditions and boundary effects, respectively (ASTM D5334-14), were neglected by visual inspection. The average of the four different evaluation methods (linear curve fitting, heating and cooling cycles; simplified method, heating and cooling cycles) was used to calculate the calibration factor for each thermocouple assuming a known thermal conductivity of 0.607 W/m.K for the stabilized water. The results for each of the five calibration tests performed are summarized in **Table 12** below and shown graphically in **Figure 24 (A-C)**. Note “H” and “C” designate a linear curve fit during the heating and cooling phases, while “HS” and “CS” indicate simplified slope method for the heating and cooling phases, respectively.



B) Calibration Factor (T2)



C) Calibration Factor (T3)

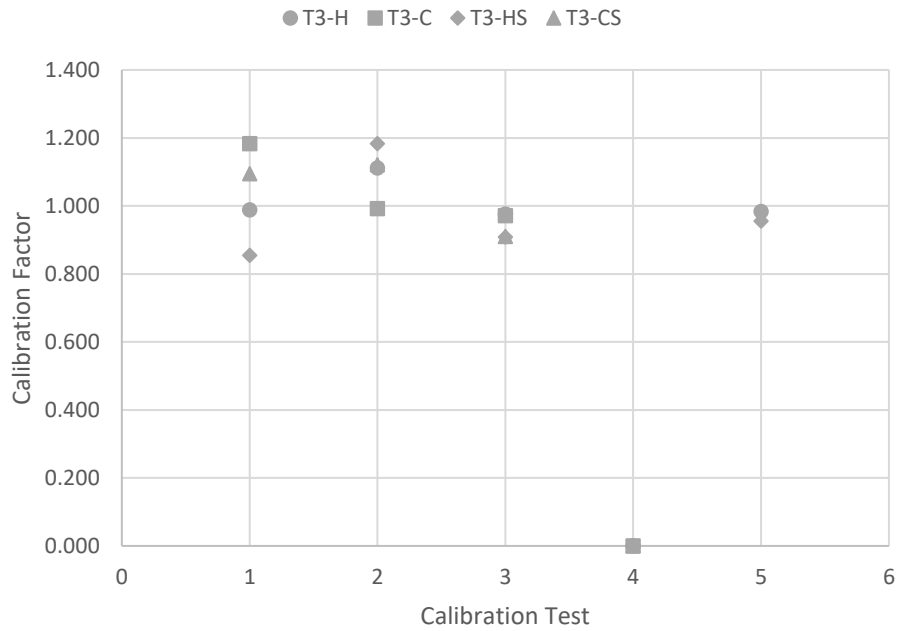


Table 12: Result of calibration testing for thermal probe using stabilized water

CALIBRATION TEST	AVERAGE ESTIMATED CALIBRATION FACTOR, C		
	T1 (Top)	T2 (Middle)	T3 (Bottom)
1	0.794	0.961	1.030
2	0.867	1.042	1.102
3	0.806	0.867	0.941
4	0.996	1.044	-
5	0.785	1.093	0.969
Average	0.849	1.002	1.010
Std. Dev.	0.079	0.080	0.062

Values for C for the middle and bottom thermocouples averaged 1.002 and 1.010 with standard deviations of 0.080 and 0.062, respectively. The top thermocouple, located closest to the exposed air, typically overestimated λ by approximately 15% likely from heat lost due to axial flow at the exposed top. Variability in the tested values are largely attributed to unshielded electronics being affected by electrical flow during heating as well as moisture infiltration. Based on the results of the calibration testing, the top thermocouple (T1) was generally used for reference only and not included in calculations of the λ to account for axial flow up the drill string. A calibration factor of 1.0 was assumed for thermocouples T2 and T3.

4.4.2 Field Testing

Testing was performed at three sites within the New Orleans area as shown on **Figure 24**. The first site, located at the offices of Eustis Engineering, L.L.C and designated as EY, is located in Metairie, Louisiana. The stratigraphy at the site can generally be characterized as surficial fill (approximately 1 to 1.5 meters) overlying Holocene deposits including swamp/marsh, interdistributary, and relic beach. The second site, a renovation of an existing building in

downtown New Orleans designated as SJS, overlays primarily point bar deposits grading from highly interbedded clays and silts into a silty sand approximately 18 meters (60 feet) below the existing ground surface. The third site, an addition to an existing warehouse in New Orleans East referred to as NOCS, can be characterized by several feet of sand fill overlying marsh/swamp, interdistributary, and abandoned distributary deposits.

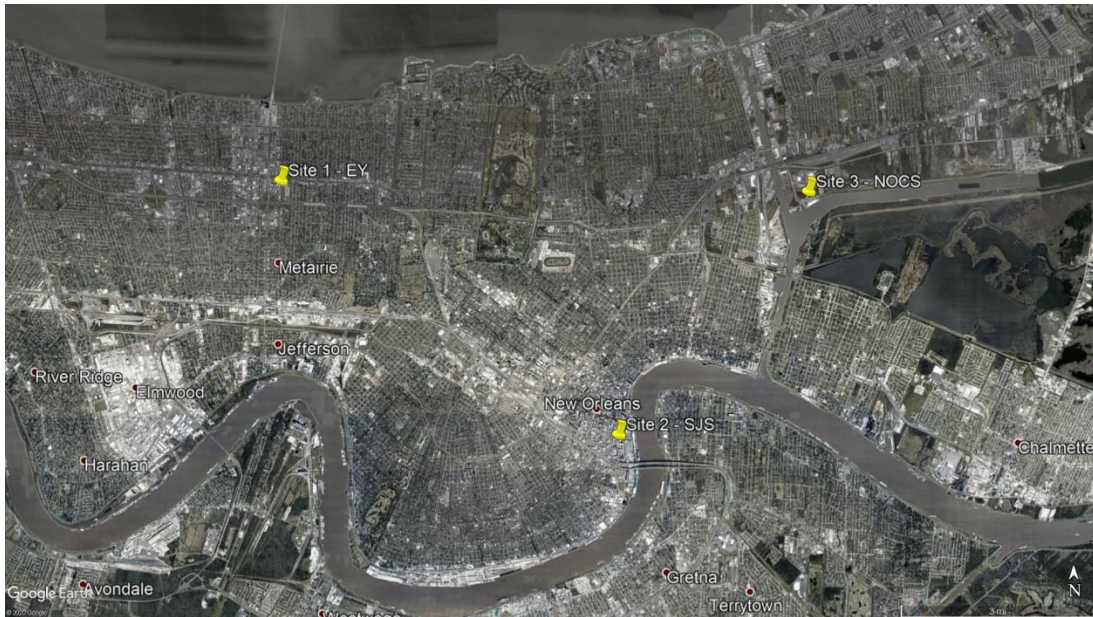


Figure 24: Locations of field testing

During field testing, the thermal probe was advanced to the planned test depths at a quasi-static hydraulic push rate of 2 cm/sec during the performance of a CPT. Prior to beginning each CPT, the probe was connected to the power and allowed to reach equilibrium over a period of approximately 15 minutes. Akrouch (2014) proposed the decay of excess heat developed from friction during the push could be used to determine λ . To evaluate this possibility, temperature was recorded throughout the soundings. A typical record of temperature during SJS-1 is provided on **Figure 25** below. Upon reaching the planned test depth, the cone temperature was allowed

stabilize for approximately 15 to 30 minutes to allow temperatures to reach equilibrium with the soils. Measurements of excess pore pressure during this stabilization period were taken during this period and continuing into the thermal loading period to evaluate their effects.

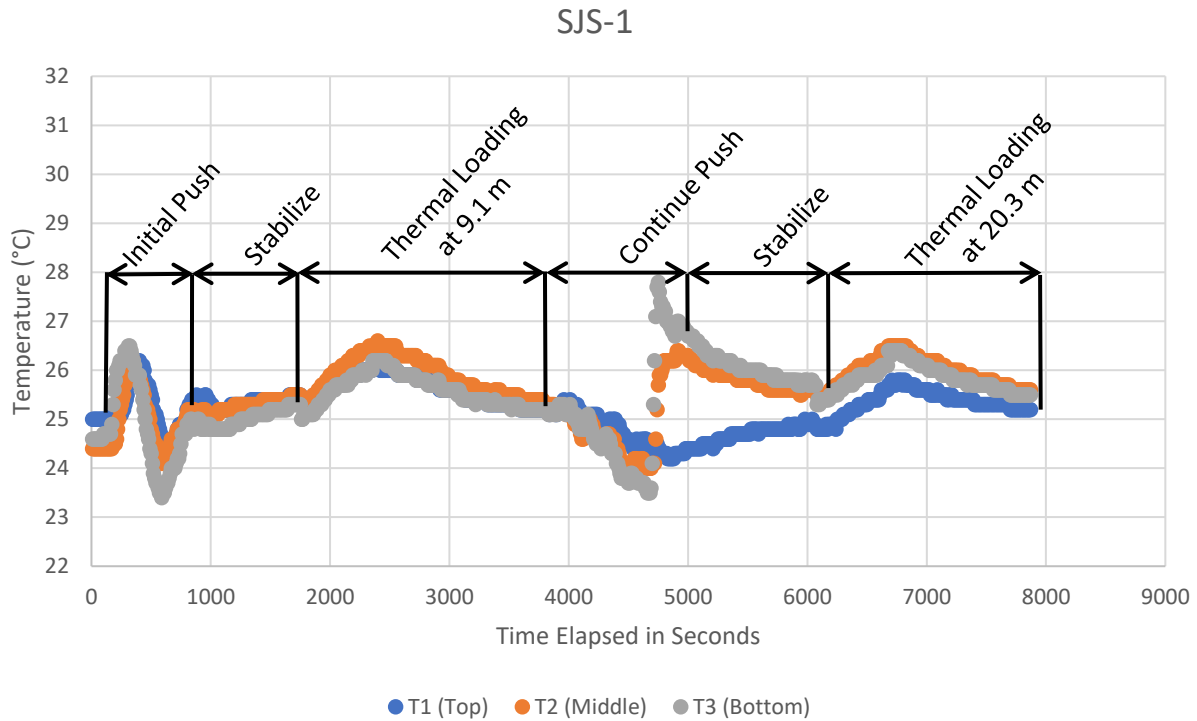


Figure 25: Temperature during CPT sounding

As can be seen, temperature response during the push can vary depending on soil/groundwater conditions as well as thermocouple position. Spikes in temperature were commonly observed when pushing in unsaturated soils above the groundwater table (as seen above in the first half of the initial push phase) or through medium dense to dense sand deposits (as seen in the continued push phase). When pushing through sand deposits, the magnitude of the temperature spike appears to be dependent on the thermocouple location, with lower thermocouples experiencing greater friction and temperature increases. On the other hand,

decreases in probe temperature when pushing through saturated soft clays (as seen above in the latter half of the initial push phase) or loose sands were also observed.

Once the probe reached thermal equilibrium, a constant voltage power source was applied to the heating elements to produce a 10 to 12 W/m heat input. The heating time required to induce a minimum +1°C change in measured temperature at all three thermocouples typically varied from 5 to 10 minutes after which the power source was shut off. Temperature was recorded throughout the heating and cooling processes by a datalogger and manually plotted to ensure thermal dissipation had reached a linear slope in log space, typically requiring 30 to 60 minutes. A typical thermal loading cycle from field testing is shown on **Figure 26**.

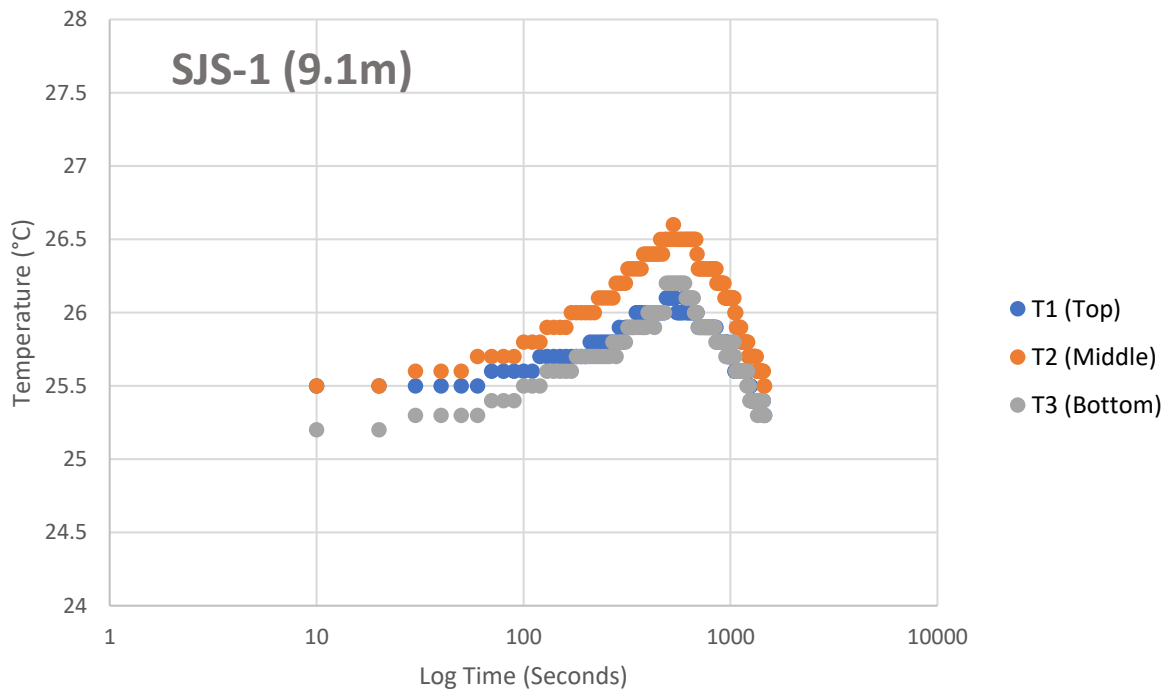


Figure 26: Typical thermal loading cycle during field testing

Simple line heat source analyses, as described in Section 4.4.1, were used to determine λ from the heating and cooling phases of the thermal loading cycles. As with the calibration tests,

thermal conductivity was estimated both by linear regression in log space and by the simplified slope methods. Estimates of thermal conductivity as measured in situ using the thermal probe, λ_p , are summarized below in **Table 13**. Data obtained from laboratory testing, including thermal conductivity λ_m , are provided in **Table 13** for reference and comparison.

Table 13: Summary of results for in situ testing of thermal conductivity

SITE	TEST	SOIL DESCRIPTION (GEOLOGY)	LABORATORY TEST DATA (IF AVAILABLE)				FIELD TEST
			ω	Υ_d		λ_m	λ_p
			(%)	(kN/m ³)	(pcf)	(W/m.K)	(W/m.K)
EY	EY-1 (3.0m)	Soft gray clay (Interdistributary)	99	6.6	42.2	1.006	1.110
	EY-1 (4.4m)	Loose gray silty sand (Relic Beach)	31	14.4	91.9	2.021	0.892
SJS	SJS-1 (9.1m)	Medium stiff gray silty clay (Point Bar)	37	12.4	78.9	1.839	1.298
	SJS-1 (20.3m)	Medium compact gray clayey silt (Point Bar)	33	13.7	86.2	2.083	1.270
	SJS-2 (9.1m)	Medium stiff gray silty clay (Point Bar)	37	12.4	78.9	1.839	0.974
	SJS-2 (21.8m)	Loose gray silty sand (Point Bar)	23	15.2	96.8	2.083	0.746
NOCS	NOCS-3 (5.5m)	Soft gray clay (Interdistributary)	91	7.7	49.0	-	1.017
	NOCS-3 (11.7m)	Medium stiff gray clay (Interdistributary)	54	11.0	69.9	1.448	1.440
	NOCS-3 (21.5m)	Medium dense gray silty sand (Abandoned Distributary)	27	14.8	94.5	-	1.596

In most cases, data taken from the middle thermocouple, T2, provided the least variability and simplest interpretation, while the data measured at the bottom thermocouple, T3, often provided very similar results but with more variability and data quality issues observed. Data taken from the top thermocouple, T1, typically resulted in estimated thermal conductivities

significantly higher than T2 and T3, indicating axial flow of heat up the drill string remained a problem in situ. For this reason, T1 was generally neglected in the averaged values reported. Standard deviations of estimated values for thermal conductivities between different thermocouple locations and evaluation methods typically ranged from 0.1 to 0.4 W/m.K.

Values of λ_p were plotted versus laboratory tests performed on soil samples taken from borings performed near the tests. These samples were primarily undisturbed samples taken using thin walled tubes; however, in cases of disturbed sampling using a split-spoon multiple samples of similar materials were combined and recompacted to an in-situ density and moisture content. These results are shown in **Figure 27** below. As can be seen, the TCT provided excellent comparison to laboratory test values between approximately 1.0 and 1.5 W/m.K. The TCT tended to underpredict the thermal conductivity as measured in the lab at thermal conductivities greater than 1.5 W/m.K. This is suggested to be the result of insufficient heat input being applied leading to overly long heating times during the field tests.

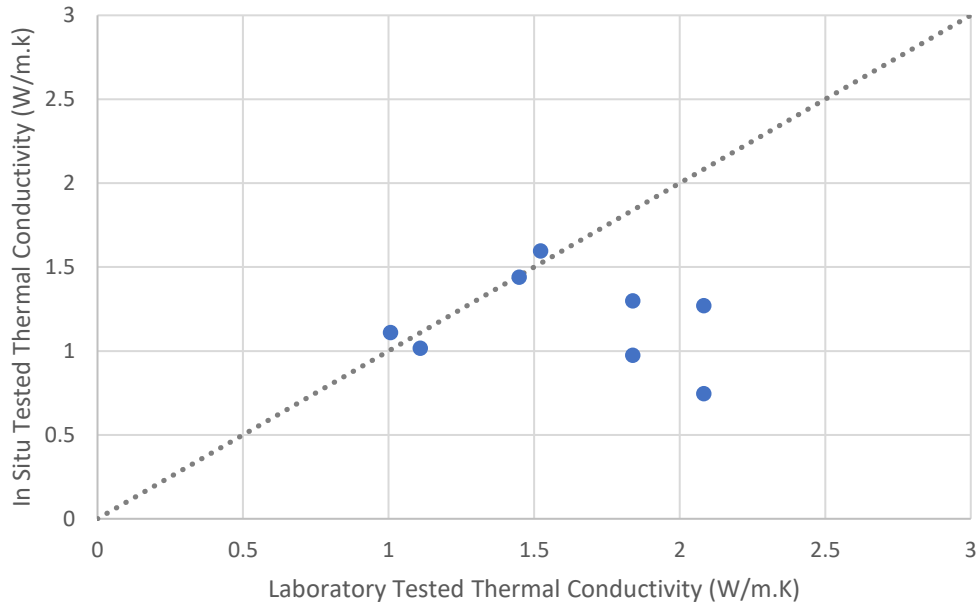


Figure 27: Comparison of in situ and laboratory test values for thermal conductivity

Attempts were made to estimate λ using the method based on dissipation as proposed by Akrouch (2014) met with limited success. Values for t_{50} , the time required to achieve 50% dissipation of the thermal pulse induced by heating, were selected by estimating the thermal peak and the point it returned to the pre-heating temperature. When used in the proposed equation, these resulted in estimated thermal conductivities ranging from 0.05 to 0.2 W/m.K, lower than should be considered reasonable for soils. It is possible the curve fitting parameters proposed by Akrouch (2014) may not be applicable to this geological setting and further research is required.

Chapter 5: Results and Discussion

5.1 Geotechnical Feasibility of Energy Piles in New Orleans

Through empirical correlations; established laboratory testing procedures; and newly developed in situ testing methods, this work developed estimates of typical values for thermal conductivity of alluvial soils encountered in foundation design in the New Orleans area. These estimates can be combined with available geological mapping performed by USACE to provide a general understanding of the suitability of soils and basic expectations for GHPs within these soils. This is shown graphically below in **Figure 28**.

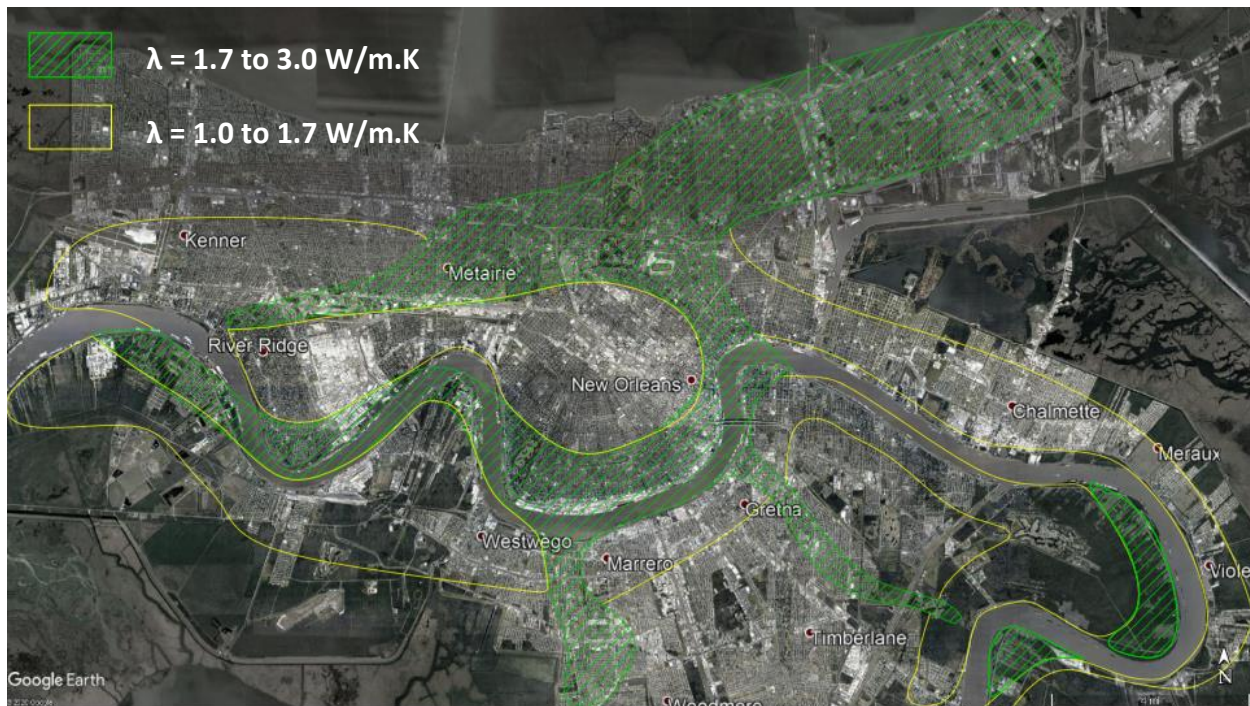


Figure 28: Estimated typical thermal conductivity

The highest thermal conductivities, and thus the greatest opportunities for GHPs installation, will typically be found in deposits of fully saturated, coarse grain materials. These

typically correspond to point bar, relict beach, or abandoned distributary geological deposits as shown by green hatching in the figure above. Based on the evaluations of λ presented in this study, typical values within these deposits may range from approximately 1.7 to 3.0 W/m.K. Saturated fines, most commonly associated with natural levee, interdistributary, or prodelta deposits, are estimated to have thermal conductivities ranging from 1.0 to 1.7 W/m.K and are delineated in yellow. Organic deposits found in swamp/marsh environments are anticipated to have typical thermal conductivities below 1.0 W/m.K.

Previous economic studies of energy piles in cooling dominated climates such as New Orleans were performed by Khan and Wang (2014) and Akrouch (2014) assuming values of thermal conductivity equal to 1.48 W/m.K and 1.87 W/m.K, respectively. The estimated performance of these systems as reported by Khan and Wang (2014) and Akrouch (2014) are summarized in **Table 14** below.

Table 14: Summary of previous economic studies (adapted from Khan and Wang, 2014; Akrouch, 2014)

STUDY	TOTAL GHX LENGTH		ASSUMED λ (W/m.K)	PERCENTAGE OF TOTAL HVAC LOAD PROVIDED BY GHP		ESTIMATED REDUCTION IN POWER USAGE (kWh per year)
	(m)	(ft)		COOLING	HEATING	
Khan and Wang (2014)	390	1280	1.48	13.34%	63.50%	~25,000
Akrouch (2014)	4,734	15,530	1.87	19.90%	68.12%	185,800

Given that the climatic conditions assumed for these two studies are typical for cooling dominated climates like New Orleans, comparisons on the system efficiency can be made based on the subsurface conditions; in this case, measured through the thermal conductivity of the soil.

Based on the evaluation of thermal conductivity presented in this study, the assumed values used for these studies appear reasonable and within anticipated values. This provides some validation to the two economic studies. Thus, the opportunity exists for significant cost savings from the use of GSHPs in New Orleans, if properly designed.

5.2 Design Responsibilities

To fully take advantage of the opportunity provided by GHPs, a better understanding of both the system and the design responsibilities is required. As described by Tapia (2017), the geothermal industry in Louisiana (and to a lesser degree, the United States in general) is still in its infancy; therefore, many of the issues and inefficiencies currently seen with GHP systems are the result of improper sizing of system components due to a lack of information, inexperience, or confusion regarding design responsibilities. In current practice, little communication is expected between geotechnical engineers evaluating subsurface conditions and mechanical engineers designing HVAC systems. Instead, design and evaluation typically flow linearly in the project lifespan from geotechnical to structural to mechanical engineers. This current practice leaves mechanical engineers to make assumptions regarding the subsurface conditions and how the GHX systems they design will interact. Proper design of energy foundations requires detailed ground investigation and interaction between all disciplines. These design considerations and responsibilities, adapted from Brandl (2006), are shown below in **Figure 29**.

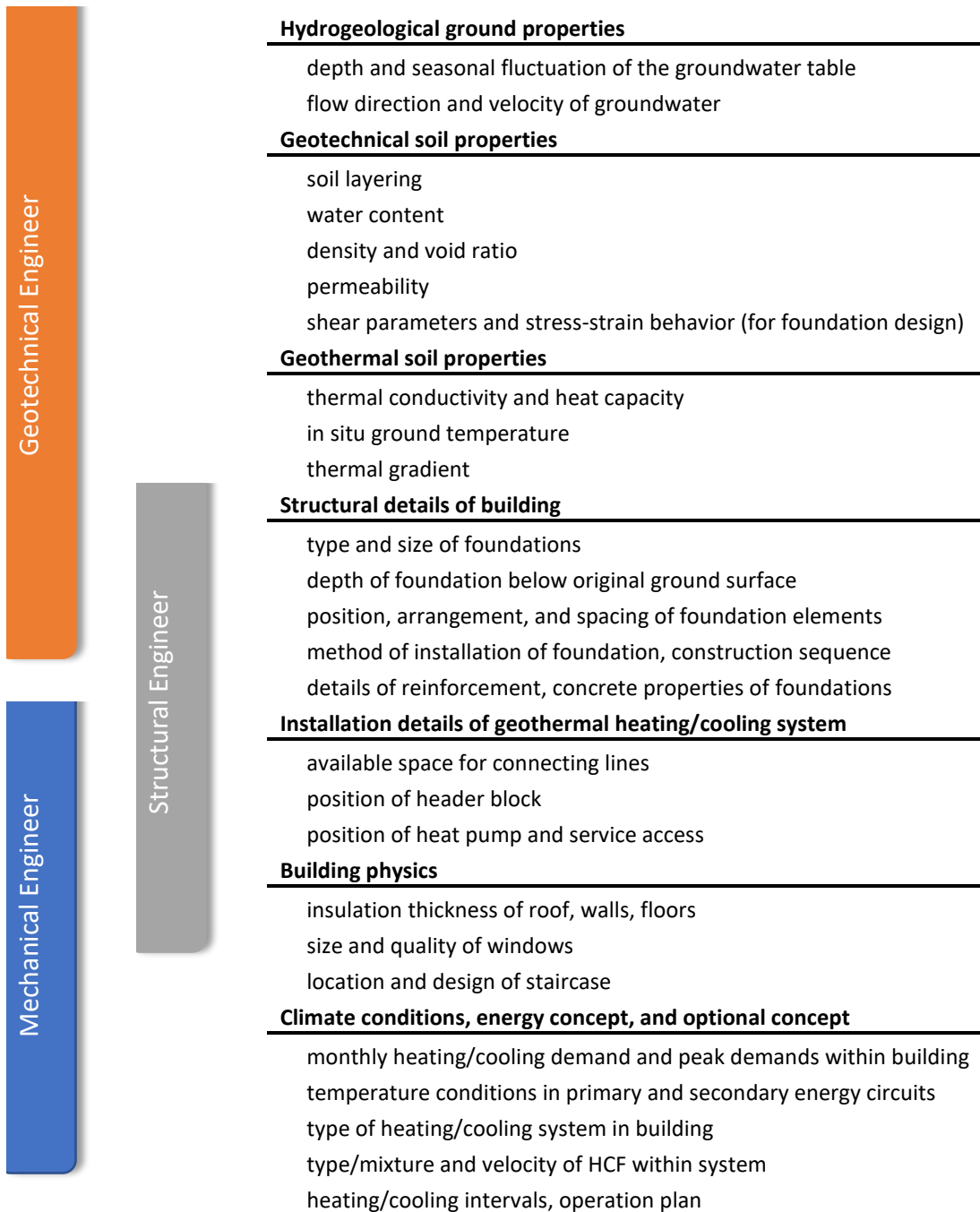


Figure 29: Summary of design parameters and responsibilities

Most parameters shown in **Figure 29** above are widely interacting and may have impacts to both later design and earlier work. Therefore, design should be considered an iterative process with communication between all disciplines essential to optimize the most cost-efficient GSHP design.

5.3 Determination of λ

One of the first steps in evaluating the thermal properties of the foundation soils for a geotechnical engineer is the determination of thermal conductivity. Although other inputs may have an impact on the way heat exchange will occur below the ground surface, thermal conductivity is often the most variable and site-specific while being the simplest to evaluate. This value can be provided to other stakeholders in the design as a means of quantifying subsurface heat exchange properties.

On a desktop study level, any of the Kersten (1949), Johansen (1975), or Côté and Konrad (2005) models appeared to provide reasonable conservative estimates of thermal conductivity with moisture content, bulk density, and soil texture being the primary inputs. Of the three, Côté and Konrad (2005) produced the least error and is recommended for use. Selection of the quartz fraction will have a significant effect on the assumed λ_s . Unless otherwise known, quartz fractions of 0% and 80% are recommended for New Orleans alluvial clays/silts and sands, respectively.

Laboratory testing of thermal conductivity on undisturbed or reconstituted samples in accordance with ASTM D5334-14 remains the most accurate means of estimating thermal

conductivity. Discrete tests performed on several borings along the depth of a boring can be combined with typical geotechnical index testing to provide excellent estimates of λ .

5.4 Recommendations for In Situ Testing of λ

While laboratory can provide accurate and repeatable estimates of thermal conductivity on undisturbed or reconstituted samples, this testing method cannot quantify the potential impact of heat convection as the result of groundwater flow in situ. Additionally, sample disturbance may result in error between laboratory estimated values and the actual performance of energy piles. Therefore, in situ testing could be considered as necessary in the future to supplement a laboratory testing program. Still in the experimental stage, these testing methods will require additional research to produce a standardized test method and make available for commercial use. Some recommendations for in situ testing based on the experiences gained in this study include:

- Thermal response of the cone during advancement to depth varies; thus, dissipation of frictional heat alone cannot be relied upon. It is recommended that a heating element be incorporated into all designs.
- ASTM D5334-14 recommends a heating element be provided such that the temperature change is less than 10 K in 1000 s. Care should be taken in sizing the heating element and power supply such that sufficient heat input is applied. Based on the heating times observed in this study, this is estimated to be approximately 60 W/m for a similarly size probe.

- Axial flow of heat up the drill string may have an influence on the estimated thermal conductivity. To reduce this potential at an individual thermocouple, the heating element is recommended to extend at least 30 cm (11.8 in) on either side of the sensor.
- The use of multiple thermocouple junctions was beneficial as it provided testing redundancy and some validation at a single test depth.
- Electronics must be properly shielded, both from water intrusion and electrical current as a result of operating the electric cone penetrometer. Ideally measurements of temperature would be taken using the CPT software, allowing for continuous graphing of data in the same manner as a PWP dissipation test.

5.5 Limitations and Future Research

This work was meant to provide a general understanding of the suitability of soils and basic expectations for system efficiencies within alluvial deposits in the New Orleans area. Variations in the actual performance of GHP systems should be expected and require a site-specific investigation be performed by a design team experienced in energy piles. However, this research can be used to better understand and model the geothermic processes that govern the performance of energy piles. While the technology is extremely promising, additional research is required to be able to optimize the design and construction of these systems and maximize the potential savings.

Additional research is recommended to further develop our understanding of the thermal behavior of Holocene alluvial soils. This would include an evaluation of appropriate values for λ_s

by examining the mineralogical composition of these soils and inversion of the Johansen (1975) method using samples with known thermal conductivities obtained through laboratory testing.

This study largely focused on thermal conductivity under the assumption that conduction was the primary method of heat transfer in soils; however, groundwater flows in the New Orleans area could significantly affect the performance of geothermal foundations. As described by Brandl (2006), high groundwater flows are beneficial in heating or cooling-dominated climates as they moderate long-term heat buildup. A methodology for understanding how groundwater flow, occurring naturally or as the result of seasonal flooding of the Mississippi River, is required to model the long-term heat balance in energy piles.

As the technology matures and understanding of the way energy piles work is expanded, optimization system components will lead to even better cost savings. By simply using the resources already available, we can reduce our energy consumption and impact on the natural environment.

References

- Abu-Hamdeh, N., Khadair, A., Reeder, R. (2001) "A comparison of two methods used to evaluate thermal conductivity for some soils", *International Journal Heat Mass Transfer*, vol. 44, no. 14, p. 1073-1078.
- Akrouch, G.A., (2014) "Energy piles in cooling dominated climates", Ph.D. dissertation, Texas A&M University, College Station, TX, USA.
- Autin, W.J., Burns, S.F., Miller, B.J., Saucier, R.T., and Snead, J.I. (1991) "Quaternary geology of the lower Mississippi Valley", *Geological Society of America, Decade of North American Geology, Quaternary nonglacial geology*, vol. 2, p. 547-582.
- ASTM, (2008) "Standard test method for determination of thermal conductivity of soil and soft rock by thermal needle probe procedure", D5334-08, West Conshohocken, PA, USA.
- ASTM, (2012) "Standard test method for electronic friction cone and piezocone penetration testing of soils", D5778-12, West Conshohocken, PA, USA.
- Bou-Mekhayel, M. (2019) "Geotechnical and geothermal properties of Louisiana coastal sediments", *University of New Orleans Theses and Dissertations*, 2589. <https://scholarworks.uno.edu/td/2589>
- Bahadori, Mehdi N. (1978) "Passive Cooling Systems in Iranian Architecture." *Scientific American*, vol. 238, no. 2, pp. 144–154., doi:10.1038/scientificamerican0278-144.
- Blum, M.D., (2007) "Large rivers and climate change, past and future", *Large Rivers: Geomorphology and Management*, ed. A. Gupta, p. 627-660, London, United Kingdom.
- Blum, M.D. and Roberts, H.H., (2012) The Mississippi Delta Region: Past, Present, and Future, *Annual Review of Earth and Planetary Sciences*, v. 40, p. 655-683
- Bourne-Webb P.J., Amatya B., Soga K., et al., (2009) "Energy pile test at Lambeth College, London: geotechnical and thermodynamic aspects of pile response to heat cycles", *Géotechnique*, vol. 59, no. 3, p. 237-249.
- Brandl, H., (2006) "Energy foundations and other thermos-active ground structures," *Géotechnique*, vol. 56 (2), p. 81-122.
- Brandon, T.L., and Mitchell, J.K., (1989) "Factors influencing thermal resistivity of sands", *Journal of Geotechnical and Geoenvironmental Engineering*, vol. 115 (12), p. 1683-1698.

- Brettmann T., Amis T., Kapps K., (2010) "Thermal conductivity analysis of geothermal energy piles", *Proceeding of the 11th International Conference on Geotechnical Challenges in Urban Regeneration*, DFI2010, London.
- BS EN 15450 (2007) "Heating systems in buildings – design of heat pump heating systems", *BSI*, p. 50.
- Campbell, G.S., Jungbauer, J.D., Bidlake, W.R., Hungerford, R.D., (1994) "Predicting the effect of temperature on soil thermal conductivity", *Soil Science*, vol. 158 (5), p. 307-313.
- Carslaw, H.S., and Jaeger, J.C., (1959) *Conduction of Heat in Solids*, Oxford Univ. Press, London, UK.
- Chen, Z.X., Guo, X.X., Shao, L.T., Li, S.Q., (2020) "On determination method of thermal conductivity of soil solid material", *Soils and Foundations*, 60, p. 218-228.
- Côté, J., and Konrad, J.M., (2005) "A generalized thermal conductivity model for soils and construction materials", *Canadian Geotechnical Journal*, vol. 42, p. 443-458.
- Day, J.W., Kemp, G.P. Freeman, A.M., and Muth, D.P., (2014) *Perspectives on the Restoration of the Mississippi Delta: The Once and Future Delta*, Springer, Netherlands.
- Deubert, R.E., (1982) Correlation of Compression Index and Soil Properties of New Orleans Area Clays. A thesis submitted to the graduate faculty Tulane University in partial fulfillment of the requirements for the degree of M.S. in the Department of Civil Engineering.
- Desmedt, J., Van Bael, J., Hoes, H., and Robeyn, N., (2010) "Experimental performance of borehole heat exchangers and grouting materials for ground source heat pumps", *International Journal of Energy Research*, vol. 36 (13), p. 1238-1246.
- De Vries, D.A., (1952) "The thermal conductivity of soil", *Mededelingen van de Landbouwhogeschool to Wageningen* 52 (1), p. 1-73, translated by Building Research Station (Library Communication No. 759), England.
- Dupray, F., Laloui, L., and Kazangba, A., (2014) "Numerical analysis of seasonal heat storage in an energy pile foundation." *Computers and Geotechnics*, 55(0), p. 67-77.
- Ewen, J., and Thomas, H.R., (1992) "The thermal probe – measurement of the thermal conductivity and drying rate of soil in the field", *Geotechnical Testing Journal*, ASTM, vol. 15 (3), p. 256-263.
- Farouki, O.T., (1986) "Thermal properties of soils", *Series on rock and soil mechanics*, vol. 11., Trans Tech Publ., Clausthal-Zellerfeld, Germany.

- Fisk, H.N., (1944) "Geological investigation of the alluvial valley of the lower Mississippi River", War Department, Corps of Engineers, Washington DC, p. 78.
- Fisk, H.N., McFarlan, E., Kolb, C.R., and Wilbert, L.J., (1954) "Sedimentary Framework of the modern Mississippi Delta." Journ. Sed. Petr., vol 24, No. 2, pp. 76-99.
- Friedman, Robert. (1984) "The Air-Conditioned Century." *American Heritage*.
- Fourier, J. B., (1822) *Théorie Analytique de la Chaleur*, translated by A. Freeman, Dover Publications, New York, NY, USA.
- Gao J., Zhang X., Liu J., et al., (2008) "Numerical and experimental assessment of thermal performance of vertical energy piles: an application", *Applied Energy*, vol. 85, no. 10, p. 901-910.
- Galloway, W.E., Whiteaker, T.L, and Ganey-Curry, P., (2011) "History of Cenozoic North American drainage basin evolution, sediment yield, and accumulation in the Gulf of Mexico basin, *Geosphere*, 7(4), p. 938-973.
- Gemant, A., (1952) "How to compute thermal soil conductivities", *Heating, Pipping, and Air Conditioning*, vol. 24 (1), p. 122-123, 1952.
- Hansson, Klas, and Lars-Christer Lundin, (2005) "Equifinality and Sensitivity in Freezing and Thawing Simulations of Laboratory and in Situ Data", *Cold Regions Science and Technology*, Elsevier, www.sciencedirect.com/science/article/pii/S0165232X05000923.
- Hamada, Y., Saitoh H., Nakamura M., et al., (2007) "Field performance of an energy pile system for space heating", *Energy and Buildings*, vol. 39, no. 5, p. 517-524.
- Henderson H.I., Carlson S.W., Walberger A.C., (1998) "North American monitoring of a hotel with room size GSHPs", *Proceedings of the IEA Room Size Heat Pump Conference*, Niagara Falls, Canada.
- Hillel, D., (1982) *Introduction to Soil Physics*, Academic Press, San Diego, CA, USA, p. 155-170.
- Horai, K.I., (1971) "Thermal conductivity of rock-forming minerals, *Journal of Geophysical Research*, 76(5), p. 1278-1308.
- Hooper, F.C., and Lepper, F.R., (1950) "Transient heat flow apparatus for the determination of thermal conductivities", *ASHVE Trans.*, 56, p. 309.

- IEEE 442-2017 (2017) "IEEE guide for thermal resistivity measurements of soils and backfill materials", *IEEE Standards Association*, The Institute of Electrical and Electronics Engineers, Inc.
- Ingersoll, J.G., (1988) "Analytical determination of soil thermal conductivity and diffusivity", *Journal of Solar Energy Division*, vol. 110, p. 306-312.
- Jalaluddin J., Miyara A., Tsubaki K., et al., (2010) "Thermal performances of three types of ground heat exchangers in short-time period of operation", *International Refrigeration and Air Conditioning Conference*, Paper 1123, available at <http://docs.lib.purdue.edu/iracc/1123>.
- Janbu, N., and Senneset, K., (1974) "Effective stress interpretation of in-situ penetration tests", *Proceedings of the European Symposium on Penetration Testing*, vol. 1, Stockholm, Sweden.
- Johansen, O., (1975) "Thermal conductivity of soils", Ph.D. thesis, Trondheim, Norway, CRREL Draft Translation 637 (1977), ADA 044002.
- Katsura T., Nakamura Y. Okawada T., et al., (2009) "Field test on heat extraction or injection performance of energy piles and its application", *Proceedings of the 11th International Conference on Thermal Energy Storage, Stockholm, EFFSTOCK 2009*, Paper 143, available at [http://intraweb.stockton.edu/eyos/energy_studies/content/docs/effstock09/Posters/146 .pdf](http://intraweb.stockton.edu/eyos/energy_studies/content/docs/effstock09/Posters/146.pdf).
- "Keeping Cool in the Face of Climate Change," *United Nations*, United Nations, 30 June 2019, news.un.org/en/story/2019/06/1041201.
- Kersten, M.S., (1949) "*Thermal properties of soils*", *Bulletin 28*, Minneapolis: Engineering Experiment Station, University of Minnesota, MN, USA.
- Kipry H., Bockelmann F., Plessner S., et al., (2009) "Evaluation and optimization of UTES systems of energy efficient office buildings (WKSP)", *Proceedings of the 11th International Conference on Thermal Energy Storage, Stockholm, EFFSTOCK 2009*, Paper 43, available at [http://intraweb.stockton.edu/eyos/energy_studies/content/docs/effstock09/Session 6 1 Case studies residential and commercial buildings/43.pdf](http://intraweb.stockton.edu/eyos/energy_studies/content/docs/effstock09/Session_6_1_Case_studies_residential_and_commercial_buildings/43.pdf)
- Khan, M., and Wang, J.X., (2014) "Study on energy foundation design in South Louisiana", *Geo-Congress 2014 Technical Papers*, GSP 234, p. 3799-3806.
- Kolb, C.R. and Van Lopik, J.R., (1958) "Geology of the Mississippi River Deltaic Plain, Southeastern Louisiana," Technical Report No. 3-483, U.S. Army Engineer Waterways Experiment Station, Vicksburg, Mississippi.

- Laloui, L., Nuth, M., Vulliet, L., (2006) "Experimental and numerical investigations of the behavior of a heat exchanger pile", *International Journal for Numerical Methods in Geomechanics*, vol. 30, no. 8, p. 783-781.
- Laloui, L., and Nuth M., (2009) "Investigations on the mechanical behavior of a Heat Exchanger Pile", *5th International Symposium on Deep Foundations on Bored and Auger Piles (BAP V)*, Universtiy of Gent, Belgium, p. 343-347.
- Laloui, L., and Donna, A.D., (2013) *Energy Geostructures: Innovation in Underground Engineering*, ISTE Ltd., London, UK.
- Lee, K.S., (2013) *Underground Thermal Energy Storage*, Springer-Verlag, London, UK.
- Lisiecki, L.E., and Raymo, M.E., (2005) "A Pliocene-Pleistocene stack of 57 globally distributed benthic $\delta^{18}O$ records" *Paleoceanography*, vol. 20.
- Lu, S., Ren, T., Gong, Y., and Horton, R., (2007) "An improved model for predicting thermal conductivity from water content at room temperature", *Soil Science Society of America*, vol. 71 (1), p. 8-14.
- Lutenegger, A.J., and Lally, M.J., (2001) "In situ measurement of thermal conductivity in soft clay", *International Conference on In-situ measurement of soil properities and case histories*, Bali, Indonesia.
- Mayne, P., (2007) "NCHRP synthesis 368, cone penetration test", NCHRP, Transportation Research Board, Washington D.C., USA.
- Mitchell, J.K., and Koa, T.C., (1951) "Measurement of soil thermal resistivity", *Journal of Geotechnical Engineering Division of the American Society of Civil Engineers*, vol. 104, GT10, p. 1307-1320.
- Montgomery, R.L., (1974) "Correlation of Engineering Properties of Cohesive Soils Bordering the Mississippi River from Donaldsonville to Head of Passes, La.," U.S. Army Engineer Waterways Experiment Station, Vicksburg, Mississippi.
- Morino K., and Oka T., (1994) "Study on heat exchanged in soil by circulating water in steel pile", *Energy and Buildings*, vol. 21, no. 1, p. 65-78.
- Nagano K., Katsura T., Takeda S., et al., (2005) "Thermal characteristics of steel foundation piles as ground heat exchangers", *Proceeding of the 8th IEA Heat Pump Conference*, Las Vegas, NV, p. 6-12.

- Narsilio, G.A., Johnston, I.W., Bidarmaghz, A., et al., (2014) "Geothermal energy: introducing an emerging technology", *Proceedings of the International Conference on Advances in Civil Engineering for Sustainable Development (ACESD 2014)*, Nakhon Ratchasima, Thailand, vol. 1.
- Nikoosokhan, S., H. Nowamooz, and C. Chazallon, (2015) "Effect of dry density, soil texture and time-spatial variable water content on the soil thermal conductivity", *Geomech. Geoeng.*
- Olgun, C.G., (2013) "Energy Piles: Background and Geotechnical Engineering Concepts", 16th Annual George F. Sowers Symposium, Atlanta, GA, USA, 7 May 2013.
- Pahud D., and Hubbuch M., (2006) "Measured thermal performances of the Dock Midfield energy pile system at Zurich airport", *14 Schweizerisches Status-Seminar, Energy und Umweltforschung im Bauwesen*, ETH Zurich, p. 217-224.
- Penland, P.S., Boyd, R., and Suter, J.R., (1988) "Transgressive depositional systems of the Mississippi River delta plain: a model for barrier shoreline and shelf sand development", *J. Sediment Res.*, vol. 58, p. 932-949.
- Penner, E., (1963) "Anisotropic thermal conduction in clay sediments", *Proceedings of the International Clay Conference*, Vol. 1, p. 363-376.
- Penner, E., (1975) "Thermal conductivity of frozen soils", *Canadian Journal of Earth Sciences*, 7: p. 982-987.
- Rao, M.V, and Singh, D.N., (1999) "A generalized relationship to estimate thermal resistivity of soils", *Canadian Geotechnical Journal*, vol. 36, p. 767-773.
- Rees, S.W., Adjali, M.H., Zhou, Z., Davies, M., and Thomas, H.R., (200) "Ground heat transfer effect of the thermal performance of the earth contact structures", *Renewable and Sustainable Energy*, vol. 3, p. 213-265.
- Remund, C. and Card, R. (2009). *IGSHPA residential and light commercial design and installation manual*. International Ground Source Heat Pump Association
- Rittenour, T.M., Blum, M.D., and Goble, R.J., (2007) "Fluvial evolution of the lower Mississippi River valley during the last 100 k.y. glacial cycle: response to glaciation and sea-level change", *Geological Society of America Bulletin*, vol. 119(5-6), p. 586-608.
- Sass, J.h., Lachenbruch, A.H., and Munroe, R.J., (1971) "Thermal conductivity of rocks from measurements on fragments and its application to heat-flow determinations, *Journal of Geophysical Research*, 76(14), p. 3391-3401.

- Saucier, R.T., (1963) *Recent Geomorphic History of the Pontchartrain Basin*, Louisiana State University Studies, Coastal Studies Series, No. 9, 114p.
- Schleiermacher, A.L.E.F., (1888) "Über die Waermeleitung der Gase", *Ann. Phys. Chem.* 34, p. 623.
- Schnürer H., Sasse C., Fisch M.N., (2006) "Thermal energy storage in office buildings foundations", *Proceedings of the 10th International Conference on Thermal Energy Storage*, ECOSTOCK, Galloway, NJ, available at http://intraweb.stockton.edu/eyos/energy_studies/content/docs/FINAL_PAPERS/11A-4.pdf.
- Sekine K., Ook R., Yokoia M., et al., (2005) "Development of a ground source heat pump system with ground heat exchanger utilizing the cast-in-place concrete pile foundations of a building", *Proceedings of the World Sustainable Buildings Conference*, Tokyo, p. 1059-1066.
- Stalhane, B., and Pyk, S., (1931) "New method for determining the coefficients of thermal conductivity", *Tek Tidskr.*, 61, p. 389.
- Tapia, C.L.D., (2017) "Analysis of cost and energy performance of geothermal heat pump systems in Southern Louisiana", *LSU Master's Theses*, 4504, https://digitalcommons.lsu.edu/gradschool_theses/4504
- Teh, C.I., and Houlsby, G.T., (1991) "An analytical study of the cone penetration test in clay", *Géotechnique*, vol. 59 (4), p. 365-375.
- Tong, B., Gao, Z., Horton, R., et al., (2016) "An empirical model for estimating soil thermal conductivity from soil water content and porosity", *Journal of Hydrometeorology*, vol. 17, p. 604-613.
- Torstensson, B.A., (1975) "Pore pressure sounding instrument", *Proceedings of Specialty Conference on In Situ Measurement of Soil Properties*, Raleigh, N.C., vol. 2, p. 48-54.
- U.S. Department of Commerce, Economics and Statistics Administration, U.S. Census Bureau, et al. May 2010. www.census.gov/content/dam/Census/library/publications/2010/demo/p25-1139.pdf.
- U.S. Army Engineer Waterways Experiment Station, (1952) *Geological Investigation of the Atchafalaya Basin and the Problem of Mississippi River Diversion*, Mississippi River Commission, Vicksburg, Mississippi.
- U.S. Army Engineer Waterways Experiment Station, (1958) *Geological Investigation of the Mississippi River-Gulf Outlet Channel*, Lower Mississippi Valley Division, Vicksburg, Mississippi.

- Van Rooyen, M., and Winterkorn, H.F., (1957) "Structural and textural influences on thermal conductivity of soils", *Highway Research Board Proceedings*, 39, p. 576-621.
- Van der Held, E.M.F., and Van Drunen, F.G., (1949) "A method of measuring the thermal conductivity of liquids", *Physics*, 15, p. 865.
- Von Herzen, R., and Maxwell, A.E., (1959) "The measurement of thermal conductivity of deep-sea sediments by a needle-probe method", *Journal of Geophysical Research*, vol. 64, no. 10, p. 1557-1563.
- Weishaupt, J., (1940) "Nichtstationäre verfahren zur bestimmung der wärmeleitfähigkeit von flüssigkeiten (non-stationary methods for determination of thermal conductivity of liquids)", *Forschung im Ingenieurwesen*, 11(1), p. 20-34.
- Welder, F.A., (1954) Deltaic Processes in Cubits Gap Area Plaquemines Parish, Louisiana. A thesis submitted to the graduate faculty of the Louisiana State University in partial fulfillment of the requirements for the degree of Ph.D. in the Department of Geology, 1954.
- Weschler, A.E., (1966) "Development of thermal conductivity probes for soils and insulations", *Cold Regions Research and Engineering Laboratory Report 182*, US Army Corps of Engineers, Hanover, NH, USA, p. 1-99.
- Winker, C.D., (1982) "Cenozoic shelf margins, northwestern Gulf of Mexico", *Gulf Coast Association of Geological Societies*, vol. 32, p. 427-448.
- Winterkorn, H.F., (1970) "Suggested method of test for thermal resistivity of soil by the thermal probe", In *Special Procedures for Testing Soil and Rock for Engineering Purposes*, *ASTM Special Technical Publication*, 479, p. 264-270.
- Wissa, A.E.Z., Martin, R.T., and Garlanger, J.E., (1975) "The piezometer probe", *Proceedings of Specialty Conference on In Situ Measurement of Soil Properties*, Raleigh, N.C., vol. 1, p. 536-545.
- Wood C.J., Liu H. Riffat S.B., (2010) "An investigation of the heat pump performance and ground temperature of a piled foundation heat exchanger system for a residential building", *Energy*, vol. 38, no. 12, p. 4932-4940.
- Zarella, A., De Carli, M., and Galgaro, A. (2013). "Thermal performance of two types of energy foundation pile: Helical pipe and triple U-tube." *Applied Thermal Engineering*, 61(2), p. 301-310.

Vita

The author is originally from Cheyenne, Oklahoma and obtained his bachelor's degree in civil engineering from the University of Oklahoma in 2015. Moving to New Orleans after graduation, he has worked first as an engineering intern and now a project engineer at Eustis Engineering, L.L.C., a geotechnical engineering consultant with a focus on the Gulf Coast. Concurrently, he has attended the University of New Orleans and received a Master's of Science in Engineering Management and a Graduate Certificate in Coastal Engineering in 2018.